國立臺灣師範大學理學院化學系

碩士論文

Department of Chemistry, College of Science

National Taiwan Normal University

Master's Thesis

以銅基金屬有機骨架於分散式固相萃取結合高效液相層析串聯質譜儀分析胺基酸之研究

Analysis of Amino Acids Using Cu-based Metal-Organic Framework in Dispersive Solid-Phase Extraction and HPLC-MS/MS

陳思蓉

Ssu-Jung Chen

指導教授： 陳頌方 博士

Advisor: Sung-Fang Chen, Ph.D.

中華民國 114 年 07 月

July 2025

Acknowledgement

I would like to express my heartfelt gratitude to Dr. Sivasankar Kulandaivel for his generous guidance and unwavering support throughout the past two years. His dedication to teaching me experimental techniques, instrumental operation, and data interpretation has been invaluable. His contributions have gone far beyond expectation, and I have often regarded him as my second advisor during my graduate studies. Words cannot fully convey my appreciation. I will always cherish the time spent working with him—without his help, I would not have achieved what I have today.

謝謝琬柔學姐這兩年來的指教，在層析與質譜等方法建立時，引導我學會相應的調整策略；謝謝冠履學長，就算您與我有一屆之隔，但仍在我初來乍到之時傳授了許多方向與知識，幫助我學習，在建立層析方法遇到困難時，給了我許多的方向或技巧、技術，即使只是一些看似平凡的建議，也使我受益良多，是我人生中非常崇拜的人之一；謝謝瀞瑩學姐這兩年來的照顧，在去年的教育訓練或在 API 4000 發生異常時，提供了許多寶貴的建議，使我學會多種處理方式；謝謝姵岑學姐悉心安排的豐富教育訓練課程，讓我在整個學習歷程中受益匪淺，同時也感謝您一年來的照顧與鼓勵。謝謝一喆學長，雖然與你共事的時間僅有一年，但在這段期間，你始終耐心地指導我，從沒有經歷過教育訓練而缺失的知識，到協助我克服論文閱讀上的困難，也在方法開發與實驗設計階段提供許多實用的建議，每當我陷入思緒混亂時，與你的討論總能協助我釐清方向，還有日常中談論棒球與啦啦隊，你在我碩班兩年的歷程中佔有極為重要的位置，我十分感謝你在這段期間給予我莫大的幫助與啟發，我也非常敬佩你能夠在碩班期間持之以恆地早睡早起、準時通勤，提前完成論文並預留時間從容準備口試，你是我最棒的學長之一，也是我心中極佳的榜樣！你對我的意義非常深遠，謝謝你這一年的照顧，未來我也希望能以你為典範，繼續努力前行；

謝謝洧辰學長，儘管你總是身負繁重的工作與代辦事項，卻依然對實驗室大小事務考慮周全，甚至連訂餐時都會細心地為身為素食主義者的我額外準備，我也非常敬佩你在理想與現實之間取得平衡，仍不斷前進的態度，雖然我們共處的時間僅有一年，但我從你身上學到了很多，若我在這段期間曾造成不便，也請你見諒，並衷心感謝你一年的照顧；謝謝雨萌學姊，感謝你教導我使用質譜儀器，你的悉心指導為我奠定了扎實的基礎，使我在碩班這兩年間的儀器操作得以順利進行，如魚得水；謝謝慧雯學姊，一年來給予我關心照顧。謝謝銘哲，在我剛進實驗室的前兩週，耐心地教導我質譜儀器的基礎知識，每次我向你借用 Agilent 1100 HPLC system 或 NanoLC autosampler 時，你也從未有過第二句話；謝謝諺霆，你總是積極處理實驗室各種瑣碎事務，也時常幫我預約 PXRD 或台科大的 FESEM，是很棒的應酬交際專家和名符其實的擋酒大王；謝謝晢析，兩年來聽了我無數次的抱怨、廢話與瑣事，還總是能給出滿滿的情緒價值，這段時間麻煩你了！但就是沒有跟你拍到畢業照有點可惜。謝謝鈺達，全世界最棒的學弟之一，很常麻煩你幫我觀察一下 Agilent 1200 的狀態，也偶爾和你抱怨些令人無言的事，謝謝你答應了我很多的請求與協助，也都有很好地完成，雖然這一年多少讓你費心，但也希望我留下的碩論資料多少對你有些幫助；謝謝品萱、芝卉、中邑與瀞文這一年的相伴。

謝謝呂家榮實驗室 A406 的人們。謝謝陳平學姐，雖然我們僅相識半年，您便出國深造，但在這段時間內，您在學理、技術與方法應用層面的指教，著實令我受益匪淺、畢生難忘，誠摯地感謝您的教導之恩，也祝福您接下來求學平安順心；謝謝博元學長，雖然我的羽球技術拙劣，你依然耐心指導我練習，在羽球技巧上我著實得益匪淺，且在處理人際關係方面，我也在你這邊學到了很多，對於我遇到很多蠢事，你也會為我抱不平，謝謝你這兩年來的照顧，祝你接下來教學一帆風順；謝謝 Hank 這位同行的素食好夥伴，你的存在對於我而言至關重要，感謝你在我迷惘之時，以我們在道場所學的古聖先賢智慧，加上你自己的經驗與建議，指引我方向，讓我知道自己可以怎麼做，這個部分我

也想向你學習！希望你接下來萬事吉祥、聖凡如意；文琪是我很好的搶票同好，無論是 Ado、Aimer 還是其他演唱會，你總是可以很快地獲取最新資訊並以絕對的實力搶到票，你的手速是我望塵莫及的，著實令我敬佩不已，希望未來也都有機會可以去日本現場看演唱會，與你交友真的很開心，祝福你出國留學平安順利；凡恩是超好的《排球少年！！》同好和 PTCG 好朋友，跟你聊排少真的很開心，還有分享遊戲抽卡、日本的旅遊景點和羽球，祝福你和你好漂亮的女朋友可以一直都這麼平安喜樂、感情和美，也祝你德國之行一帆風順、一路平安。謝謝秦雍，無論是聊羽球、KPOP，還是聽我發牢騷，你總是給予我莫大的包容與情緒支持，承蒙你的包容與關照了！我的經驗告訴我，雖然人生有很多破事，但是能遇到你這麼好，還會在口試前送來點心和可愛史迪奇的學弟，實屬不幸中的大幸！祝福你沒有這種不幸，抑或也有這種不幸中的大幸！同樣來自中原、明明差不多時間被錄取但只認識半年、拍照技術還很好的和維，謝謝你提供我許多關於材料分析的實用建議，尤其是在 Diamond 畫圖上的協助，還需要你把電腦搬來搬去的，著實煩你費心了！若是將來有我可以幫上忙的地方，我也必定在所不辭；謝謝思涵，經常在我抱怨時傾聽、給予情緒價值，又或是一起預定媽媽便當的超好吃果仁乾拌麵，明明自己也有很多公務纏身，與你相處真的很開心！祝福你實驗一切順利，未來平安喜樂；還有很常訂飲料還讓我蹭飲料的冠龍學長，謝謝學長一年來的照顧！最後，是我全 A406 最應該感謝的人，從碩一修習電分析化學開始便對我照顧有加，對我而言宛若天使般的晉哲，從協助我安裝 Origin、Chemdraw 等分析軟體、指導我首次操作校內 SEM 等儀器，還有聽到我甲酸噴濺受傷還近乎每周關心我傷口復原情況，明明不是你造成的但卻比肇事者還深切的關心、遇到一堆令人惱怒的事情時總會耐心聽我傾訴並陪我抱怨、偶爾也會聽我分析我的數據和我一起想辦法思考實驗上的問題、閒暇空檔的 PTCG 對戰或是一起出去買午餐，甚至是書報或口試報告練習，就算聽不懂也還是很努力地從頭到尾聽完，我的碩士生活幾乎五分之一的時光都有你的影子，謝謝你，是我兩年碩士生涯中最難能可貴的機遇之一，

我很榮幸能這兩年能有你的陪伴！我很榮幸能在這段日子裡有您的陪伴，也衷心祝福您未來的人生旅途一帆風順。

很榮幸這兩年能與曉潔成為隔壁實驗室的同學，在借用冰箱、器材或藥品時也多有協助，也給你添了不少的麻煩，謝謝你平時總是很有精神地與我打招呼、噓寒問暖及相互鼓舞，提供了我很多的情緒價值與正能量，謝謝你從大學至今的這六年來的照顧！祝福你日後一帆風順；也謝謝佳璟，平時借用 pH meter 與烘箱多有叨擾，祝你畢業快樂、前程似錦；亦寧是我在學習材料相關的各式表徵測試用儀器，最好的學習夥伴之一，與你一起學習使我受益匪淺，謝謝你這段時間的陪伴與交流；還有雖然我們只認識短短一個月，且經凡恩提起才知道你也來自中原的逸塵，是平日或周末晚上做實驗時常遇見的實驗好夥伴很高興認識你，祝你碩二順利，不用像我待到那麼晚。

謝謝從大學時期就一直對我有諸多照顧的林奇宏，從大三無機化學的指教到系學會日常，甚至是我剛進師大時協助我辦理就學及指導教授，以及日後請教 XRD 和 XPS，始終給予我極大的幫助，還曾帶我去吃許多好吃的餐廳！或在我情緒低落或身心俱疲時的日常慰問，真誠地感謝您一直以來的陪伴與照顧，並祝您順利完成學業，前程似錦；謝謝林冠丞，經常在限動看到我熬夜至極、疲勞至極、心情低落時給我很多溫暖的建議與提醒，還有很擔心我地叫我快點去休息，在我迷茫的時刻，也會給予我很多的建議、幫助我理清思緒，雖然兩年見面次數不多，但我仍深切感受到您的關心與鼓勵，謝謝你一直以來的陪伴與指引，你是很棒的朋友！謝謝沈宗奇，雖然你的這兩年過得也相當辛苦，甚至未來仍可能面對不少挑戰，但還是給了我很多日常的關心，特別是我甲酸噴濺受傷的那段時間，你對我的慰問次數與程度，遠勝過整個實驗室的總和，雖然這件事……冠丞、奇宏和你都很為我抱不平，謝謝你們！每次在我熬的要死要活、遇到令人咋舌的荒謬事件或陷入崩潰時，所給予的支持與建議。你也是我很重要的 Duolingo 夥伴，我也立志像你一樣，努力完成法文 500 天連續挑戰！也很喜歡你彈的鋼琴，祝福你能朝著自己的人生方向堅定前行；謝謝廖敬華從

大學到現在的諸多照顧，及樂於與我分享許多新奇又有趣的事物，像是 Native Mass 或醣合成相關領域的發展，也時常給我許多人生方向的建議與指引，雖然你總鼓勵我繼續攻讀博士，但目前我還沒有打算跨出這一步，不過你給我的鼓勵與方向，我都會放在心中，也許有朝一日就派得上用場；謝謝碩一時期，為了幫我取得一篇文獻補充資料，而伸出援手的劉昱君、許友齊、安妍、世蓉等人，也感謝之翎、詩屏，以及許許多多大學同學，雖然無法一一列名，但你們每一次的幫助我都銘記在心。誠摯地謝謝你們！

謝謝簡敦誠老師實驗室的進志學長，每次在我借藥品的時候總是二話不說地幫我查找；謝謝在我碩士這兩年期間的十三位室友，包括彥驊學姐、懷恩和很多人，我總是很晚才回去宿舍，謝謝你們平時的包容和時常聽我喋喋不休地分享日常以及抱怨生活瑣事，在我遇到問題時也會給我一些建議，謝謝！

也感謝道場上的許多道伴，包括葉原禎、游翔臻、易融、嘉茵、筠清、宗佑、宗敏、宇力哥哥、緯驊哥哥、夢婷姐姐、文彰哥哥、卉榆、敏涵，還有更多更多曾給我幫助與鼓勵的人。謝謝你們總是願意陪我談心、邀我參與活動、幫我出謀劃策，或適時地送來溫暖的建議與貼心的關懷。你們的關心真的非常之暖心。未來我想參與道務，這個部分我會在之後的日子裡盡我所能的。

誠摯地感謝《排球少年！！》的日向翔陽，雖然我的最愛角色是孤爪研磨，但是每當我瞪著日以繼夜做完的實驗，但無法解釋或與預想完全不同的數據時，我就會想到你，從第一季到第四季，甚至是在《劇場版 排球少年！！ 垃圾場的決戰》中，儘管你擁有出色的反應神經與體能，但在缺乏訓練背景、經常被質疑與貶低的狀態下，你做了什麼？「天賦異稟的體格、優秀傑出的體能，不同於這些條件的武器，『好難熬，真的好想停下來』從這個念頭產生瞬間後的一步……」想到你就算累死累活，還是會一刻不停歇地拼命接球，想到第四季開頭，即便全世界都在否定你的努力與價值，你仍不斷地思索自己在做什麼、能做什麼、還可以嘗試什麼，這樣的精神，深深打動著我，鼓舞我想著「我要如何走出『一步』」，然後開始動腦思考「一定有什麼事情是我可以做的、是我可

以解釋的，我一定可以做些什麼！」是你，使我即使在通宵實驗、身心俱疲的時刻，就算百般的痛苦又灰暗的日子裡，不斷地思考，思考我可以做什麼、可以嘗試什麼，你是我實驗過程中不可或缺的精神支柱，如太陽般和煦、如沐春風，是我非常不可或缺的太陽，謝謝你的存在，帶給我莫大的勇氣與動力前行。

真誠地謝謝《世界計畫：繽紛舞台！》，雖然劇情中沒有魔法，也沒有奇蹟般的翻轉，但正因如此，角色們在遭遇困難時的真實掙扎與內心拉扯，總讓我深受感動，並獲得源源不絕的勇氣。青柳冬彌，為了夢想毅然走出家裡反對，就算如此也不斷地正視自己的內心，或與家人正面的溝通，正視其問題；白石杏，儘管在天賦卓越且努力的新星小豆澤心羽面前顯得渺小，卻仍選擇不直視並勇敢前行；東雲彰人，即使遭受諸多批評，依舊努力拼命練習、追逐夢想。但最令所我共鳴的，是東雲繪名，她並沒有特別耀眼的才能，甚至被父親唱衰了整整三四年，即便如此，她仍然握緊畫筆，持續創作，就算瞭解前行的痛苦，她也仍舊堅持她所選擇的路，她讓我明白，真正重要的不是別人說了什麼，而是我自己選擇了什麼、願意做什麼、又願意為之努力到什麼程度。

謝謝我人生中的精神聖經《元素三部曲》，書中的「Dum Spiro, Spero.」與「生命之所以可貴，是在於個人擁有選擇的權利。」皆是我很重要的座右銘，而小說中的其他字句，如「如果要成功的保證才開始，我們一生將無法成就任何有價值的事。」也在關鍵時刻支撐著我，帶給了我許多勇氣與力量向前。這套書帶給了我莫大勇氣，是對我而言意義非同小可的一套小說，謝謝它的存在。

在這裡特別感謝我的家人們。謝謝我的阿嬤，雖然您已經過世了，但沒有從小到大的悉心照顧，不會有今天的我，我一直將您給我的護身符放在身上，特別是晚上在實驗室熬夜或通宵時，因為我真的很怕鬼，但我相信您還有觀世音菩薩會保佑我，謝謝您一直以來的照顧和庇佑，我很想念您，非常非常想念；謝謝我的阿公，從小到大的細心照顧，雖然我的潔癖和晚睡總是讓你很頭疼，但是每次我回家吃晚餐，你總是會準備很多我喜歡吃的菜，謝謝您一直以來的照顧！給您添麻煩了；謝謝爸爸媽媽，總是會問我需不需要很多東西，需要的

會幫我採買，我在家時，喝咖啡也總是有我的那一份，又或者回家工作，很常借我書房的電腦螢幕讓我比較好做事，金錢上部分也有許多的支援，雖然很常會嫌棄我沒有好好照顧自己的身體或者是沒有自己去賺錢，但還是各方面幫助了我很多，謝謝您從小到大的養育之恩、資源支持以及引領我的思考模式，雖然我不能說是很聰明，但對於我的邏輯思考以及思考實驗設計、前因後果以及機制上面的推敲，奠下了良好基礎，誠摯地謝謝你們。謝謝我的妹妹小宥，雖然從小打到大，但每當我遇到一些事情找你抱怨或是不知道怎麼解決的時候，你總是會有很多旁觀者清的見解，讓我有一些方向知道自己可以做些什麼；謝謝弟弟小冠，很常幫家裡大大小小的事情，我身為姐姐的我也受到你不少照料；怡怡，你還是好好讀書吧。謝謝典煌叔叔，雖然很少見面但是每次見面總是會給我許多建議，特別是對於次世代定序、蛋白質體學或代謝體學等業界趨勢，給了我許多實驗邏輯思考上的方向，也不斷地鼓勵我要保持一顆不斷貪婪學習的心態，因為我還是學生，我還有學習、犯錯的權利，我記得您的指教；謝謝鐘凰阿姨，給了我很多建議的同時甚至還問我有沒有需要高解析質譜儀，雖然我碩士用不到但我很樂意學！而在層析方法和萃取方法方面也得到了不少的建議，謝謝你們的照顧！最後，給你們添了很多麻煩，還有雖然不是故意也不是我造成的，但還是不小心受的傷，讓你們擔心了我很抱歉。

非常感謝指導教授陳頌方老師，明明九月才與您談話的第一天貿然請您收我作為研究生，您卻接受，且在這個得來不易的環境與資源中，我受到了許多非凡的薰陶，了解了許多專業技術上的知識，也將其知識藉由我的論文，應用的更加透徹，謝謝您兩年來的指教。

感謝口試委員曾素香博士，在百忙中撥冗參與我的畢業口試，指出了論文陳述上的錯誤及相關方法的問題，讓我有可以更加改善的空間；也謝謝口試委員林嘉和教授，誠摯地感謝您在畢業口試時的悉心引導與指教，經由您循序漸進的問題循循善誘著我，促進我的邏輯思維，讓我對於我的實驗機制及其作用，有如明心見性般，更加地清楚及透徹，對論文整體也有更高的掌握度。您們不

吝提出問題與寶貴的建議，讓我能夠重新審視實驗，讓論文更加完整。

Merci à moi-même. Durant ces deux années de master, j’ai travaillé sans relâche : réalisant des expériences jour et nuit, traitant les données, réfléchissant aux résultats, concevant les prochaines étapes. À force de persévérance, j’ai atteint ce résultat. Merci sincèrement à moi. J’ai vraiment donné le meilleur de moi-même durant ces deux années. À moi, dans le futur, si tu lis ces lignes, souviens-toi : tu as survécu à cette période qui ressemblait à une mort intérieure. Tu es extraordinaire, vraiment extraordinaire. Continue d’avancer, continue de te battre. Tu peux le faire — j’en suis sûre.

中文摘要

胺基酸廣泛參與生物體內之蛋白質合成、能量代謝及訊息傳遞等生命活動，並在醫學診斷、營養評估、食品品質控管及環境監測中扮演關鍵角色。然而，複雜樣品基質中含有的干擾物質常導致胺基酸分析面臨高背景雜訊、離子抑制及偵測靈敏度不足等問題。為克服上述挑戰，本研究合成一種陰離子銅基金屬有機骨架材料 (Cu-PyC NH_4^+ MOF)，其負電荷骨架源自雙去質子化之吡唑-4-羧酸酯配體，並由 NH_4^+陽離子平衡，應用於分散式固相萃取 (dSPE) 以陽離子交換機制選擇性吸附胺基酸，其中胺基酸的質子化銨基團 ($-NH_3^+$) 取代 NH_4^+ 離子。此 MOF 具備高比表面積、規則微孔結構與含氮/含氧官能基團，可與胺基酸形成氫鍵與靜電作用，提供良好的萃取選擇性與效率。實驗中進行萃取與洗脫條件之系統性優化，達成多數分析物回收率超過 80% 並具可接受的重現性，並將所得萃取液以高效液相層析串聯質譜儀 (HPLC-MS/MS) 進行分析，搭配醯胺管柱進行非衍生化分離。應用於即溶咖啡樣品，該方法展現足夠的靈敏度以偵測複雜基質中的微量胺基酸。本研究所建立之陰離子 Cu-MOF/dSPE 結合 LC-MS/MS 方法，提供一選擇性高、快速且環保的胺基酸分析平台，具應用於食品、醫療與環境等領域的實用潛力。

關鍵字： 胺基酸、Cu-PyC NH_4^+ MOF、陰離子金屬有機骨架、分散式固相萃取、Amide column、HPLC-MS/MS

Abstract

Amino acids play essential roles in protein biosynthesis, energy metabolism, and cellular signaling, making their accurate quantification critical in clinical, nutritional, food, and environmental analyses. However, complex sample matrices often contain interfering substances that hinder detection by causing ion suppression and elevated background noise. To overcome these challenges, this study synthesized an anionic copper-based metal-organic framework (Cu-PyC NH_4^+ MOF), characterized by a negatively charged framework derived from doubly deprotonated pyrazole-4-carboxylate ligands and balanced by NH_4^+ counterions, and applied it as a dispersive solid-phase extraction (dSPE) adsorbent for the selective enrichment of amino acids via a cation-exchange mechanism, where protonated ammonium groups of zwitterionic amino acids displace NH_4^+ ions. The synthesized MOF exhibits high surface area, microporosity, and functionalized surfaces capable of forming hydrogen bonding and electrostatic interactions with zwitterionic amino acids. Extraction and elution conditions were systematically optimized, resulting in recoveries exceeding 80% for most analytes and acceptable reproducibility. The extracted analytes were subsequently analyzed using high-performance liquid chromatography-tandem mass spectrometry (HPLC-MS/MS) with an amide column, enabling derivatization-free separation and quantification of 15 amino acids. Applied to instant coffee samples, the method demonstrated sufficient sensitivity for trace-level detection in complex matrices. This anionic MOF-based dSPE method coupled with LC-MS/MS provides a selective, rapid, and environmentally friendly platform for amino acid analysis, with practical applicability in food, clinical, and environmental fields.

Keywords: Amino Acids、Cu-PyC NH_4^+ MOF、Anionic metal-organic framework、Dispersive solid-phase extraction、Amide column、HPLC-MS/MS

Table of Contents

List of Tables

List of Figure

Chapter 1 Introduction

1.1 Amino Acid

1.1.1 Amino Acid

Amino acids, as the fundamental building blocks of proteins, are indispensable to the metabolism of virtually all living organisms, participating in processes such as protein biosynthesis, enzymatic catalysis, metabolic regulation, and cellular signaling.

The scientific investigation of amino acids originated in the early 19th century, with the first documented isolation of asparagine from asparagus juice by Louis-Nicolas Vauquelin and Pierre Jean Robiquet in 1806, marking the earliest identification of a nitrogen-containing organic compound from a biological source. This was followed by the discovery of cystine by William Hyde Wollaston in 1810, isolated from a urinary calculus, which underscored the presence of amino acids in pathological conditions. In 1820, Henri Braconnot employed acid hydrolysis to isolate glycine from gelatin, establishing this technique as a cornerstone for the subsequent identification of amino acids from proteins. As analytical methods advanced in the mid-19th century, amino acids were characterized as organic compounds featuring an amine ($-NH_2$) and a carboxylic acid (-COOH) group attached to a central α-carbon. Significant progress was achieved in the late 19th century when Emil Fischer advanced the field by elucidating the stereochemistry of amino acids and synthesizing peptides, thereby confirming their role as monomeric units of proteins. His seminal work (1899-1907) established that amino acids polymerize via peptide bonds to form proteins. The complete set of 20 standard proteinogenic amino acids was delineated by 1935, with threonine identifed as the final member through nutritional studies by William Cumming Rose. These foundational discoveries not only advanced

biochemical knowledge but also provided the basis for subsequent developments in analytical methods for amino acid characterization and quantification.[1, 2]

The investigation of amino acids spans diverse scientific domains, including biochemistry, analytical chemistry, and related disciplines. This interdisciplinary framework encompasses their essential functions in protein biosynthesis and cellular metabolism in humans, as well as in plant growth, microbial regulation, medical diagnostics, and disease pathogenesis. These multifaceted applications underscore the centrality of amino acids in biological and chemical research, establishing a basis for the subsequent examination of their classification, functional roles, and analytical methodologies in the following sections. [3, 4]

1.1.2 Amino Acid Categories

Amino acids are systematically categorized based on their chemical structure, nutritional essentiality, metabolic behavior, and biological function, reflecting their diverse roles in biological systems and influencing analytical approaches such as adsorption mechanisms in chromatography. Chemically, they are classified according to the properties of their side chains (R-groups), which determine key physicochemical characteristics like polarity, charge, hydrophobicity, and solubility. These properties are crucial for understanding how amino acids interact with stationary phases in separation techniques, where nonpolar side chains promote hydrophobic interactions, while polar or charged groups facilitate ionic or hydrogen bonding.

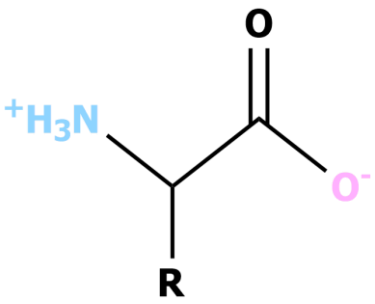

Figure 1. Structure of an α-Amino Acid in Its Zwitterionic Form.

Side chains are broadly grouped into four categories: nonpolar (hydrophobic), polar uncharged (hydrophilic), acidic (negatively charged at physiological pH), and basic (positively charged at physiological pH). Nonpolar amino acids, such as alanine, valine, leucine, isoleucine, proline, phenylalanine, tryptophan, and methionine, feature aliphatic or aromatic R-groups that minimize water interactions, enhancing their affinity for nonpolar adsorbents in reverse-phase chromatography. Polar uncharged amino acids, including serine, threonine, cysteine, tyrosine, asparagine, and glutamine, contain hydroxyl, sulfhydryl, or amide groups that enable hydrogen bonding, potentially leading to stronger retention on polar stationary phases like hydrophilic interaction liquid chromatography (HILIC). Acidic amino acids, such as aspartic acid and glutamic acid, carry carboxyl groups that ionize to form negative charges, promoting electrostatic interactions with positively charged adsorbents. Basic amino acids, including lysine, arginine, and histidine, possess amine or guanidino groups that protonate to positive charges, facilitating ion-exchange mechanisms with negatively charged surfaces. These classifications not only dictate protein folding and stability but also impact analytical selectivity, where side chain properties influence elution order and resolution in LC-MS/MS methods.

Biologically, amino acids are divided into proteogenic and non-proteogenic types. Proteogenic amino acids comprise the 20 standard α-amino acids encoded by the

genetic code for ribosomal protein synthesis in eukaryotes (21 in some prokaryotes, including selenocysteine), all of which are L-enantiomers except glycine (achiral). These include the nine essential amino acids (histidine, isoleucine, leucine, lysine, methionine, phenylalanine, threonine, tryptophan, and valine) that humans cannot synthesize and must obtain from diet, and the remaining non-essential ones (alanine, arginine, asparagine, aspartic acid, cysteine, glutamic acid, glutamine, glycine, proline, serine, and tyrosine) produced endogenously. Conditionally essential amino acids, such as arginine and glutamine, become vital under stress, injury, or metabolic disorders, emphasizing their role in nutrition and disease diagnostics.

Non-proteogenic amino acids, numbering over 500 naturally occurring variants, are not genetically encoded for protein synthesis but arise from metabolic pathways, post-translational modifications, or environmental sources. Examples include D-enantiomers (e.g., D-serine, a neurotransmitter co-agonist), β-amino acids (e.g., β-alanine in coenzyme A), γ-amino acids (e.g., γ-aminobutyric acid (GABA) as an inhibitory neurotransmitter), and modified residues like hydroxyproline (from collagen hydroxylation) or ornithine (in the urea cycle). Many non-proteogenic amino acids mimic proteogenic ones, potentially leading to misincorporation into proteins or toxicity (e.g., β-methylamino-L-alanine (BMAA) linked to neurodegenerative diseases). Their diverse structures—often with altered side chains or stereochemistry—pose challenges in analysis, requiring chiral separation to distinguish enantiomers and isomers, as their adsorption behaviors differ significantly from proteogenic counterparts due to variations in polarity and charge.[5-10]

These categorization schemes are pivotal in biomedical, nutritional, and analytical contexts, guiding dietary formulations, clinical diagnostics, the optimization of separation methods, and the selection of extraction techniques. For instance, understanding side chain interactions informs not only adsorption

mechanisms in chromatography—where polar and charged groups enhance retention via ionic or hydrophilic forces—but also extraction strategies, such as tailoring solvent polarity to match amino acid hydrophilicity or hydrophobicity to improve yield and purity from complex matrices. This framework thus provides a foundation for exploring their functional applications and analytical methodologies in subsequent sections.

1.1.3 Amino Acid Application

Amino acids exhibit multifaceted roles in biological systems, extending beyond their fundamental function as constituents of proteins. Their applications encompass biochemistry, medicine, nutrition, agriculture, and biotechnology, influencing diverse processes from cellular metabolism to disease management.[3, 11] In ribosomal protein synthesis, only 22 amino acids (21 in eukaryotes and 22 in prokaryotes) are genetically encoded, all of which are α-amino acids and predominantly L-enantiomers (with the exception of glycine, which is achiral).[12] These proteinogenic amino acids, including methionine, glutamine, and proline, also fulfill secondary metabolic roles; for instance, methionine participates in cholesterol metabolism[13], glutamine maintains hepatic pH homeostasis[14], and proline regulates mitochondrial function[15]. Non-proteinogenic amino acids, exceeding 500 naturally occurring variants, further expand these functions; they originate from metabolic pathways, post-translational modifications, environmental sources, or synthetic engineering, and may mimic proteinogenic amino acids, occasionally resulting in erroneous incorporation into peptides via ribosomal or non-ribosomal synthesis mechanisms.[16, 17]

In neuroscience and pharmacology, amino acids serve as neurotransmitters or their precursors. Gamma-aminobutyric acid (GABA), glutamine, and D-serine modulate signaling at GABA and N-methyl-D-aspartate (NMDA) receptors.[18, 19]

Metabolic intermediates such as tyrosine and tryptophan are precursors to hormones like dopamine and serotonin, respectively.[11] Clinically, amino acid concentrations in biological fluids act as biomarkers for physiological status, with perturbations indicating disorders such as phenylketonuria, wherein elevated phenylalanine levels impair neurological development.[20] Therapeutically, non-proteinogenic amino acids like levodopa (L-DOPA), a dopamine precursor, are employed in Parkinson's disease management owing to its capacity to traverse the blood-brain barrier via amino acid transporters.[16] Emerging therapeutic applications include L-theanine for schizophrenia treatment[21] and L-serine for potential neuroprotection against cyanobacterial toxins or motor neuron disease.[17, 22] In biotechnology, engineered amino acids enhance the stability and specificity of therapeutic peptides.[23]

From a nutritional perspective, amino acids are pivotal in dietary formulations. Essential amino acids (e.g., histidine, isoleucine, leucine, lysine, methionine, phenylalanine, threonine, tryptophan, and valine in humans) must be acquired exogenously, as they are not synthesized endogenously, whereas non-essential amino acids (e.g., alanine, arginine, asparagine, aspartic acid, cysteine, glutamic acid, glutamine, glycine, proline, serine, and tyrosine) are produced internally.[3, 24] Conditional essentiality may arise under conditions of stress, injury, or disease, rendering non-essential amino acids like arginine and glutamine indispensable.[25] In agriculture, optimizing amino acid profiles in animal feed promotes livestock growth and development by ensuring a balanced intake of essential and non-essential amino acids.[24] Fitness supplements frequently incorporate branched-chain amino acids (leucine, isoleucine, valine) or non-proteinogenic variants such as norvaline to support muscle recovery and performance.[26, 27]

Toxicity constitutes another critical domain, particularly for non-proteinogenic amino acids synthesized by bacteria, algae, and plants for allelopathic or defensive

purposes.[28, 29] Acute toxins like domoic acid induce amnesic shellfish poisoning[30], while chronic exposure to β-methylamino-L-alanine (BMAA) or azetidine-2-carboxylic acid (Aze) has been implicated in neurodegenerative disorders such as amyotrophic lateral sclerosis (ALS) or multiple sclerosis.[17, 31, 32] The analysis of these compounds in environmental matrices is often confounded by the presence of isomers (e.g., BMAA and its three cyanobacterial-derived analogs), underscoring the necessity for precise identification to evaluate ecological and health risks.[33]

These diverse applications highlight the centrality of amino acids in scientific inquiry, fostering advancements in diagnostics, therapeutics, and sustainable practices. A comprehensive understanding of their roles enables targeted interventions in human health, agriculture, and environmental monitoring.

1.1.4 Amino Acid Analysis

The analysis of amino acids poses distinct challenges attributable to their polar character, low molecular weight, and absence of intrinsic chromophores or fluorophores in most instances.[34, 35] Amino acids may occur in samples as free entities or bound within proteins or peptides, necessitating specialized extraction, separation, and detection methodologies.[36] Free amino acids preserve their native configuration, whereas bound forms are liberated via enzymatic digestion or chemical hydrolysis (e.g., acid hydrolysis employing HCl).[37, 38] In complex biological matrices such as fluids, tissues, or environmental samples, extraction typically involves protein precipitation, solvent-based approaches, or solid-phase extraction (SPE) for sample cleanup to mitigate matrix interferences.[34] Hydrolysis may yield post-translationally modified residues or non-covalently associated amino acids, requiring cautious interpretation to circumvent analytical artifacts.[39, 40]

Separation is imperative given the structural diversity of amino acids and potential contaminants. Chromatographic techniques predominate, including thin-layer chromatography (TLC), gas chromatography (GC), and liquid chromatography (LC) modalities such as high-performance liquid chromatography (HPLC) and ultra-high-performance liquid chromatography (UHPLC).[41, 42] The polarity of native amino acids impedes retention in reverse-phase LC, prompting the adoption of alternatives like hydrophilic interaction liquid chromatography (HILIC) or ion-exchange chromatography.[34] Capillary electrophoresis (CE) provides a non-chromatographic separation option, albeit less prevalent.[43] Derivatization mitigates these constraints by augmenting hydrophobicity, ionization efficiency, and detectability.[44] Pre-column derivatization (e.g., with o-phthalaldehyde (OPA), fluorenylmethyloxycarbonyl chloride (FMOC), or dansyl chloride) facilitates reverse-phase LC and enhances sensitivity, while post-column derivatization (e.g., with ninhydrin) enables immediate post-separation detection[34, 45] Chiral analysis, increasingly essential for differentiating D- and L-enantiomers, utilizes chiral stationary phases or derivatizing reagents such as Marfey's reagent.[34]

A notable advancement in non-derivatized analysis involves the use of amide-based stationary phases in HILIC mode, which offers several advantages for separating native amino acids. These columns provide enhanced retention through hydrogen bonding and electrostatic interactions, improving resolution without the need for derivatization steps that can introduce variability, artifacts, or additional sample preparation time.[34, 46] Moreover, amide columns exhibit compatibility with mass spectrometry (MS) detection, enabling direct analysis of underivatized samples with reduced risk of column fouling and better suitability for high-throughput workflows.[35, 36] This approach is particularly beneficial in metabolomics and clinical applications where preserving the native state of analytes is desirable to minimize

chemical alterations.

Detection strategies are selected based on the application: spectrophotometric detectors (UV, visible, or fluorescence) are apt for derivatized amino acids, whereas mass spectrometry (MS), especially tandem MS (MS/MS), affords superior specificity for both native and derivatized forms.[34] LC-MS/MS is preferred for its sensitivity, supporting targeted analyses (e.g., multiple reaction monitoring for quantitation) or untargeted profiling (e.g., full-scan modes for discovery) in intricate samples.[36] Challenges such as isomer resolution (e.g., leucine/isoleucine or BMAA isomers) demand optimized gradients or specialized columns.[33] Quantitation necessitates internal standards, often isotopically labeled analogs, to compensate for matrix effects and ionization inconsistencies.[33]

Recent innovations, including HPLC-MS/MS, have expedited analysis durations and augmented resolution, facilitating high-throughput applications in metabolomics and clinical diagnostics.[34] Nonetheless, method selection hinges on sample characteristics, amino acid form (native versus derivatized), and objectives (e.g., chiral versus achiral). Prospective developments may incorporate microfluidics or artificial intelligence-driven data interpretation to bolster precision and accessibility.

1.2 Metal-Organic Framework

1.2.1 Introduction

Metal-organic frameworks (MOFs) are a class of crystalline porous materials made up of metal ions or clusters coordinated to multidentate organic ligands, forming highly ordered three-dimensional networks. The concept of MOFs is rooted in early coordination chemistry, with historical examples like Prussian Blue—an iron-cyanide polymer synthesized in the 1700s and later identified as a mixed-valent Fe(II)/Fe(III) framework. In 1897, Hofmann and colleagues synthesized a nickel-based coordination network, and in 1964, J.C. Bailar formally introduced the term "coordination polymer," laying the conceptual groundwork for modern MOFs. Over the past two decades, advances in synthetic and crystallographic techniques have transformed these early structures into a new class of materials with precisely tunable properties.[47]

Modern MOFs are recognized for their ultra-high surface areas, tunable pore sizes and shapes, and remarkable structural diversity. These characteristics stem from their modular architectures, wherein both the metal nodes and organic linkers can be thoughtfully selected or modified to achieve the desired functionality. Consequently, MOFs can engage in a broad range of chemical interactions, facilitating their use in gas storage and separation[48-50], heterogeneous catalysis[51], chemical sensing[52, 53], drug delivery[54], and beyond[55].[56, 57]

Recently, the tunable porosity, surface chemistry, and framework topology of MOFs have made them highly attractive for analytical sample preparation, particularly in solid-phase extraction (SPE) and dispersive SPE (dSPE) techniques. MOFs can interact selectively with target analytes through mechanisms such as hydrogen bonding, electrostatic interactions, π-π stacking, and metal-ligand

coordination. These interactions enable efficient enrichment, separation, and detection of trace-level compounds from complex matrices. Building on these advantages, our research explores the use of MOFs as high-performance adsorbents in SPE systems, targeting the selective extraction of environmentally and biologically relevant analytes[58,59-61].

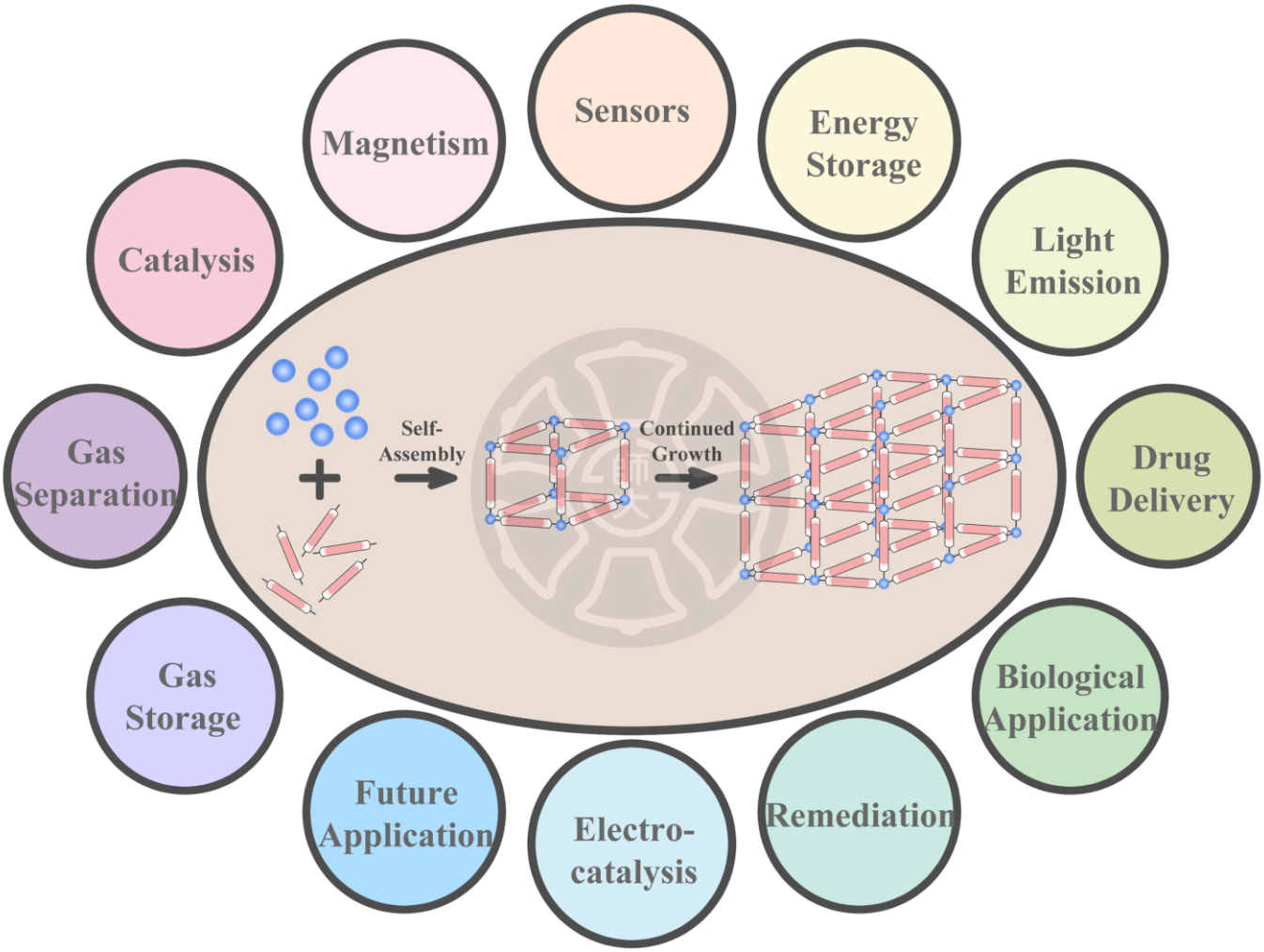

Figure 2. MOF Formation and Application.

1.2.2 Structural Modularity of MOFs

Metal Nodes

The metal centers in MOFs serve as structural nodes and play a crucial role in defining coordination geometry, pore architecture, and framework stability. These can include single metal ions (e.g., MOF-74: Zn^{2+} [62], HKUST-1: Cu^{2+} [63], MIL-101: Fe^{3+} [64]) or metal clusters (e.g., UiO-67[65]: Zr_6, PCN-250: Fe_3[66], CAU-6: Al_{13}[67]), which act as primary or secondary building units (SBUs). The coordination number, ionic radius, and oxidation state of the metal influence both the robustness and the functionality of the MOF. Importantly, the framework's chemical stability is heavily dependent on the nature of the metal; for instance, MOFs incorporating soft metal ions (e.g., Cd^{2+}) often show poor resistance under acidic or basic conditions.[56, 68]

Organic Linkers

The organic ligands bridge the metal nodes and define the overall topology, pore size, and flexibility of the MOF. Common linkers include carboxylates, azolates, phosphonates, and sulfonates. The length and rigidity of the linker determine the dimensionality and pore accessibility, while functional groups (e.g., $–NH_2$, –OH, –COOH) modulate surface interactions with guest molecules. Longer or more flexible linkers may increase porosity but also raise the risk of framework interpenetration or collapse during synthesis or solvent removal.[56, 68]

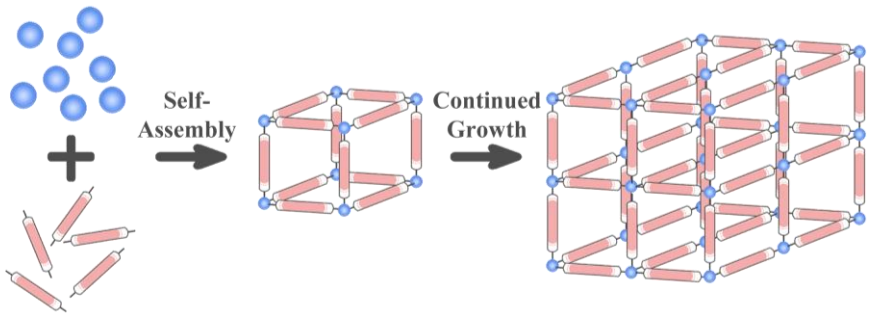

Figure 3. Scheme of MOF Formation in Synthesis Process.

pH Stability and Environmental Responsiveness

MOF stability across different pH environments is an influential factor for practical applications, especially in aqueous systems used for solid-phase extraction. In general, MOFs based on high-valent metal clusters such as Zr^{4+} (e.g., UiO-type MOFs) or Al^{3+} (e.g., MIL-53, MIL-101) exhibit excellent stability in acidic or basic media. Conversely, frameworks built from low-valent or soft metals tend to degrade in harsh conditions (e.g., pH ≤ 2 or ≥ 11). The presence of acid/base-stable linkers and strong metal–ligand coordination bonds can further enhance resilience. These characteristics make selected MOFs ideal candidates for SPE applications involving complex or variable matrices, such as environmental waters or biological fluids.[69]

1.2.3 Cu-PyC NH_4^+ MOF

The MOF employed in this study, formulated as $NH_4[Cu_3(\mu_3\text{-}OH)(\mu_3\text{-}4\text{-carboxypyrazolato})_3]$, was synthesized with slight modifications from previously reported procedures[70, 71]. The synthetic route is divided into three stages: *ligand deprotonation and metal dissolution*, *homogeneous mixing and incubation*, and *acid-triggered crystallization and isolation*.

Stage I: Ligand Deprotonation and Metal Ion Release

1H-pyrazole-4-carboxylic acid was initially dispersed in deionized water. The zwitterionic nature of the molecule, with acidic –COOH and basic pyrazole functionalities, affords moderate aqueous solubility. Upon addition of aqueous ammonium hydroxide, complete dissolution occurred via deprotonation of both the carboxylic and pyrazole protons:

$$H_2PyC + 2NH_4OH \rightarrow (NH_4)(PyC) + 2H_2O$$

In parallel, copper(II) nitrate trihydrate was dissolved in water, releasing Cu^{2+} and nitrate ions:

$$Cu(NO_3)_2 \cdot 3H_2O \rightarrow Cu^{2+} + 2NO_3^- + 3H_2O$$

Stage II: Homogeneous Mixing and Pre-Nucleation Equilibrium

The deprotonated PyC^{2-} ligand and Cu^{2+} solution were combined under ultrasonication to ensure homogeneity. The resulting solution consisted of dissociated species in equilibrium:

$$3Cu^{2+} + 3PyC^{2-} + NH_4^+ + NO_3^- + OH^-$$

At this stage, no framework assembly occurs due to the absence of a kinetic or thermodynamic driving force for coordination polymerization.

Stage III: MOF Nucleation via Acid-Induced Self-Assembly

Following 16-18 hours of incubation, the pH was reduced via dropwise addition of hydrochloric acid. This neutralized excess hydroxide and promoted the *in situ* hydrolysis of coordinated water, leading to the localized formation of μ_3–OH^- bridges and subsequent cluster formation:

$$3H_2O + Cu^{2+} \rightarrow Cu_3(\mu_3 - OH) + 3H^+$$

This initiated the self-assembly of trinuclear $Cu_3(\mu_3–OH^-)$ clusters, which further coordinated with three bridging PyC^{2-} ligands to generate the anionic MOF framework:

$$3Cu^{2+} + 3PyC^{2-} + OH^- \rightarrow [Cu_3(\mu_3 - OH)(PyC)_3]^-$$

$$NH_4^+ + [Cu_3(\mu_3 - OH)(PyC)_3]^- \rightarrow NH_4[Cu_3(\mu_3 - OH)(PyC)_3]$$

The resulting blue crystalline solid was collected via centrifugation, washed sequentially with water and ethanol to remove unreacted salts and byproducts (e.g., NH_4Cl), and dried. This purification step is critical to preserve pore accessibility for subsequent extraction applications.

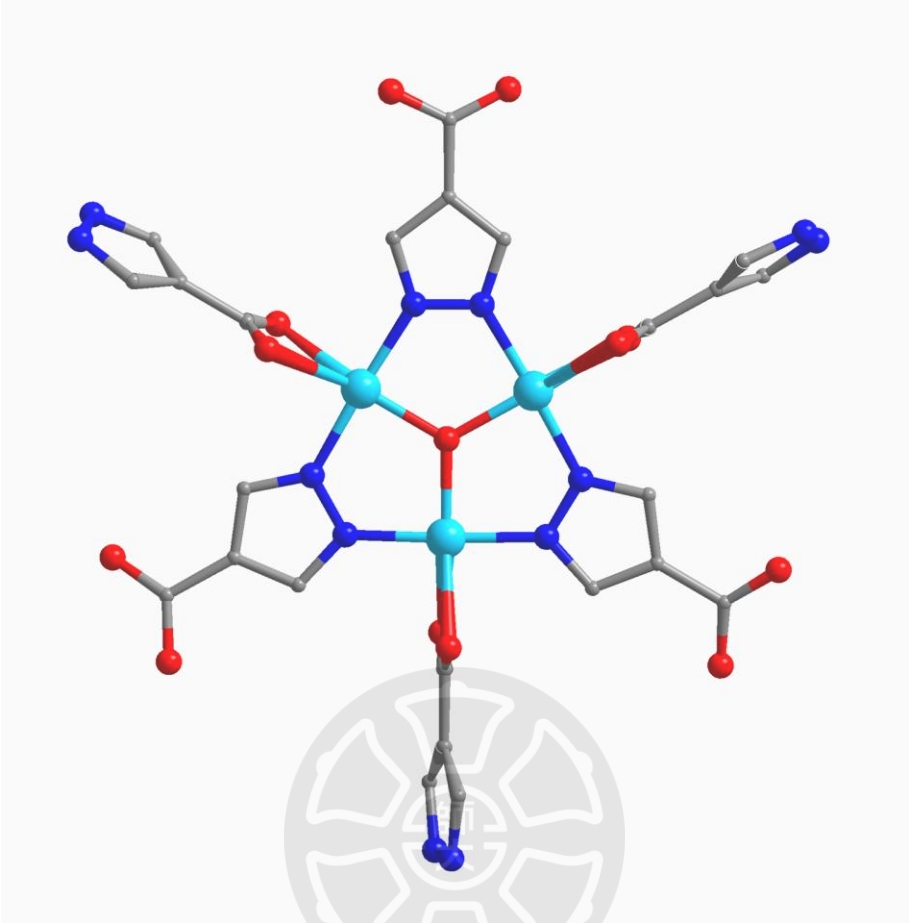

Figure 4. $Cu_3(\mu_3\text{-}OH)$ Clusters Coordinated with PyC^{2-} Ligands to Form $Cu_3(\mu_3\text{-}OH)(PyC^{2-})_3$ Unit.

Crystal Structure and Framework Topology

The structure of $NH_4[Cu_3(\mu_3\text{–}OH^-)(PyC^{2-})_3]$ is constructed from trinuclear $Cu_3(\mu_3\text{–}OH^-)$ SBUs, where three Cu^{2+} ions adopt a nearly coplanar geometry, bridged centrally by a μ_3-hydroxo group. These SBUs are extended into a three-dimensional framework by 4-carboxypyrazolato ligands, which coordinate via their carboxylate oxygen and pyrazole nitrogen atoms in a ditopic fashion.

The resulting network adopts an hxg topology and crystallizes in the cubic Fd-3c space group, characterized by high symmetry and periodic porosity (~1.3 nm). The framework is inherently anionic, with NH_4^+ ions serving as counterbalancing species. This combination of robust metal-ligand connectivity and symmetric topology yields excellent aqueous and thermal stability, key features for solid-phase extraction.

Furthermore, the microporous structure and polar internal surface—stemming from the carboxylate and pyrazole functional groups—facilitate strong interactions with polar analytes. These features render the MOF highly suitable for adsorption of small, water-soluble molecules such as amino acids, which is the focus of the subsequent extraction experiments.

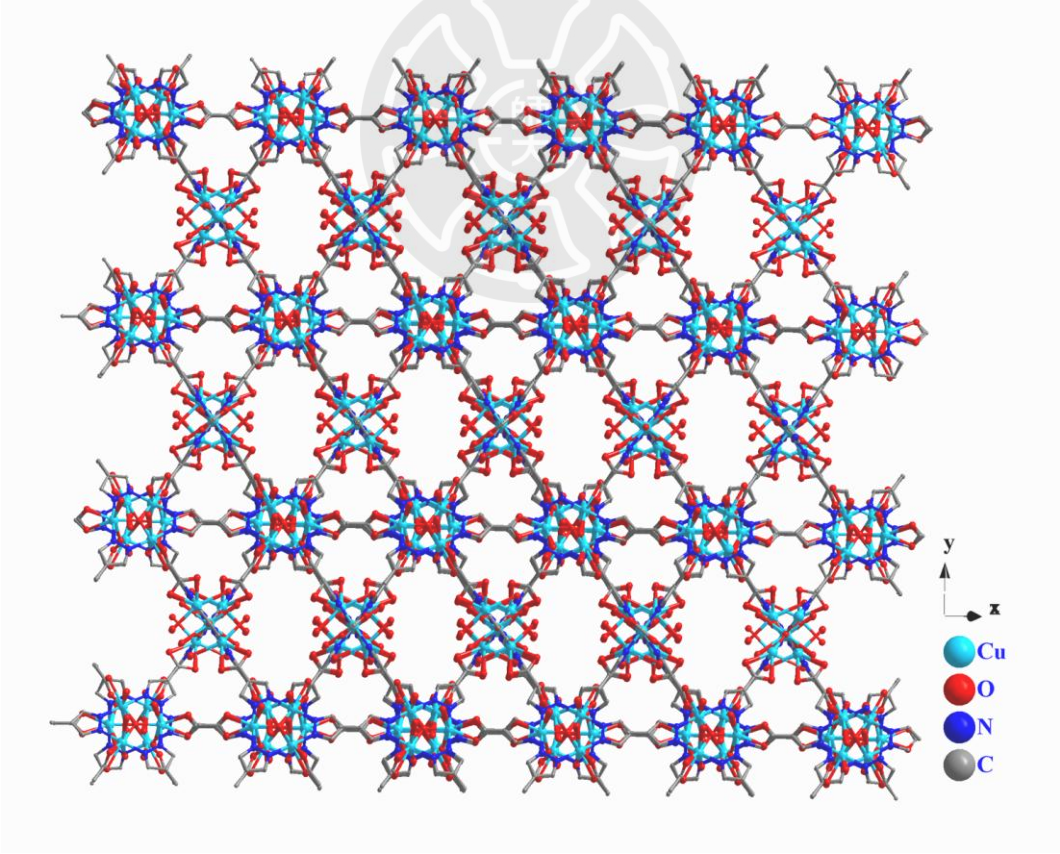

Figure 5. Cu-PyC MOF Structure Viewed along the Z-Axis.

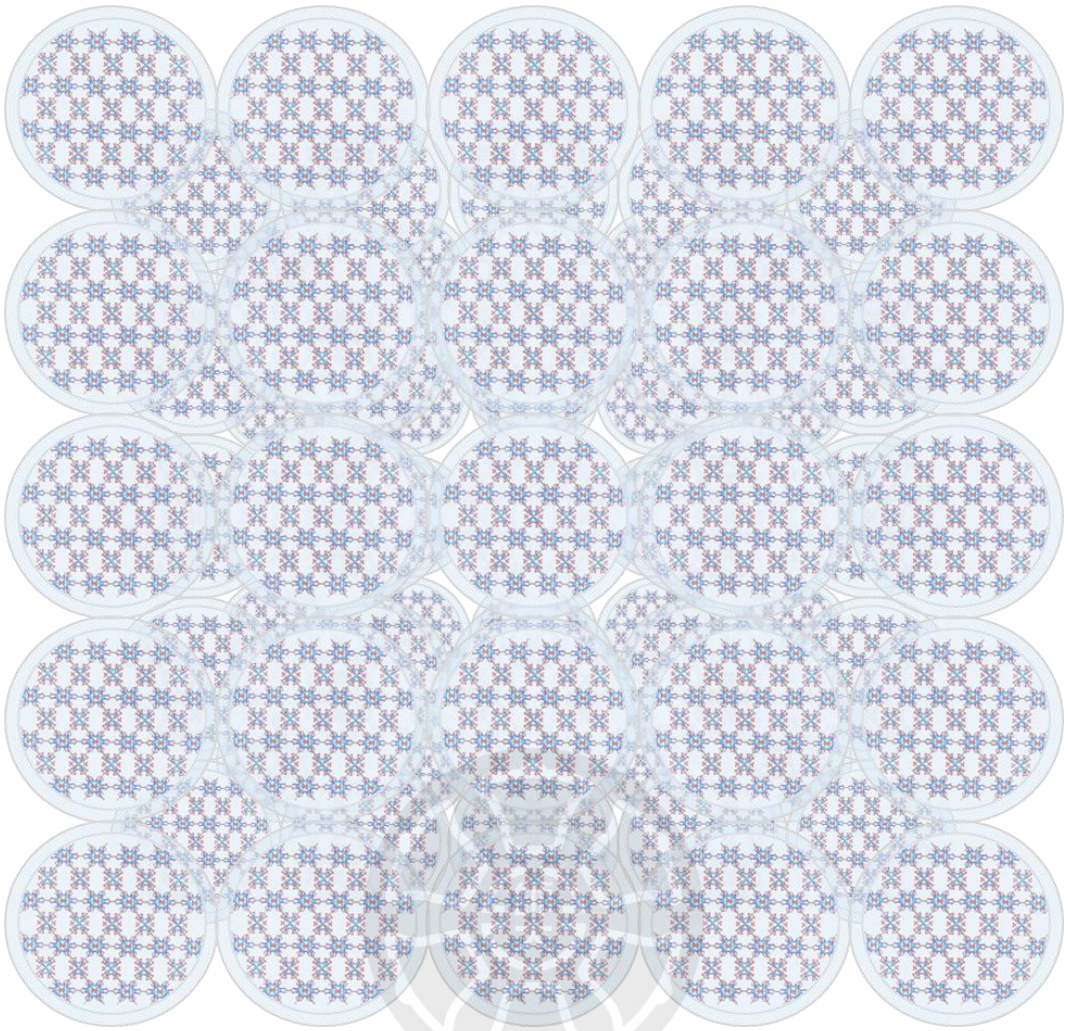

Figure 6. Schematic illustration of a MOF particle dispersed in a solution medium.

1.3 Sample Preparation

1.3.1 Sample Preparation

Sample preparation is a critical yet often underestimated step in analytical workflows. Despite being time-consuming and labor-intensive, it is indispensable for data quality. This is particularly true in complex matrices (e.g., biological, pharmaceutical, environmental, and food samples), where direct analysis is rarely feasible due to sample heterogeneity, trace-level analytes, and interfering substances. Without appropriate preparation, matrix components may suppress or enhance signals, contaminate analytical instruments, and ultimately compromise accuracy and precision. In essence, the goal of sample preparation is to isolate target analytes from the sample matrix, enhance their detectability, and transform the sample into a form compatible with the analytical system. This includes improving selectivity by eliminating interferences, increasing sensitivity through pre-concentration, and ensuring instrumental compatibility by adjusting pH, solvent composition, and physical state. These roles have become even more critical as modern instruments (e.g., LC-MS/MS) achieve lower detection limits, making even minor interferences problematic.

Historically, sample preparation techniques evolved to address challenges in isolating analytes from complex matrices. One of the earliest examples is the Soxhlet extractor, introduced by Franz von Soxhlet in 1879, which enabled continuous solid–liquid extraction using solvent reflux—a concept still used in fat and oil analysis today.[72] In the early 20th century, precipitation, drying, liquid–liquid extraction (LLE), and deproteinization were developed to address the need for cleaner samples in gravimetric or titrimetric analyses. A pivotal shift occurred in 1941, when A. J. P. Martin and R. L. M. Synge introduced counter-current extraction (CCE) to separate

amino acids based on distribution coefficients. Their theoretical contributions laid the groundwork for partition chromatography and ultimately led to the development of gas chromatography and liquid chromatography—technologies that redefined the role of sample preparation as indispensable rather than auxiliary.[73]

Since then, numerous techniques have been developed or refined to meet the increasing demands of modern analytical chemistry. LLE, while still widely used, has largely been supplemented or replaced by more efficient and selective methods such as solid-phase extraction (SPE), microwave-assisted extraction (MAE), solid-phase microextraction (SPME), and dispersive solid-phase extraction (dSPE). Each of these methods was introduced to overcome specific limitations, including excessive solvent consumption, lengthy procedures, poor automation potential, or inadequate selectivity.

Today, sample preparation continues to evolve in response to emerging challenges, such as the need for multi-residue detection in complex food and environmental matrices, the miniaturization of workflows, and the principles of green analytical chemistry. An ideal method is expected to be universal, fast, cost-effective, selective, and environmentally sustainable—attributes that often conflict in practice and must be carefully balanced during method development.[74]

1.3.2 Solid Phase Extraction

Solid-phase extraction (SPE) is a widely used sample preparation technique developed in the late 1970s to address the limitations of liquid–liquid extraction. The introduction of commercial prepacked cartridges, such as Sep-Pak® by Waters in 1977, represented a pivotal development in standardizing and simplifying extraction procedures.

SPE is based on the selective retention of target analytes on a solid adsorbent, which is chosen to interact more strongly with the analytes than with other matrix components. The SPE procedure involves conditioning the adsorbent, loading samples to selectively retain analytes, washing away interferences, and finally eluting analytes with an appropriate solvent. Unwanted substances are removed by washing with a mild solvent, and finally, the analytes are eluted with a stronger solvent that disrupts the analyte–adsorbent interaction.

In a typical SPE procedure, the sample solution is passed through a cartridge or disk packed with a solid adsorbent. Target analytes are selectively retained through interactions such as hydrophobic forces (e.g., C18-bonded silica for nonpolar compounds), ion exchange (for charged species), or hydrogen bonding. Its versatility, low solvent consumption, and suitability for automation have made SPE a standard method. It is widely used in environmental, pharmaceutical, and food analysis.

Nevertheless, conventional SPE methods often involve multiple conditioning and elution steps and may be less effective when dealing with samples containing particulates or highly polar compounds. These limitations have prompted the development of alternative approaches, such as dispersive solid-phase extraction (dSPE), which enhances contact efficiency and simplifies the workflow.

1.3.3 Dispersive Solid Phase Extraction

Dispersive solid-phase extraction (dSPE) was developed as a simplified variant of conventional SPE, first proposed in 2002 and formally described in 2003 by Anastassiades and Lehotay as part of the QuEChERS method for pesticide residue analysis. This technique was developed to address the laborious steps and cartridge dependency of traditional SPE and has since been widely adopted in food, environmental, and clinical analyses owing to its simplicity and high-throughput capability.[75]

A typical dSPE procedure starts with an organic extract (e.g., acetonitrile or ethanol) containing both analytes and matrix interferences. The extract is introduced into a tube pre-filled with selected adsorbents and drying salts. In contrast to cartridge-based SPE, dSPE disperses adsorbent particles directly within the sample, maximizing the surface contact between the adsorbent and analytes. Following vigorous mixing and subsequent centrifugation, matrix interferences or analytes—depending on the adsorbent used—are adsorbed onto the adsorbent particle. The supernatant containing unwanted components is then discarded. To elute the adsorbed analytes, an appropriate solvent with stronger affinity to the analytes is added. The eluate is then collected and concentrated, if necessary.

This approach is especially effective for complex sample matrices where rapid cleanup is essential. It offers a streamlined, scalable alternative to traditional solid-phase extraction, providing both selectivity and efficiency in sample preparation. It requires only a small amount of solvent and a relatively short extraction time. It is particularly advantageous for separating and enriching trace analytes in complex matrices, and its integration into modern analytical workflows, such as LC-MS/MS, makes it ideal for routine and multi-residue determinations. It is one of the key

technologies widely used in the analysis of food and biological samples in recent years. However, it also presents limitations: the choice of adsorbent must be highly specific, as there is no gradient elution or stepwise control as in cartridge SPE. In this study, a metal-organic framework (MOF) was selected for amino acid extraction owing to its tunable adsorption properties.

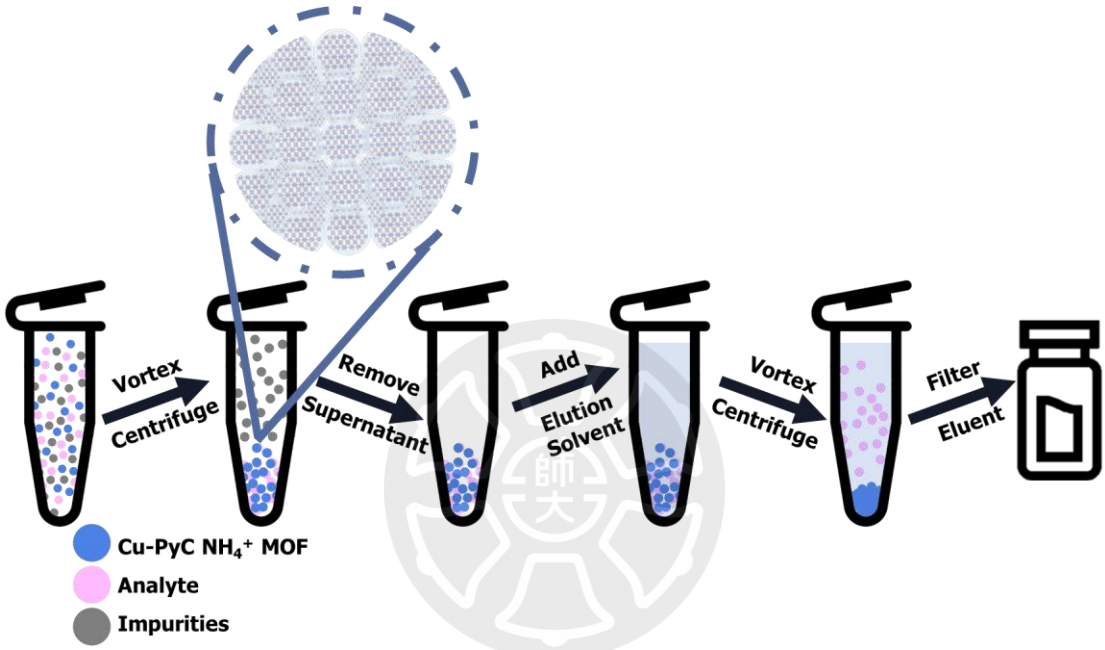

Figure 7. Schematic of dSPE using Cu-PyC NH_4^+ MOF for amino acid extraction

1.4 High Performance Liquid Chromatography

1.4.1 Chromatography

Chromatography is a powerful and versatile analytical technique used for the separation, identification, and quantification of diverse analytes within complex mixtures. The separation relies on the differential distribution of analytes between the stationary and mobile phases. Separation is achieved through interactions of analytes with either phase as the mobile phase flows through or across the stationary phase. Due to its high sensitivity, resolution, and methodological versatility, chromatography plays a crucial role in chemical, biological, pharmaceutical, environmental, and many other analytical fields.

The foundation of chromatographic techniques was established in 1906 when Russian botanist Mikhail Tsvet first separated plant pigments using a glass column packed with calcium carbonate (described as “white chalk and alumina” in the original literature). This process resulted in distinct colored bands—a visual phenomenon that inspired the term 'chromatography,' derived from the Greek words chroma (color) and graphō (writing). Although Tsvet did not provide a theoretical explanation for the separation mechanism, his observations marked the inception of chromatographic technique development.

Chromatography represents a broad and fundamental category within analytical chemistry. Depending on analyte properties—such as volatility, polarity, or thermal stability—the appropriate physical state of the mobile phase is selected, classifying chromatographic techniques into three primary categories: gas chromatography (GC), liquid chromatography (LC), and supercritical fluid chromatography (SFC). Within LC, analyte properties and operational conditions influencing retention or resolution determine the optimal separation mechanism—such as partition, adsorption, or size-

exclusion chromatography—to achieve high selectivity and efficiency.

Among various chromatographic methods, partition chromatography is widely used across multiple fields. This method was developed in 1941 by A. J. P. Martin and R. L. M. Synge, refining the earlier work of Mikhail Tsvet. The technique relies on the differential partitioning of analytes between two immiscible liquid phases — one immobilized on an inert solid support serving as the stationary phase, and the other as the mobile phase. In their study, water was used as the stationary phase, retained on a solid carrier such as silica, while an organic solvent like chloroform served as the mobile phase. The separation mechanism in this system is governed by the analytes' partition coefficients, which dictate their distribution between two immiscible phases, resulting in separation based on subtle differences in solubility. This study established the theoretical foundation of liquid-liquid chromatography, enabling the successful separation of amino acids and peptides. Their pioneering work earned them the Nobel Prize in Chemistry in 1952 and laid the groundwork for modern liquid-phase separation techniques.

The implementation of various chromatographic techniques requires either simple or advanced analytical platforms. A simple example is thin-layer chromatography (TLC), which employs specialized thin-layer plates coated with stationary phases. More sophisticated analytical platforms include high-performance liquid chromatography (HPLC), ultrahigh-performance liquid chromatography (UHPLC), and nano-liquid chromatography (nanoLC).

1.4.2 High Performance Liquid Chromatography

In 1966, Csaba Horváth and his student at Yale University developed a high-pressure liquid chromatographic system using small-particle packing materials and a pump capable of operating at up to 4,000 psi, to achieve the ion-exchange separation of organic compound[76]. This system[77], later developed into what became known as the LCS-1000 prototype with, represented a critical milestone in the evolution of modern high-performance liquid chromatography (HPLC).

1968, Waster Associates released the first commercially available HPLC instrument, ALC-100. Further advancement followed, with the introduction of 6,000-psi system in 1972, along with innovations such as septumless injectors. These developments shifted the emphasis from "high pressure" to "high performance." Over the subsequent decades, improvements in instrumentation, column technologies, and flow control significantly enhanced resolution and speed. In the early twenty-first century, systems capable of operating at ultra-high pressures (15,000–20,000 psi) and the corresponding column were introduced.

Meanwhile, progress was also made in instrumental configurations, such as the development of two-dimensional and multidimensional HPLC platforms. Today, HPLC continues to be a fundamental analytical technique across scientific disciplines and remains a field of ongoing technological refinement.

HPLC is one of the most powerful and versatile analytical platforms in modern chemistry. Through the coordinated use of variable mobile phases and chemically diverse stationary phases—under different column configurations such as length, inner diameter, and particle size—HPLC enables the separation, identification, and quantification of compounds via multiple chromatographic mechanisms, including partition chromatography and affinity chromatography. With the integration of

advanced detection systems—such as ultraviolet-visible (UV-Vis) detectors and mass spectrometry (MS)—HPLC provides high sensitivity, resolution, reproducibility, and robustness. These attributes have made HPLC widely applicable across biological, pharmaceutical, food and beverage, environmental, and other domains.

1.4.3 Stationary Phase in HPLC Column

Separation in HPLC results from complex interactions. Factors such as column length, inner diameter, particle size, and various other conditions can influence separation performance. Among these, the stationary phase is one of several critical components contributing to chromatographic separation. Based on the interaction mechanisms between analytes and the stationary phase, HPLC columns are generally categorized into five types: adsorption chromatography, partition chromatography, ion-exchange chromatography, size-exclusion chromatography, and affinity chromatography.

Adsorption Chromatography

This separation technique is the earliest form of chromatographic separation by Tswett. It relies on the interaction between analytes (adsorbates) and the surface of solid stationary phase (adsorbent). As the mobile phase carries the sample through the column, compounds with stronger adsorption to stationary phase elute more slowly, resulting in longer retention times. This mechanism is employed in techniques such as thin-layer chromatography (TLC), activated carbon-based separations, and normal-phase liquid chromatography. In normal-phase chromatography—a subtype of column chromatography—highly polar stationary phases, such as silica or alumina, are used to separate analytes based on polarity, placing it under the category of adsorption chromatography.

Partition Chromatography

This technique operates through a liquid–liquid partitioning mechanism. A thin film of liquid stationary phase is coated onto a solid support, such as silica, allowing solutes to distribute between this stationary liquid and the flowing mobile phase. Reverse-phase chromatography, the most prominent application of partition chromatography, separates compounds based on their differing solubilities in the polar mobile phase and the nonpolar stationary phase. The more hydrophobic compounds tend to remain in the stationary phase longer, while more polar compounds elute more quickly with the mobile phase.

Ion-Exchange Chromatography

This method achieves separation by using ion-exchange resins as the stationary phase—developed in the mid-1930s—along with an aqueous buffer as the mobile phase. This technique laid the theoretical groundwork for the successful separation and detection of amino acids and other ionic compounds in complex matrices following World War II. Separation occurs through the differential affinities of ionic compounds toward the oppositely charged stationary phase. By the type of ionic groups present, this chromatography can be classified into cation exchange chromatography and anion exchange chromatography. Both forms are commonly employed in HPLC systems and have broad applications in fields.

Size-Exclusion Chromatography

Size-exclusion chromatography (SEC), or gel chromatography, is a powerful technique for separating substances by molecular size. The stationary phase typically consists of small silica (~10 μm) or polymer particles that form a uniform porous network, allowing solutes and solvents to flow through during separation. The separation is driven by size exclusion: large molecules are too big to enter the pores, causing them to pass through the column quickly and elute first, while small

molecules enter the pores and take a longer path, leading to later elution. What makes this method unique is the separation depends purely on size differences, without any chemical or electrostatic interactions between the analytes and the stationary phase.

Affinity Chromatography

This chromatographic method utilizes specific interactions to separate target analytes, facilitated by an affinity ligand covalently bonded to a solid support. As the mixture passes through the column, analytes with specific binding affinity are retained by the immobilized ligand — such as antibodies, enzyme inhibitors, or other recognition molecules — while non-specific compounds, including matrix interferences, are washed away with the mobile phase. After the undesired substances are removed, the bound analytes are eluted by changing the buffer conditions, completing their isolation and purification[78, 79].

1.4.4 Amino Acid Separation Mechanism in This Study

Previous literature has reported various HPLC approaches for amino acid separation, including the use of C18 and HILIC columns. In this research, we utilized an amide column with a mobile phase containing ammonium formate (as a buffer salt) and formic acid (as an additive), under a tailored gradient. The separation is governed by three coexisting chromatographic mechanisms, with column efficiency interpreted by the Van Deemter equation.

Mechanism I: Partition Chromatography

The primary mechanism responsible for the separation of the fifteen amino acids is partition chromatography. This separation is driven by a carefully designed gradient and the distinct partition coefficients of individual analytes, which together facilitate their differential migration and resolution.

In a chromatographic system, the equilibrium between the analyte distributed in the stationary phases (*S*) and the mobile phase (*M*) can be described as:

$$A_S \rightleftharpoons A_M$$

The equilibrium constant (*K*), also referred to as the partition coefficient or distribution constant, is defined as:

$$K = \frac{(a_A)_S}{(a_A)_M} = \frac{\gamma_S \cdot c_S}{\gamma_M \cdot c_M}$$

where a_A represents the activity of analyte *A*, γ_S and γ_M are the activity coefficients in the stationary and mobile phases, respectively, and c_S and c_M are the corresponding molar concentrations.

Since activity coefficients are often difficult to determine, and ionic strength in this system is well controlled through the addition of ammonium formate, it is reasonable to assume ideal behavior and approximate activity coefficients as unity. This simplifies the equation to:

$$K = \frac{c_S}{c_M}$$

In biphasic systems, the partition coefficient (*P*) is typically defined as the ratio of the analyte's concentration in the organic phase to that in the aqueous phase:

$$P = \frac{c_{Organic\ phase}}{c_{Aqueous\ phase}}$$

and more conveniently expressed as:

$$\log P = \log\left(\frac{c_{Organic\ phase}}{c_{Aqueous\ phase}}\right)$$

Based on these partitioning principles, the applied gradient was designed to achieve effective separation under partition chromatography conditions.

Mechanism II: Adsorption Chromatography

The second mechanism in this developed method is adsorption chromatography, which is associated with the amide-functionalized stationary phase. Unlike

conventional bare silica or reversed-phase columns, the amide column exhibits mixed-mode behavior, incorporating not only partitioning but also adsorption interactions—such as dipole-dipole interactions and hydrogen bonding—between analytes and the amide groups on the stationary phase surface. These interactions contribute to additional retention, particularly for highly polar amino acids. As the gradient increases the polarity of the mobile phase, these interactions are gradually weakened, leading to analyte elution.

Figure 8. Structure of the Amide-Bonded Stationary Phase.

Mechanism III: Ion-Exchange-Like Interaction

Ion-exchange-like interaction represents the third chromatographic mechanism involved in this approach. As the stationary phase lacks dedicated ionic functional groups, this mechanism does not fully align with the classical definition of ion-exchange chromatography. However, pH adjustment using formic acid may create an environment that mimics ion-exchange behavior. Under acidic conditions (pH 3.1), amino acids predominantly exist in their cationic forms (refer to the pK values in Table 1). Although the amide-functionalized stationary phase is not formally charged, weak electrostatic interactions may occur between the positively charged analytes and residual polar sites—such as polar functionalities on the bridged ethylene hybrid (BEH) particle surface. These interactions may slightly affect retention behavior, particularly for amino acids bearing polar or aromatic side chains.

Van Deemter Equation

These three retention mechanisms can be further interpreted through a unified physical model of separation efficiency, described by the Van Deemter equation:

$$H = A + \frac{B}{u} + (C_S + C_M) \cdot u$$

where H represents the height equivalent to a theoretical plate (HETP, in centimeters), and u is the linear velocity of mobile phase (cm/s), calculated from the flow rate. The term A (eddy diffusion) reflects the multiple flow paths that different that different analytes can traverse depending on the characteristics of the packing structure, is primarily affected by particle size, particle geometry, and the overall packing characteristics of the column. The term B is the longitudinal diffusion coefficient, influenced by analyte diffusivity. The terms C_S and C_M represent the mass transfer coefficient in the stationary and mobile phase, respectively, and are dependent on both analyte properties. These terms explain the physical contribution to band broadening during chromatographic separation[79].

Table 1. Physical Property of Fifteen Amino Acids

Amino acid	Structure	Mass Weight (g/mol)	Log P [a]	pK_1 (COOH)	pK_2 (NH_2)	pK_3 (side chain)	pI [b]
Glycine	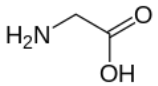	75.07	-3.21	2.34	9.60	-	5.97
Alanine	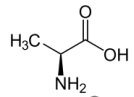	89.09	-2.85	2.34	9.69	-	6.00
Serine	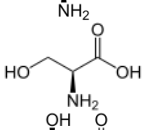	105.09	-3.07	2.21	9.15	-	5.68
Threonine	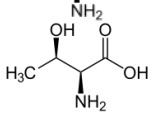	119.12	-2.94	2.09	9.10	-	5.60
Valine	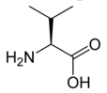	117.15	-2.26	2.32	9.62	-	5.96
Methionine	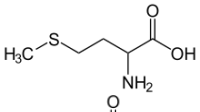	149.21	-1.87	2.28	9.21	-	5.74
Proline	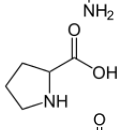	115.13	-2.54	1.99	10.60	-	6.30
Phenylalanine	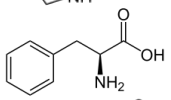	165.19	-1.38	1.83	9.13	-	5.48
Tyrosine	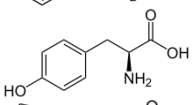	181.19	-2.26	2.20	9.11	-	5.66
Tryptophan	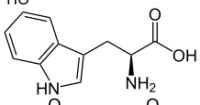	204.22	-1.06	2.38	9.39	-	5.89
Glutamine	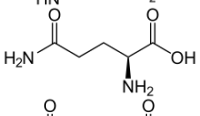	146.14	-3.64	2.17	9.13	-	5.65
Glutamic acid	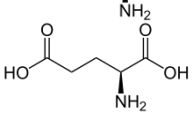	147.13	-3.69	2.19	9.67	4.25	3.22
Histidine	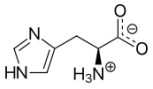	155.15	-3.32	1.82	9.17	6.00	7.59
Lysine	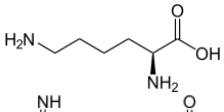	146.19	-3.05	2.18	8.95	10.53	9.74
Arginine	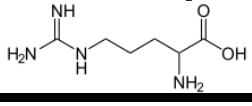	174.2	-4.2	2.17	9.04	12.48	10.76

[a] Partition coefficient (*P*). [b] Isoelectric point (pI)

1.5 Mass Spectrometry

1.5.1 Mass Spectrometry

Mass spectrometry is a powerful analytical technique known for its exceptional sensitivity, specificity, selectivity, rapid analysis capability, and broad applicability in qualitative and quantitative analysis across diverse analytes. The versatility of this technique is further enhanced by adjustable instrumental components, such as ion sources, mass analyzers, and detectors.

he original concepts of 'cathode', 'anode', and 'ion' were introduced in his 1894 publication, *Experimental Researches in Electricity*, by Joseph John Thomson.[80] J. J. Thomson discovered the electron and defined its mass-to-charge ratio (m/z) in 1897, building on his earlier work published in 1894, and earning him the 1906 Nobel Prize in Physics. In 1913, J. J. Thomson, who received the Nobel Prize in Physics, built the first parabola mass spectrograph to separate isotopes, such as neon-20 and neon-22, as described in his book *Rays of Positive Electricity and Their Application to Chemical Analysis*. This work established the relationship between isotopic abundances and atomic weights, indirectly supporting quantitative mass spectrometry. Building upon Thomson's work, Francis William Aston developed the first 'mass spectrograph', employing gas discharge tubes under parallel electric and magnetic fields and photographic detection of ions. This method is now recognized as electron ionization (EI). These achievements earned Aston the 1922 Nobel Prize in Chemistry.[81] Based on the preparation of previous generations, Josef Mattauch and Richard Herzog developed the double-focusing mass spectrograph in 1934. This instrument separated the isotope by using the 31.82° electric sector and 90° magnetic sector to achieve the separation and focus multiple ions in one plate.[82] In the 1940s, Alfred Nier designed a simplified 60° sector field mass spectrometer, featuring a smaller size and reduced

magnetic power consumption, which improved resolution and sensitivity. Its straightforward design and high resolution made it widely applicable for uranium isotope separation (U^{235} and U^{238}) during World War II. In 1953, Nier collaborated with Edward Joseph Johnson and built the Nier-Johnson mass spectrometer by combining electrostatic and magnetic analyzers in a unique configuration. Due to the refinements to the 90° electric sector and 60° magnetic sector design, this instrument achieved the highest mass resolution of its time. In the same year, Wolfgang Paul and Helmut Steinwedel invented the Quadrupole Mass Filter, which selected and filtered ions using radio frequency (RF) and direct current (DC) voltages. This research laid the foundation of modern routine LC-MS, such as triple quadrupole mass spectrometry, and its contribution won the 1989 Nobel Prize in Physics.[83] In the same era, the concept of time-of-flight (TOF) mass spectrometry was first proposed by William E. Stephens in 1946 at the meeting of the American Physical Society.[84] This concept was initially demonstrated experimentally by Alastair Ewan Cameron and David F. Eggers, Jr. in 1948[85], and significantly improved by William C. Wiley and Iain H. McLaren in 1955[86].

In 1956, Dow Chemical first successfully coupled gas chromatography with mass spectrometry, laying the foundation for chromatography-mass spectrometry techniques. Chemical ionization (CI) was developed by Melvin Stephen Bruce Munson and Frank Henry Field in 1966[87]; electrospray ionization (ESI) was developed by Malcolm Dole and his group at Northwestern University in 1968[88]; atmospheric pressure chemical ionization (APCI) was developed by E. C. Horning and colleagues in 1973[89]. Each technique introduced distinct ionization methods, broadening the scope and applicability of mass spectrometry. Fourier Transform Ion Cyclotron Resonance Mass Spectrometry (FT-ICR MS) was developed by Melvin B. Comisarow and Alan G. Marshall in 1974 and commercialized by Bruker in 1982.

This advancement significantly improved the resolution and accuracy of mass spectrometry for analyzing complex mixtures and large molecules such as proteins, and remains widely used today.[90] In 1977, Richard A. Muller introduced isotope separation and dating analysis using accelerator mass spectrometry (AMS), publishing his results in *Science*. AMS remains widely employed for archaeological dating applications.[91] John Bennett Fenn significantly advanced biomolecular analysis using electrospray ionization (ESI), earning him the 2002 Nobel Prize in Chemistry. Additionally, Finnigan MAT introduced the first commercial ion-trap mass spectrometer in 1983. Matrix-assisted laser desorption/ionization (MALDI) was first introduced in 1985[92], with practical demonstration provided by Koichi Tanaka of Shimadzu Corporation in 1988[93], who later shared the 2002 Nobel Prize in Chemistry. In 1999, Alexander Makarov joined Thermo Fisher and led the development of the first high-resolution mass spectrometer without a magnetic field, launched commercially in 2005 as the Orbitrap. To date, innovative mass spectrometric techniques continue to emerge, ensuring its broad and evolving applications.[94-96]

As technology has advanced and analytical needs have diversified, mass spectrometry has evolved into various types with distinct configurations. A mass spectrometer typically consists of a sample inlet, ion source, mass analyzer, detector, and data system.

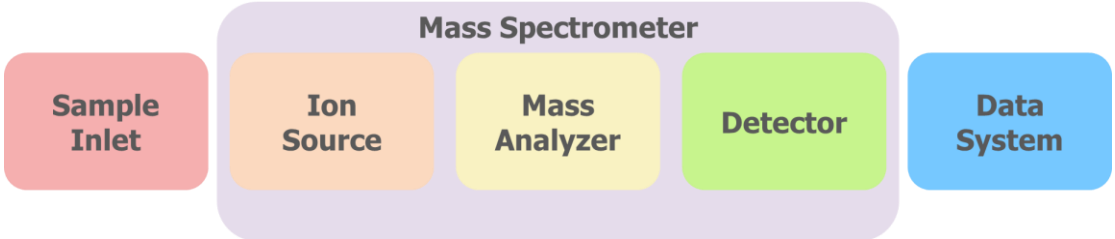

Figure 9. Schematic Diagram of a Mass Spectrometry System.

The sample inlet is the component that introduces the sample into the mass spectrometer. Direct introduction methods include flow injection analysis (FIA), whereas indirect methods involve coupling with platforms such as liquid chromatography (LC) and gas chromatography (GC). The ion source ionizes the sample and removes neutral species, transmitting only ions into the mass analyzer. Ionization methods vary in principle and application, including electronic ionization (EI, 1918), chemical ionization (CI, 1966), electrospray ionization (ESI, 1968/1984), atmospheric pressure chemical ionization (APCI, 1973), fast atom bombardment (FAB, 1974), inductively coupled plasma (ICP, 1980), matrix-assisted laser desorption/ionization (MALDI, 1985), surface enhanced laser desorption/ionization (SELDI, 1993), surface assisted laser desorption/ionization (SALDI, 1995-1999), atmospheric pressure photoionization (APPI, 1999), desorption/ionization on silicon (DIOS, 1999), desorption electrospray ionization (DESI, 2004), and direct analysis in real time (DART, 2005). Mass analyzers are components that separate, filter, and select ions based on their mass-to-charge ratio (m/z), kinetic energy, or spatial behavior under optimized electric or magnetic fields. Its type include double-focusing electrostatic and magnetic sector instruments (1934), time-of-flight (TOF, 1946) analyzers, quadrupole mass filters (Q, 1953), ion cyclotron resonance (ICR, 1974) instruments, accelerator mass spectrometers (AMS, 1977), quadrupole ion traps (IT, 1983), and Orbitrap analyzers (1999). Regardless of the type of mass analyzer used, ions are eventually directed to the detector, which captures and converts their signals for analysis. Detectors include Faraday cup detectors (1830), electron multipliers (EM, 1930), photomultiplier tubes (PMT, 1930/1936), microchannel plates (MCP, 1959), and image current detectors (1974). Once the signal is captured by the detector, data acquisition software processes and displays the analytical results.

Experiments were conducted using an API 4000^{TM} (Figure 10). This instrument features APCI/ESI ion sources, a triple quadrupole mass analyzer, and an MCP detector. In the following sections, we describe the components and operating principles of this instrument in greater detail.

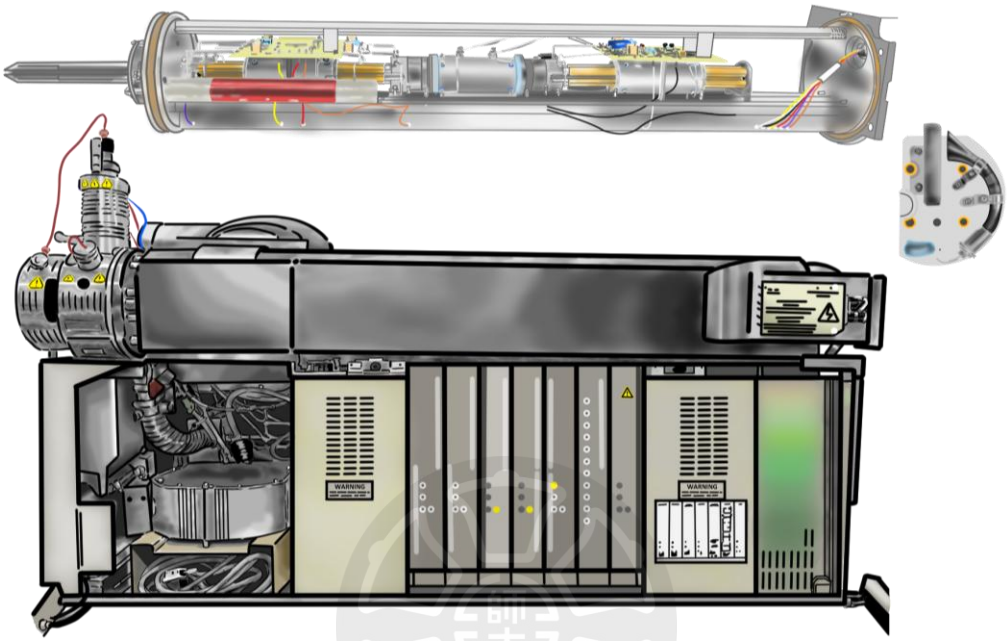

Figure 10. Internal Architecture of API 4000^{TM}, illustrating its Ion Source, Triple Quadrupole Mass Analyzer, and MCP Detector.

1.5.2 Electrospray Ionization

The earliest development of electrospray ionization (ESI) was pioneered by Malcolm Dole and his group in 1968. In their study, the samples (macroions) were injected directly in liquid form for electrospray ionization, utilizing a high potential difference to ionize and primarily relying on inertia to deliver analyte ions to the Faraday cage for detection.[88] Although this study focused on the ionization of macroions and employed a simple construction that resulted in poor resolution—thus receiving limited attention at the time—it nevertheless laid the foundational framework for the future development of mass spectrometry for large molecules.

Building upon Dole's pioneering research and leveraging subsequent technological advancements, Fenn and his team optimized the conditions for ESI, including capillary size, electrospray voltage, and related parameters. The improved ESI source was integrated with a single quadrupole mass analyzer, enabling the selective transmission of analyte ions by adjusting voltage settings to remove background ions and suppress chemical noise. Protein samples were subsequently analyzed to demonstrate the practical applicability of this technique. The results clearly established that ESI could generate multiply charged ions from large biomolecules, thereby facilitating their detection within the limited m/z range of conventional mass analyzers. These innovations substantially enhanced the utility of ESI in biological analysis, expanding its use across proteomics, metabolomics, and pharmaceutical research. This breakthrough ultimately led to John B. Fenn being awarded the Nobel Prize in Chemistry in 2002.

Upon sample introduction into the mass spectrometer, the electrospray ionization (ESI) source plays a crucial role in converting analytes into gas-phase ions. In positive ion mode, the sample solution is continuously delivered through a steel capillary, to which a high positive voltage (often 3-6 kV) is applied. Assisted by coaxial nebulizer gas and thermal energy, the liquid emerging from the tip forms a Taylor cone and breaks into charged droplets. These droplets undergo desolvation through solvent evaporation and are subsequently subjected to Coulomb repulsion, eventually leading to Coulomb explosion when the repulsive force surpasses surface tension. This process, known as the ion evaporation model, effectively liberates analyte ions into the gas phase.

The resulting multiply charged ions significantly extend the detectable mass range of biomolecules, allowing even large molecules to fall within the low m/z detection window of conventional mass analyzers. Additionally, the presence of

multiple charges enhances ion transmission efficiency and fragmentation performance in tandem MS analysis.

Following ionization, the gaseous ions are directed into the mass spectrometer's interface region and enter the mass analyzer. In this study, the ESI source was coupled to a triple quadrupole mass analyzer. The fundamental operation and advantages of this tandem mass analyzer are described in the next section.

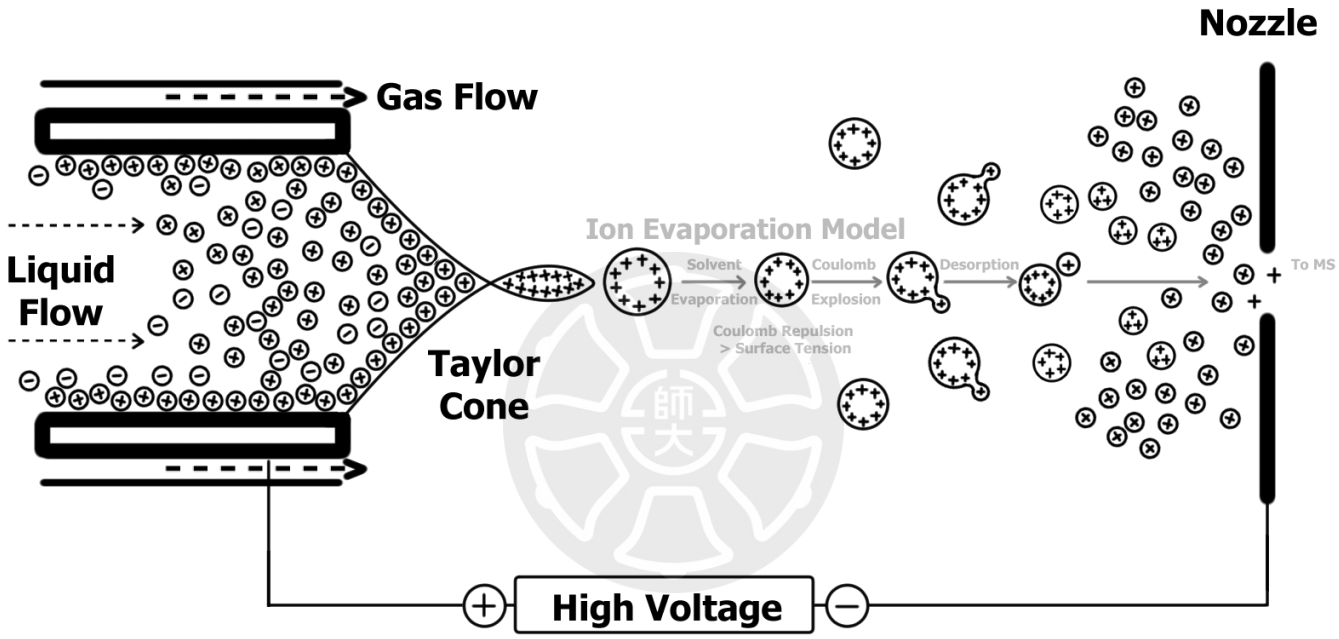

Figure 11. Electrospray Ionization via the Ion Evaporation Model

1.5.3 Triple Quadrupole Tandem Mass Spectrometer

Triple quadrupole tandem mass spectrometer (TQMS) represents one of the most widely used analytical platforms for targeted quantitative analysis. Introduced in the late 1970s, TQMS systems are composed of three quadrupole units arranged in series: the first (Q1) and third (Q3) quadrupoles act as mass filters, while the second (Q2) serves as a collision cell that facilitates fragmentation of selected precursor ions via collision-induced dissociation (CID).

In a typical tandem MS workflow, ions generated from the ion source (e.g., ESI) are directed into Q1, where precursor ions of interest are selected based on their mass-to-charge ratio (m/z). These selected ions are then fragmented in Q2 through collisions with an inert gas, such as nitrogen. The resulting product ions are subsequently analyzed in Q3, which can either scan over a range of m/z or be fixed to detect specific transitions. This configuration enables a variety of scan modes, including full scan, product ion scanning, and, most importantly, multiple reaction monitoring (MRM) (Figure 12).

MRM mode is particularly advantageous in quantitative analyses due to its superior selectivity and sensitivity. In this mode, both Q1 and Q3 are set to transmit predefined m/z values corresponding to a specific precursor-to-product ion transition. By excluding non-target ions at both stages, MRM significantly reduces background interference and enhances signal-to-noise ratios. This dual-filtering mechanism not only improves detection limits but also ensures reliable quantification, especially in complex matrices. As shown in Figure 12, each MRM transition is defined by fixed Q1 and Q3 values, allowing the mass spectrometer to monitor multiple analytes simultaneously by rapidly switching between different transition pairs.

Tailoring MRM transitions for target compounds is a major advantage of TQMS, making it widely used in bioanalysis, clinical diagnostics, food safety, and environmental monitoring. In this study, the triple quadrupole mass analyzer operated in MRM mode to quantify amino acids with high specificity and reproducibility.

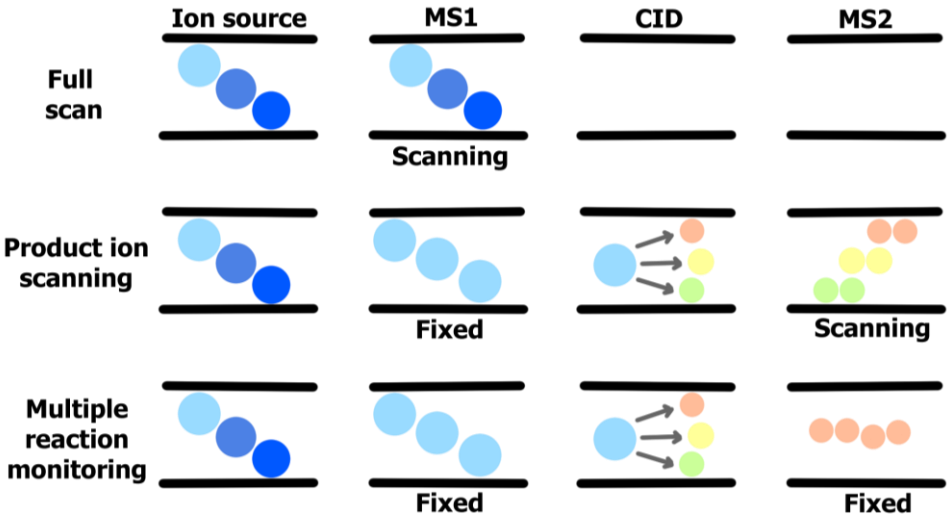

Figure 12. Scheme of scan modes of a triple quadrupole mass spectrometer.

1.6 Motivation

Amino acids are fundamental biomolecules essential for various physiological and environmental processes, including protein synthesis, metabolic regulation, and neurotransmitter function. Their accurate quantification is crucial in fields such as medical diagnostics, nutritional assessment, food quality control, and environmental monitoring, where imbalances can indicate disease states, nutritional deficiencies, or contamination in complex matrices like biofluids, coffee, or other food products. However, analyzing amino acids in real-world samples presents significant challenges due to their zwitterionic nature, high polarity, and lack of strong UV-absorbing chromophores, which complicate chromatographic retention and detection without chemical derivatization.

Traditional methods often rely on derivatization to enhance separation and sensitivity in techniques like HPLC-MS/MS, but these approaches introduce drawbacks, including prolonged preparation times, variable reaction efficiencies, poor reproducibility, and potential interference from multi-derivatives or unreacted reagents. For instance, common reagents like 9-fluorenylmethyl chloroformate (FMOC-Cl) or o-phthalaldehyde (OPA) require controlled conditions and can lead to incomplete reactions or toxicity concerns, particularly in complex matrices where ion suppression and matrix effects further hinder accuracy. Recent studies highlight these issues, emphasizing the need for derivatization-free workflows to minimize preparation artifacts and improve throughput.

To address these limitations, this study explores a derivatization-free approach using a Cu-based metal-organic framework (Cu-PyC MOF) in dispersive solid-phase extraction (dSPE) coupled with HPLC-MS/MS for amino acid analysis. Cu-PyC MOF, known for its oxidoreductase-like catalytic activity and high selectivity, enables efficient extraction and cleanup of amino acids from complex matrices by leveraging its porous structure and functional groups for targeted adsorption, while reducing solvent use and adhering to green analytical principles. Recent advancements in MOF-based dSPE, such as amino-functionalized UiO-66-NH2 for enhanced extraction of analytes in aqueous samples, demonstrate improved sensitivity and selectivity compared to conventional methods. By integrating this with HPLC-MS/MS, the proposed workflow aims to achieve rapid, reproducible quantification with minimal interference, offering a promising solution for routine analysis in food and biological samples.

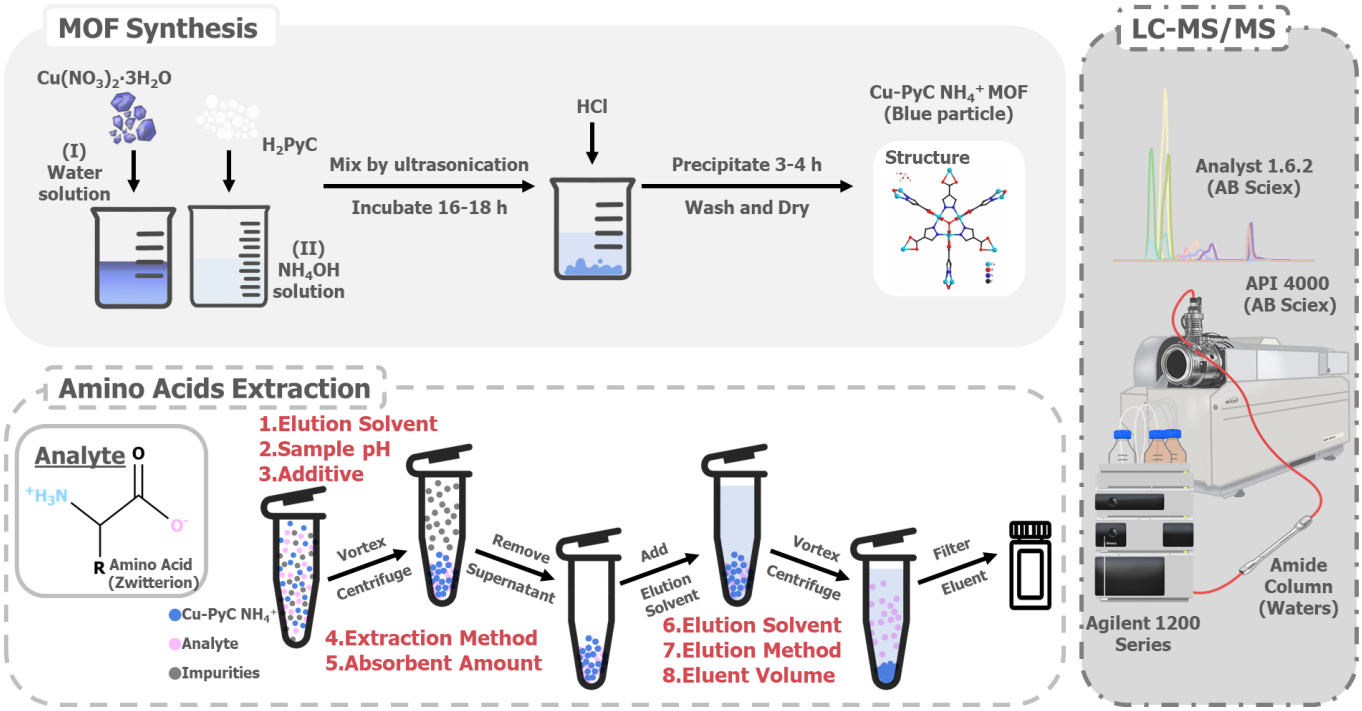

Figure 13. Schematic illustration of the overall workflow for amino acid analysis using Cu-PyC NH_4^+ MOF-based dSPE and LC-MS/MS.

Chapter 2 Experimental Section

2.1 Materials and Reagents

All fifteen amino acid standards including glycine (Gly), L-alanine (Ala), L-serine (Ser), L-threonine (Thr), L-valine (Val), L-methionine (Met), L-proline (Pro), L-phenylalanine (Phe), L-tyrosine (Tyr), L-tryptophan (Trp), L-glutamine (Gln), L-glutamic acid (Glu), L-histidine (His), L-lysine (Lys), and L-arginine (Arg) were purchased from Sigma-Aldrich (St. Louis, MO, USA).

1H-pyrazole-4-carboxylic acid (98%) was purchased from Combi-Blocks (San Diego, CA, USA). Cupric nitrate trihydrate (99.0–104%) and ammonium formate (97%) were purchased from Sigma-Aldrich (St. Louis, MO, USA).

HPLC-grade acetonitrile (ACN) and methanol (MeOH) were obtained from Merck (Darmstadt, Germany). Ultra-pure water was purified using a Milli-Q® Direct 3 system (Merck Millipore, Darmstadt, Germany). ACS reagent-grade ethanol (EtOH), hydrochloric acid (HCl, 36.5–38%), sodium hydroxide (NaOH, 98.2%), and formic acid (FA, 100%) were purchased from J.T. Baker (Avantor Performance Materials, Center Valley, PA, USA). ACS reagent-grade acetic acid (AA, 100%) and ammonium hydroxide (NH_4OH, 28–30%) were obtained from Honeywell Fluka (Charlotte, NC, USA). L-lactic acid (85.0-92.0%) was purchased from FUJIFILM Wako Pure Chemical Corporation (Osaka, Japan).

2.2 Apparatus

Several analytical techniques were used to characterize the synthesized materials. Powder X-ray diffraction (PXRD) was performed using a Bruker D8 Advance Eco diffractometer (Bruker, Karlsruhe, Germany) with Cu Kα radiation (λ = 1.54178 Å), operated at 40 kV and 40 mA at room temperature. The morphology and elemental composition of the samples were examined using a JEOL JSM-6500F field-emission scanning electron microscope (FE-SEM; JEOL Ltd., Tokyo, Japan), equipped with an energy-dispersive X-ray spectroscopy system (EDS; Oxford Instruments, Abingdon, UK). Functional groups and coordination environments were characterized by attenuated total reflectance Fourier-transform infrared spectroscopy (ATR-FTIR), using INVENIO® FT-IR Spectrometers (Bruker, Billerica, MA, USA). Nitrogen adsorption–desorption isotherms were measured at 77 K using a Micromeritics 3Flex physisorption analyzer (Micromeritics Instrument Corporation, Norcross, GA, USA) to determine the Brunauer–Emmett–Teller (BET) surface area and pore size distribution. Prior to measurements, the samples were degassed under vacuum at 120 °C to remove residual guest molecules and solvents. Micropore volume and pore size distributions were estimated from the adsorption isotherms using the non-local density functional theory (NLDFT) model.

2.3 Method

2.3.1 Cu-PyC NH_4^+ MOF Synthesis

The Cu-PyC NH_4^+ MOF was synthesized via a modified aqueous procedure based on previous reports.[70, 71] Briefly, 1120.0 mg of 1H-pyrazole-4-carboxylic acid (H_2PyC) was dissolved in 50.0 mL deionized water with 6.5 mL ammonium hydroxide solution (25% w/w NH_3) in a 150.0 mL Pyrex bottle. Separately, 2410.0 mg of $Cu(NO_3)_2 \cdot 3H_2O$ was dissolved in 20.0 mL deionized water in a 100.0 mL Pyrex bottle. Both solutions were sonicated until fully dissolved. The copper(II) solution was then added to the ligand solution under gentle shaking, forming a homogeneous blue mixture. The reaction was allowed to proceed at room temperature for 16-18 hours. Subsequently, 5.0 mL of concentrated HCl (36.5-38.0%) was added dropwise, promoting precipitation of the product over 3-4 hours. The resulting blue solid was collected by centrifugation, washed three times with deionized water and ethanol, and dried at 75 °C for 24 hours. The obtained Cu-PyC NH_4^+ MOF was stored for further characterization and application.

2.3.2 Sample Preparation using Cu-PyC NH_4^+ MOF

A standard solution mixture containing 15 amino acids was prepared, with each individual amino acid at a concentration of 1.0 μg/mL. To achieve this, stock solutions of each amino acid were first prepared: 1.0 mg of each standard was dissolved in 1.0 mL of pure water (except for tyrosine, which was dissolved in 0.1 M hydrochloric acid due to its low solubility in water). These stock solutions (1.0 mg/mL) were then appropriately diluted and mixed to yield a 50.0 μg/mL mixed standard solution, which was further diluted to 10.0 μg/mL. Subsequently, 100.0 μL of the 10.0 μg/mL mixed standard solution was added to the extraction solution (700.0 μL ethanol, 200.0 μL

water, and 0.5 μL formic acid) in a centrifuge tube containing 50 mg of Cu-PyC NH_4^+ MOF adsorbent. The mixture was vortex-mixed for 10 minutes to ensure homogeneous adsorption, followed by centrifugation at 15,000 rpm and 4°C for 5 minutes. After discarding the supernatant, 1,200.0 μL of 1% hydrochloric acid was added for elution, followed by another 10-minute vortex-mixing step. The eluate was obtained by centrifugation at 15,000 rpm and 4°C for 5 minutes, filtered through a 0.22 μm hydrophilic PTFE filter to remove particulates, and diluted fivefold with deionized water prior to LC-MS/MS analysis.

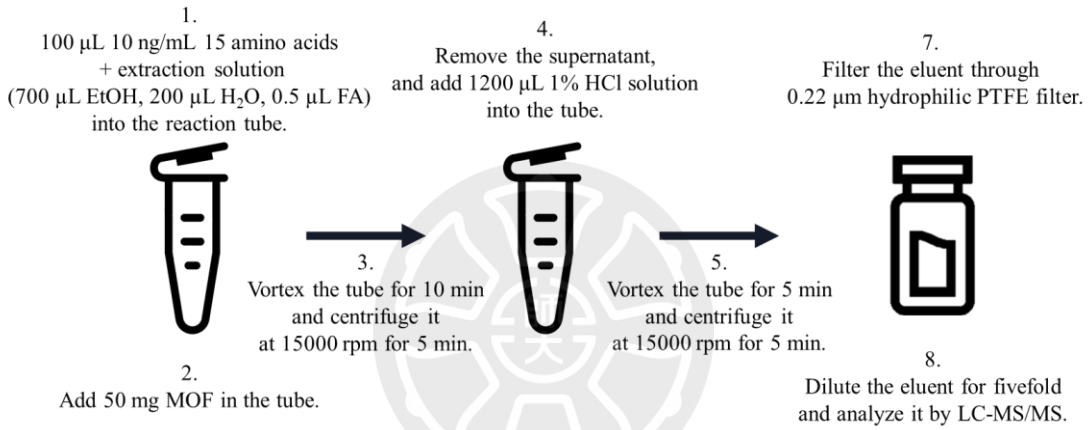

Figure 14. Scheme of sample preparation protocol

2.3.3 Sample Preparation in Instant Coffee

Instant coffee powder (10 mg) was dissolved in 10 mL of pure water and diluted tenfold (to a final volume of 100 mL). A 100 μL aliquot of this diluted coffee solution was transferred to the extraction solution (700 μL ethanol, 200 μL water, and 0.5 μL formic acid) in a centrifuge tube containing 50 mg of Cu-PyC NH_4^+ MOF adsorbent. The mixture was vortex-mixed for 10 minutes to facilitate adsorption, followed by centrifugation at 15,000 rpm and 4°C for 5 minutes. After discarding the supernatant, 1,200 μL of 1% hydrochloric acid was added to desorb the analytes. The mixture was vortex-mixed again for 10 minutes and centrifuged at 15,000 rpm and 4°C for another

5 minutes. The resulting eluate was filtered through a 0.22 μm hydrophilic PTFE filter, diluted fivefold with deionized water, and analyzed by LC-MS/MS. For quantification, a 100 ng/mL amino acid standard solution was spiked into the final diluted eluate.

2.3.4 HPLC-MS/MS System Condition

The chromatographic analysis of amino acid were performed an Agilent 1200 HPLC System (Agilent, USA) coupled with a binary pump, a vacuum degasser, an autosampler. The separation was achieved on an XBridge^{TM} Premier BEH Amide column (2.1 × 100 mm, 2.5 μm, 130 Å, Waters, USA) at a flow rate of 0.2 mL/min and a column temperature of 40°C. The mobile phases were 1 mM ammonium formate in H_2O/ACN (90/10, v/v) (A) and 1 mM ammonium formate in H_2O/ACN (10/90, v/v) (B), both adjusted to pH 3.1 with formic acid. The chromatographic separation was conducted for 15 min with the following gradient: 0-1.5 min, 86% B; 1.5-7.0 min, 86% to 30% B; 7.0-9.0 min, 30% B; 9.0-9.1 min, 30% to 86% B; 9.1-15.0 min, 86% B. The injection volume was 5 μL.

MS was performed on an API 4000^{TM} (AB Sciex, Canada) with Turbo V^{TM} ion source equipped with electrospray ionization (ESI) in positive ion mode. The ionization voltage was set to 5500 V while the source temperature was set to 400°C. Other MS parameters were as follows: collision gas (N_2), 4 psi; curtain gas (N_2), 20 psi; gas 1 (nebulizer gas), 30 psi; gas 2 (heating gas), 30 psi. The scan type was multiple reaction monitoring (MRM) mode and the analyte parameters are shown in Table 2.

Data acquisition used Analyst software version 1.6.2 (AB Sciex, Canada).

2.4 Method Validation

The developed method was validated based on linearity, sensitivity (limits of detection, LOD; limits of quantification, LOQ), accuracy, precision (intra-day and inter-day), and matrix effect. Quantitative analysis of amino acids was performed using an external standard method.

Linearity was evaluated using calibration curves obtained weighted (1/x) linear regression of peak area versus analyte concentration. Calibration curves for 14 amino acids were constructed at eight concentration level (10, 20, 50, 100, 200, 500, 1000, 2000 ng/mL), while glycine was calibrated at six points (50, 100, 200, 500, 1000, 2000 ng/mL), each analyzed in triplicate. Sensitivity was determined by the LOD and LOQ, defined by signal-to-noise (S/N) ratios of 3 and 10, respectively.

Accuracy was evaluated by spiking amino acid standards into real sample matrices at three levels (100 and 1000 ng/mL), each analyzed in triplicate. Accuracy was expressed as recovery (%), calculated using the following equation:

$$Recovery\ (\%) = \frac{Mass_{spiked} - Mass_{non-spiked}}{Mass_{theoretical\ spiked}} \times 100$$

Precision was assessed as repeatability (intra-day, n = 3) and intermediate precision (inter-day, n = 3), and expressed as relative standard deviation (RSD, %):

$$RSD(\%) = \left(\frac{S}{\bar{x}}\right) \times 100$$

Where S is the standard deviation and $\bar{x}$ is the mean.

Chapter 3 Results and Discussion

3.1 HPLC-MS/MS Condition

3.1.1 Mass Spectrometry Method Development

Initially, we detected 15 amino acids using the full scan mode in both positive and negative ion modes, allowing observation of amino group fragmentation in positive ion mode and carboxyl group fragmentation in negative ion mode. As shown by the results, all amino acids exhibited higher intensity in positive ion mode compared to negative ion mode. Thus, the positive ion mode was selected for further optimization of detection conditions. For enhanced MS/MS detection of analytes, a 500 ng/mL single amino acid standard solution was injected into the instrument. We chose at least one pair of precursor and product ion with highest intensity for each amino acid. Afterwards, we conducted detailed optimization of MRM parameters, including declustering potential (DP), entrance Potential (EP), collision energy potential (CE), and collision cell exit potential (CXP), to maximize analyte intensity.

The optimized MRM parameters are presented in Table 2. It can be observed that during collision-induced dissociation, the majority of amino acids exhibit cleavage of the carboxyl group and the α-amino group, corresponding to the $[M+H-46]^+$ or $[M+H-17]^+$ fragment ions. As a result, these ions demonstrated significant intensities and served as the principal fragments for amino acid fragmentation, consistent with findings reported in previous studies[97, 98]. We will apply the optimized conditions for the ensuing experiments.

Table 2. Optimized MS Parameters of Fifteen Amino Acids

Amino acid	Structure	Retention time (min)	Precursor ion (m/z)	Product ion (m/z)	DP [a] (V)	EP [b] (V)	CE [c] (V)	CXP [d] (V)
Glycine	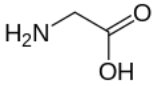	5.76	76	30	50	10	22	4
Alanine	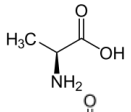	4.94	90	44	51	11	16	1
Serine	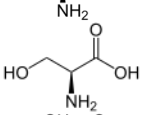	6.93	106	60 70	22	5	18 17	2 5
Threonine	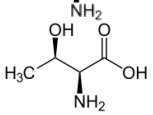	5.54	120	74 56	44	11	14 24	5 2
Valine	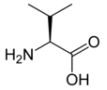	3.59	118	72 55	43	5	15 30	5 9
Methionine	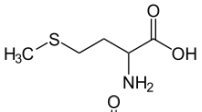	3.17	150	61 56	43	10	31 25	2 2
Proline	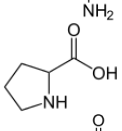	3.80	116	70 75	28	5	22 7	5 5
Phenylalanine	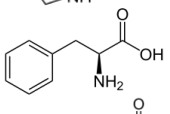	2.60	166	120 131	46	15	16 17	10 10
Tyrosine	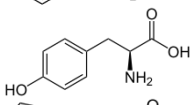	3.55	182	136 123	44	10	17 23	10 9
Tryptophan	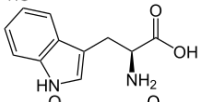	2.56	205	146 188	50	11	24 14	12 15
Glutamine	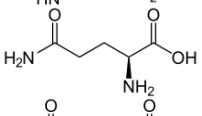	6.77	147	84 130	35	10	24 13	5 10
Glutamic acid	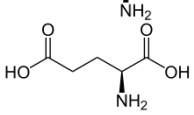	5.65	148	84 102	40	10	22 15	6 8
Histidine	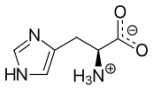	9.67	156	110 95	50	8	19 24	19 4
Lysine	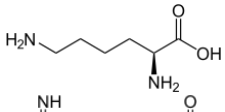	9.75	147	84 130	40	10	24 13	6 22
Arginine	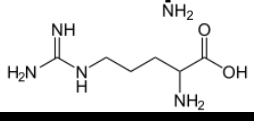	9.59	175	70 116	70	4	32 19	11 5

[a] Declustering potential. [b] Entrance potential. [c] Collision energy potential. [d] Collision cell exit potential

3.1.2 Liquid Chromatography Method Development

To determine optimal conditions for amino acid separation, a 100 ng/mL amino acid standard mixture was injected into three columns under consistent chromatographic conditions: Kinetex® EVO C18 column (2.1 × 100 mm, 2.6 μm, 100 Å, Phenomenex), the Kinetex® F5 Core-Shell column (2.1 × 100 mm, 2.6 μm, 100 Å, Phenomenex), and the XBridge™ Premier BEH Amide column (2.1 × 100 mm, 2.5 μm, 130 Å, Waters). The C18 and F5 columns failed to retain most amino acids. In contrast, the Amide column improved the separation of most amino acids.

To optimize the separation strategy, we referred to the literature[97] and chose to use ammonium formate and ammonium acetate to enhance peak shape. Our results showed that peak shape improved when both ammonium formate and ammonium acetate were present. Without these buffer salts, the retention time would become unstable. However, excess amounts of these buffer salts can cause ion suppression and increase the overall LOD and LOQ in amino acid detection, with ammonium acetate showing more severe effects than ammonium formate. Based on these results, we opted to apply 1 mM ammonium formate to optimize the experimental conditions.

The amount of formic acid used was informed by reference[99] to achieve better peak shape. Excessive addition of formic acid caused excessive retention of amino acids, leading to carryover. Consequently, we determined an optimal concentration of formic acid to adjust the mobile phase to pH 3.1, thereby refining our experimental conditions. The optimized retention times of the 15 amino acids are listed in Table 2, with representative chromatograms illustrated in Figure 15.

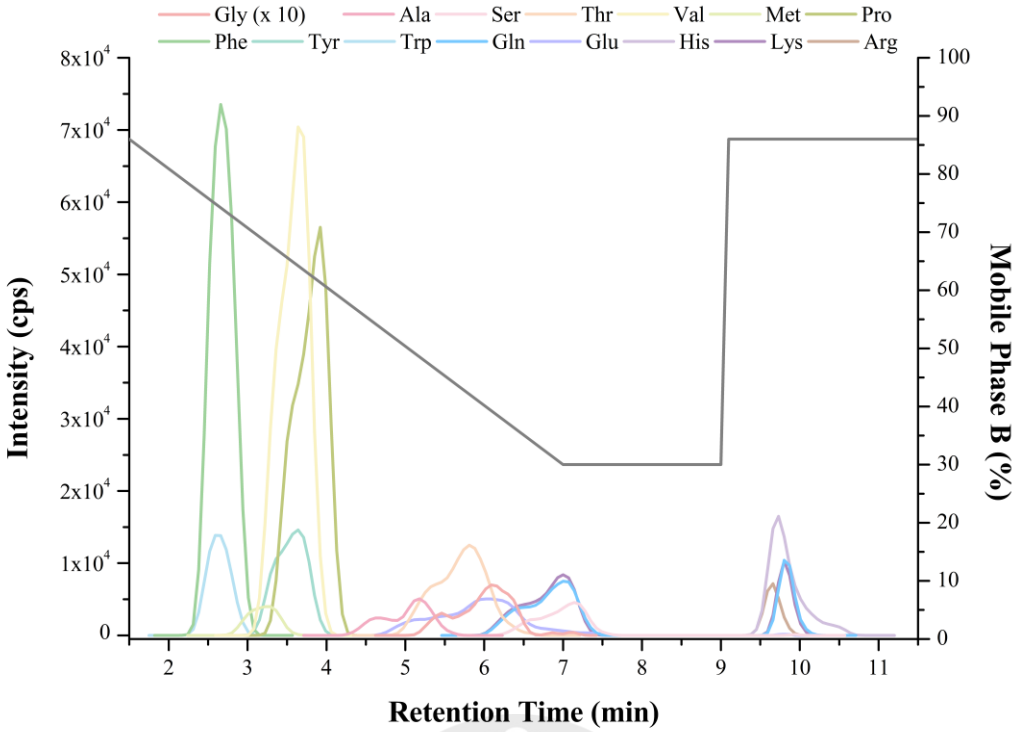

Figure 15. Representative LC-MS/MS Chromatograms of Fifteen Amino Acids under Optimized Conditions.

3.2 Characteristics of Cu-PyC NH_4^+ MOF

Following the optimized synthesis method based on previous literature[70, 71], $NH_4[Cu_3(\mu_3\text{-}OH)(\mu_3\text{-}4\text{-}PyC)_3]$ was successfully synthesized in a shotern reaction time and with increased yield efficiency.

3.2.1 Powder X-Ray Diffraction

The structural integrity and crystallinity of the synthesized MOF were confirmed by powder X-ray diffraction (PXRD). As shown in Figure 16, the obtained PXRD pattern exhibits characteristic diffraction peaks at 2θ values of 8.26° (220), 10.12° (222), 11.7° (400), 14.34° (422), and 17.58° (600), matching the standard simulated pattern (CCDC No. 767852). These PXRD results validate the successful synthesis of Cu-PyC NH_4^+ MOF with the correct and expected crystalline structure.

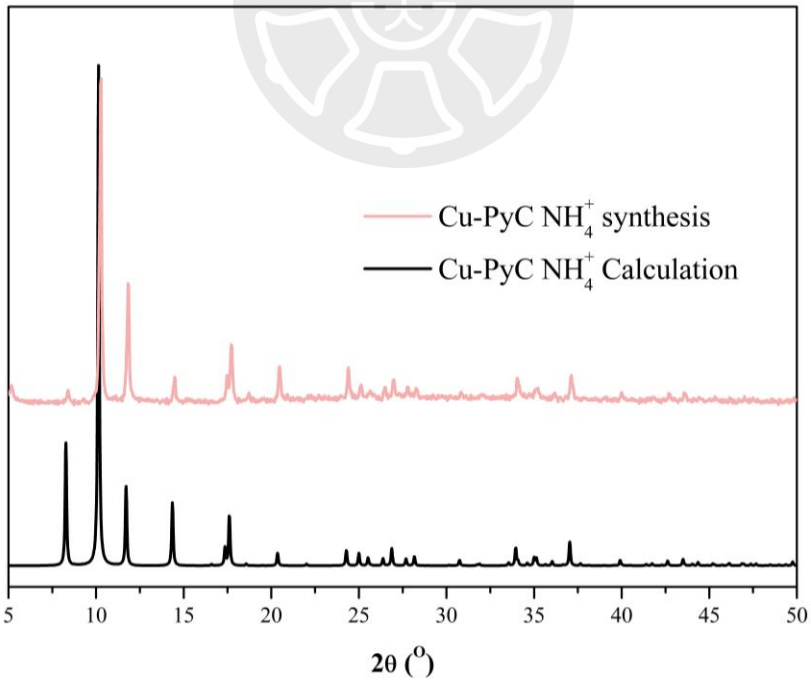

Figure 16. PXRD Pattern Comparison Between Synthesized Cu-PyC NH_4^+ MOF and The Calculated Structure.

3.2.2 Field Emission Scanning Electron Microscope

The morphology of the synthesized MOF nanoparticles was examined by field emission scanning electron microscopy (FESEM). Figure 17 illustrates the broad particle size distribution and distinct octahedral morphology observed at various magnifications. These observations further confirm the successful synthesis and structural integrity of the Cu-PyC NH_4^+ MOF.

(a) **(b)**

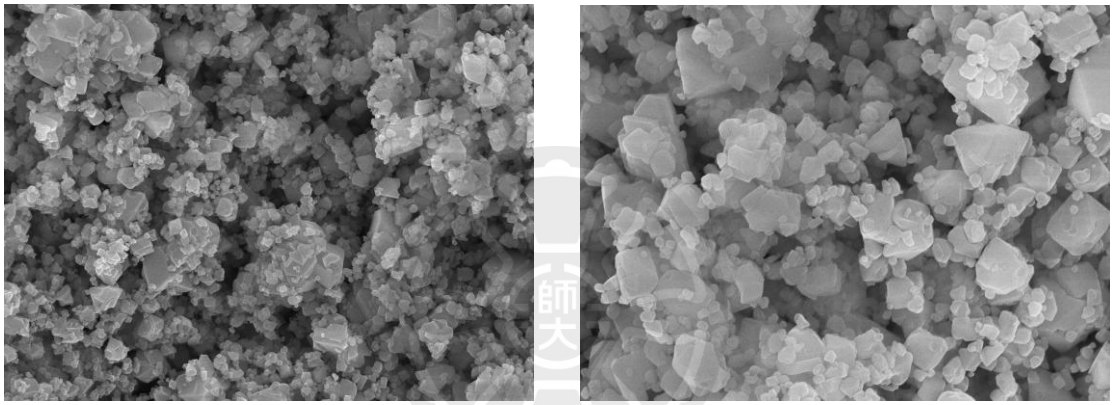

Figure 17. FESEM images of Cu-PyC NH_4^+ MOF at magnifications of (a) ×5,000, and (b) ×10,000.

Energy-dispersive X-ray spectroscopy (EDS) analysis and elemental mapping were also performed on the region shown in Figure 17(a), and the results are presented in Figure 18. The uniform distribution of elemental intensities observed in the EDS mapping images indicates a homogeneous incorporation of metal ions and organic ligands within the MOF crystals. This result reflects effective control over the nucleation and growth conditions during synthesis, leading to highly crystalline and chemically homogeneous MOF products.

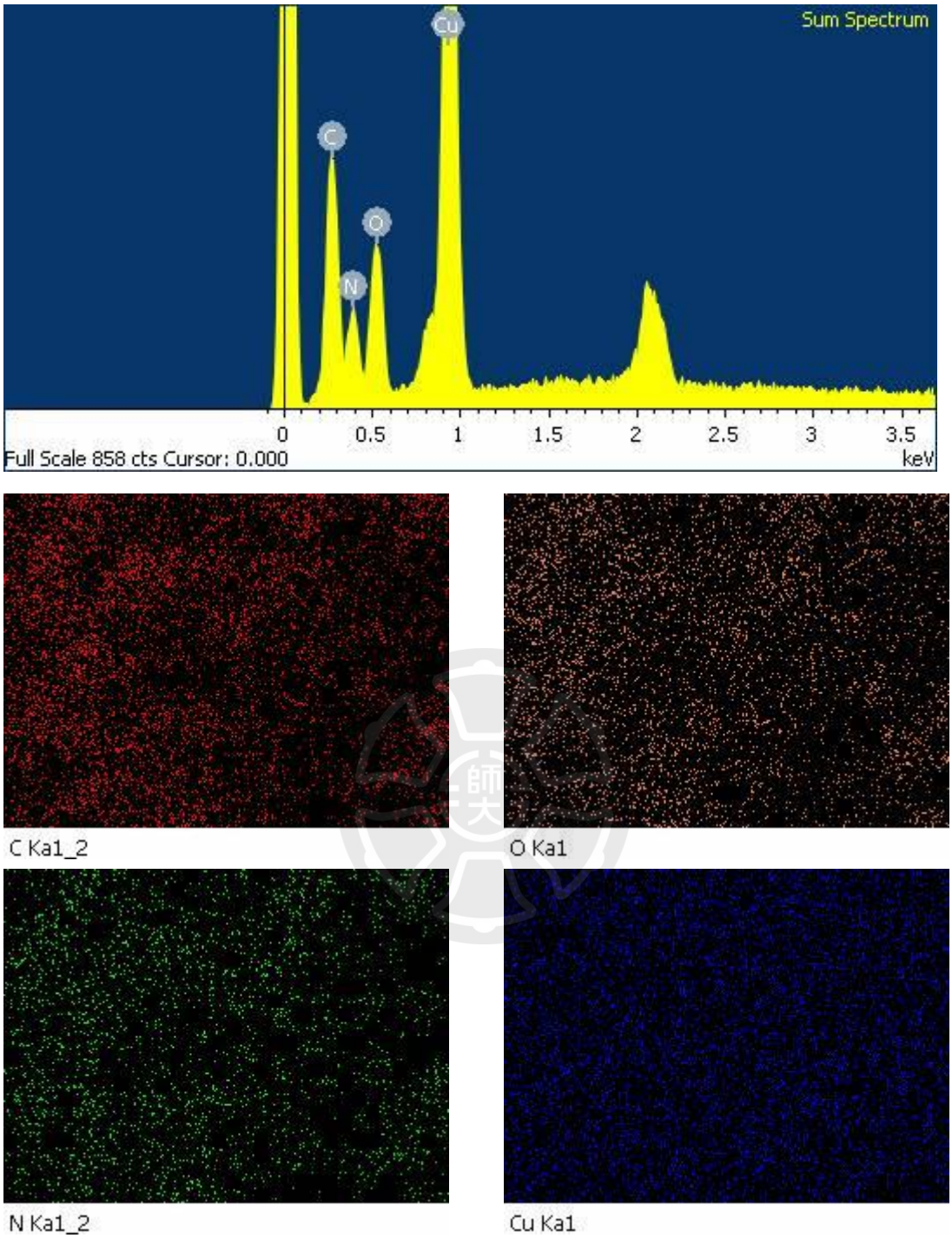

Figure 18. EDS elemental mapping images of Cu-PyC NH_4^+ MOF displaying uniform distribution of carbon (C), oxygen (O), nitrogen (N), and copper (Cu).

3.2.3 Fourier-Transform Infrared Spectroscopy

The functional groups and coordination modes of the synthesized MOF were confirmed using attenuated total reflectance Fourier-transform infrared spectroscopy (ATR-FTIR), and the results are presented in Figure 19. The characteristic absorption band observed at 1537 cm^{-1} is attributed to the asymmetric vibrations of the carboxylate groups ($–COO^–$) from the ligands, clearly indicating successful coordination to Cu^{2+} ions. These carboxylate vibration modes provide indirect evidence for metal-ligand bonding, confirming the successful formation of the MOF structure. The absorption bands appearing at 1291 cm^{-1}, 1178, and 1157 cm^{-1} can be assigned to the stretching vibrations of C–N and N–Cu–N, while the feature at 457 cm^{-1} corresponds to the Cu–O vibration, further validating the coordination bonds formed between copper ions and the organic ligand within the synthesized framework. These spectral features are consistent with those reported in previous literature[100], supporting the successful incorporation of functional groups and the formation of the intended MOF structure.

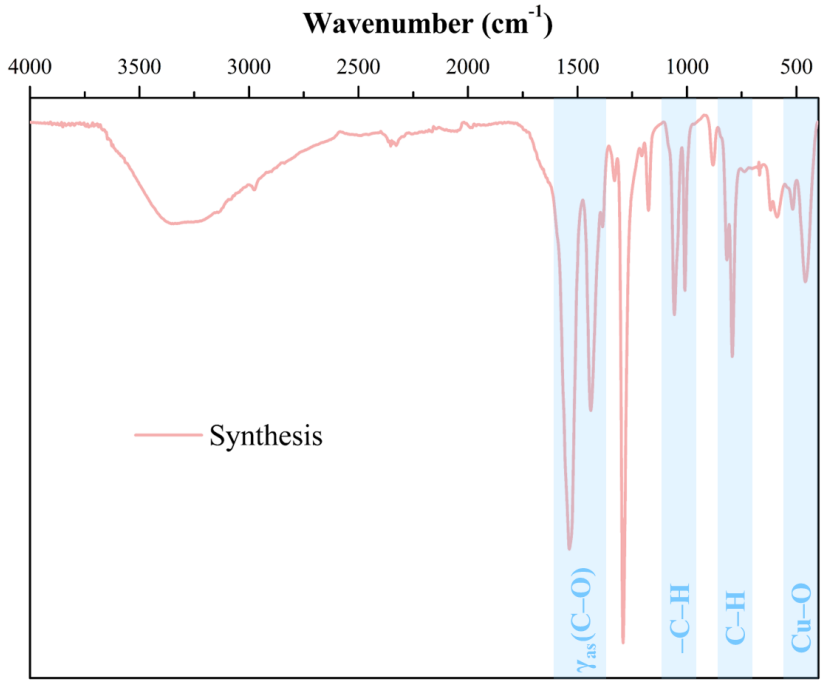

Figure 19. ATR-FTIR Spectrum of Synthesized Cu-PyC NH_4^+ MOF.

3.2.4 Sorption Isotherms and Pore Size Distribution

After activation under vacuum for 24 hours, nitrogen adsorption-desorption measurements of the synthesized MOF sample were performed, as shown in Figure 20. The resulting nitrogen adsorption-desorption isotherm exhibits a typical Type I profile, indicating that the Cu-PyC NH_4^+ MOF possesses microporous characteristics. The Brunauer–Emmett–Teller (BET) surface area and pore volume were determined to be 596.63 m^2g^{-1} and 0.29 cm^3g^{-1}, respectively. Pore size distribution analysis based on the nitrogen adsorption data revealed that the average pore size of the synthesized Cu-PyC NH_4^+ MOF is approximately 9.50 Å, classifying it as a supermicroporous material.

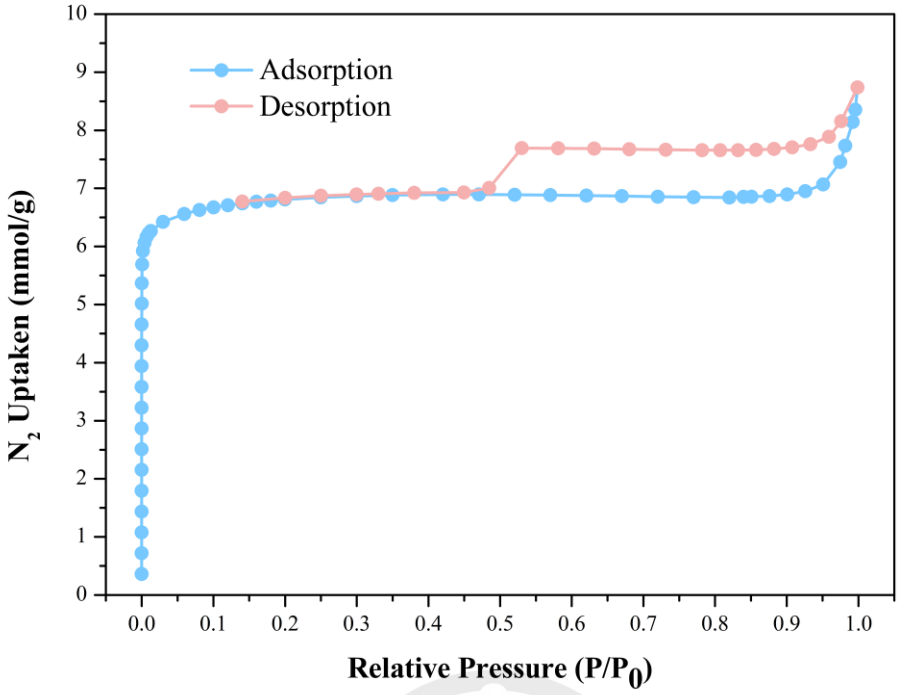

Figure 20. Nitrogen Adsorption-Desorption Isotherm of Synthesized Cu-PyC NH_4^+ MOF.

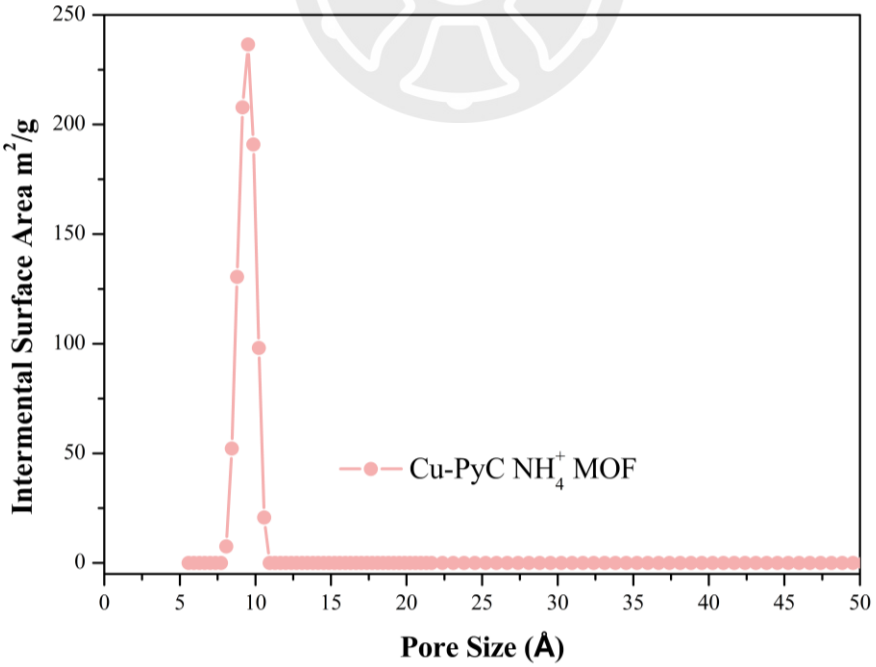

Figure 21. Pore Size Distribution of Synthesized Cu-PyC NH_4^+ MOF.

3.3 Sample Preparation Optimization

The primary objective of sample preparation is to eliminate interferences, purify samples, and enrich analytes, thus ensuring accurate qualitative and quantitative analyses. Systematic optimization experiments were essential to establish effective conditions for amino acid extraction using Cu-PyC NH_4^+ MOF.

3.3.1 Extraction Solvent

To achieve efficient amino acid extraction using Cu-PyC NH_4^+ MOF, adsorption efficiencies were systematically evaluated across various organic solvent-water mixtures. Ethanol and methanol were specifically selected due to their intermediate polarity, which provides an optimal balance for amino acid adsorption onto the MOF. Strong non-polar solvents (e.g., acetonitrile or isopropanol) were excluded due to insufficient amino acid dissolution, while excessively polar solvents (e.g., pure water) were avoided since they predominantly dissolve amino acids rather than promoting their adsorption onto the MOF surface.

As illustrated in Figure 22, the mixture containing 70% ethanol in water exhibited the highest extraction efficiency under these conditions. This observation supports our hypothesis that solvents positioned at either polarity extreme result in lower extraction performance, confirming the necessity of utilizing solvents with moderate polarity for effective amino acid extraction.

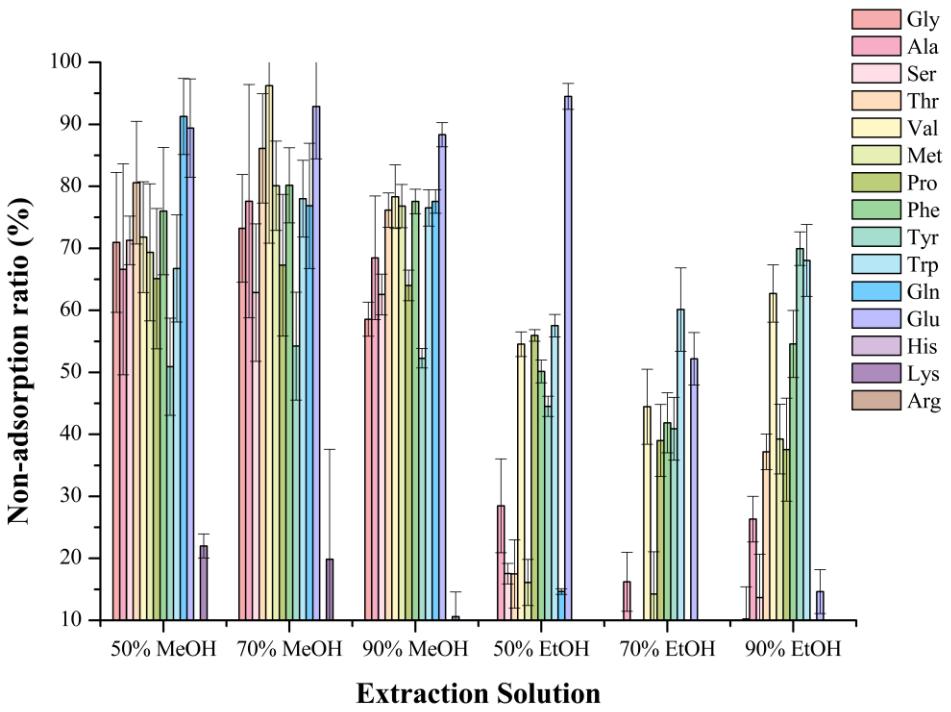

Figure 22. Extraction Solvent Optimization in Extraction Conditions.

3.3.2 Sample pH

In consideration of the zwitterionic properties of amino acids, we referred to previous literature[101, 102] which specifically addressed optimization strategies for analytes possessing zwitterionic characteristics or zwitterionic functional groups structurally analogous to those of amino acids.

However, results shown in Figure 23 indicated that adjusting the pH of samples did not improve extraction efficiency as anticipated. In fact, samples with pH adjustment exhibited lower adsorption efficiency compared to those without pH adjustments. Two possible explanations could account for these results. First, unlike the highly polar solvents used in the referenced studies, our extraction solvent (70% ethanol in water) is moderately polar solution. Thus, pH adjustments might be ineffective or even counterproductive under these conditions. Second, the introduction

of pH-adjusting additives might lead to competitive interactions between these ions and amino acids, for adsorption sites on the MOF surface, thereby reducing overall adsorption efficiency. Taking these considerations into account, further experiments were conducted without adjusting the sample pH.

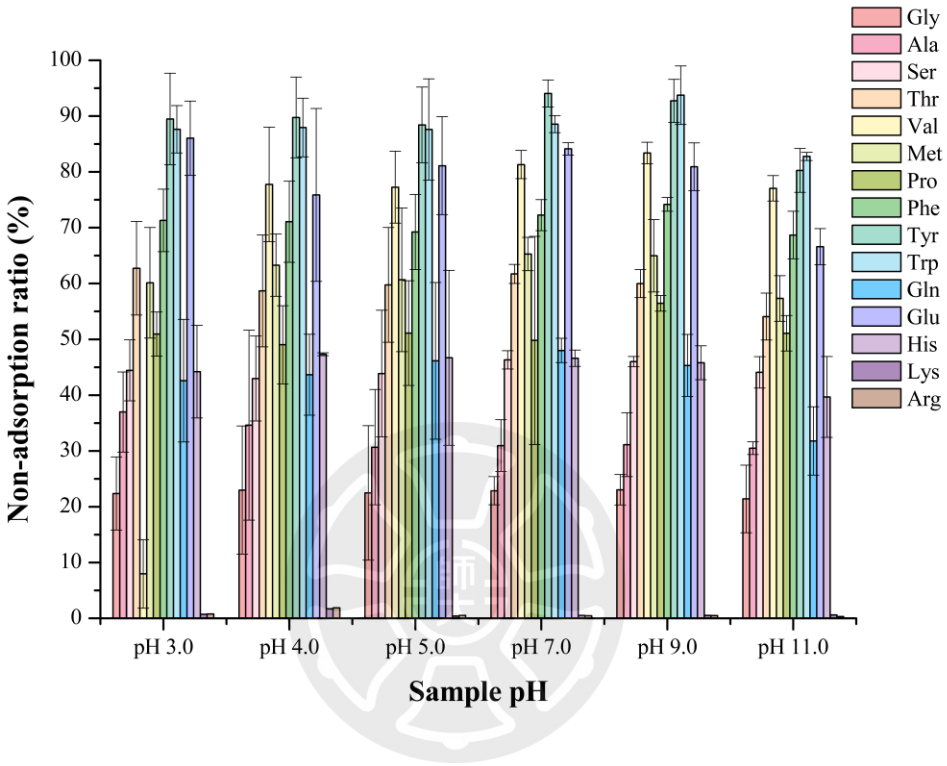

Figure 23. Sample pH value Optimization in Extraction Conditions.

3.3.3 Additive Addition

A small amount of an additive may improve the interactions between amino acids and adsorption sites on the MOF surface, thus enhancing extraction efficiency. Consequently, optimizing and clearly distinguishing among non-additive, acidic, and basic additive conditions at trace levels under highly organic conditions is crucial.

Figure 24 illustrates the adsorption efficiencies achieved with various additives. Among them, 0.1% formic acid significantly improved adsorption compared to no additives. In contrast, 0.1% acetic acid and 0.1% lactic acid slightly decreased the

overall adsorption efficiency compared to the non-additive control. Meanwhile, 0.25% ammonium hydroxide induced a contrasting adsorption trend—reducing the adsorption of polar amino acids while slightly enhancing that of non-polar amino acids.

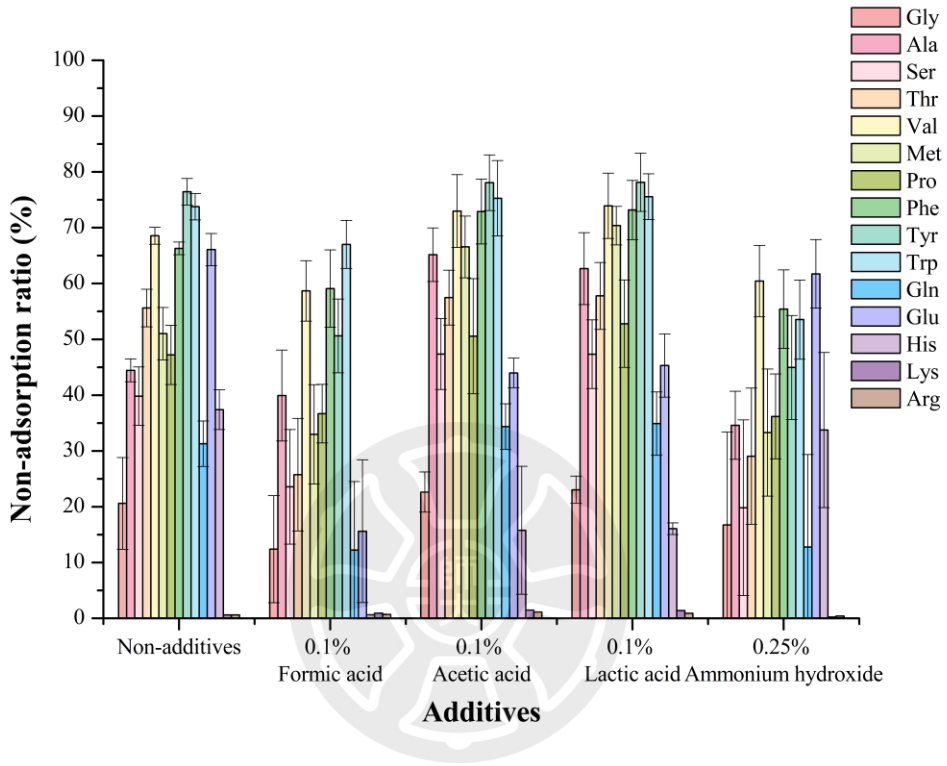

Figure 24. Additive Addition Optimization in Extraction Solution.

The superior performance of formic acid, compared to acetic acid and lactic acid, can be attributed to its stronger acidity (pKa = 3.75) and smaller molecular size. As previously discussed, highly acidic or basic additives often fail to improve extraction efficiency in high-organic solvents, possibly due to competition with analytes for adsorption sites. In contrast, weak acidic additives with small molecular size, such as formic acid, may act like surfactants—inducing partial protonation and modifying MOF surface polarity or functionality. These effects can enhance amino acid adsorption even under high-organic extraction conditions. On the other hand, acetic

acid acid (pKa = 4.76) and lactic acid (pKa = 3.86) exhibit weaker acidity than formic acid and possess larger molecular sizes. These properties likely limit their ability to modify the MOF surface or influence the adsorption environment. As a result, they may contribute to site blocking or competitive interference, rather than promoting adsorption.

Conversely, the addition of 0.25% ammonium hydroxide led to a distinct shift in extraction behavior, reflected in decreased adsorption of polar amino acids and enhanced adsorption of non-polar amino acids. This phenomenon may result from increased solvent polarity upon ammonium hydroxide addition, which alters solvation dynamics. The resulting environment may favor desolvation and adsorption of non-polar analytes while simultaneously reducing interactions with polar amino acids.

Previous results led to further optimization of the extraction, achieved by varying formic acid concentrations. The information presented in Figure 25 also corroborates our earlier discussion on 0.25% ammonium hydroxide. At 0.2% formic acid, a divergent adsorption trend compared to 0.1% formic acid was observed: reduced adsorption of polar amino acids and enhanced adsorption of non-polar amino acids. This phenomenon may be attributed to changes in solvent polarity and solubility, where a higher concentration of acidic additive increases the polarity of the extraction solution, thereby altering the extraction environment. This observation supports the selection of 0.05% formic acid for subsequent experiments.

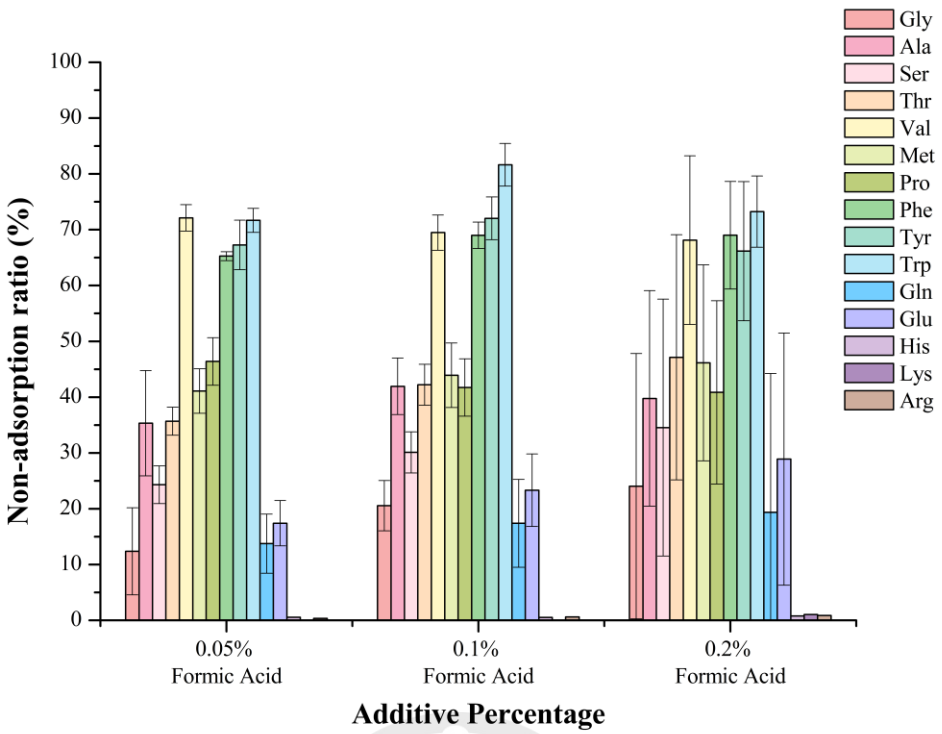

Figure 25. Additive Percentage Optimization in Extraction Solution.

3.3.4 Extraction Method

Different extraction methods utilize distinct energy-transfer mechanisms, resulting in varying adsorption efficiencies Ultrasonication enhances adsorbent dispersion by generating acoustic cavitation using high-frequency sound waves, which facilitates deeper solvent penetration and promotes analyte adsorption. Shaking facilitates sample movement, improving mass transfer by enhancing surface contact and reducing boundary layer resistance. Vortexing rapidly disperses adsorbent particles by disrupting the interface between the solid and liquid phases. Therefore, identifying the most effective extraction method is crucial for optimizing analyte recovery in this study.

Under these optimized conditions, the extraction efficiencies of ultrasonication, shaking (100 rpm), and vortexing (level 10) are compared (Figure 26). Before

comparing these methods, uniform dispersion of adsorbent in each extraction system was ensured using a consistent vortex method. Figure 26 illustrates adsorption efficiencies from highest to lowest as follows: vortexing, shaking, and ultrasonication. The lower extraction efficiency observed with ultrasonication likely results from inadequate adsorbent dispersion. Although proper dispersion was initially achieved, sedimentation occurred during ultrasonication due to gravitational effects and the orientation of the reaction tube, resulting in poor adsorbent dispersion and consequently reducing extraction efficiency. Compared to ultrasonication, the shaking method exhibited superior performance due to continuous and homogeneous mixing. However, the extraction efficiency of shaking was lower than that of vortexing, likely due to differences in their energy transfer mechanisms. Shaking reduces the boundary layer gently and mixes the two phases homogeneously, whereas vortexing disrupts the boundary layer vigorously and directly. The intensity of energy delivered during vortexing is greater and more dynamic compared to shaking. Consequently, the vortexing duration was further optimized.

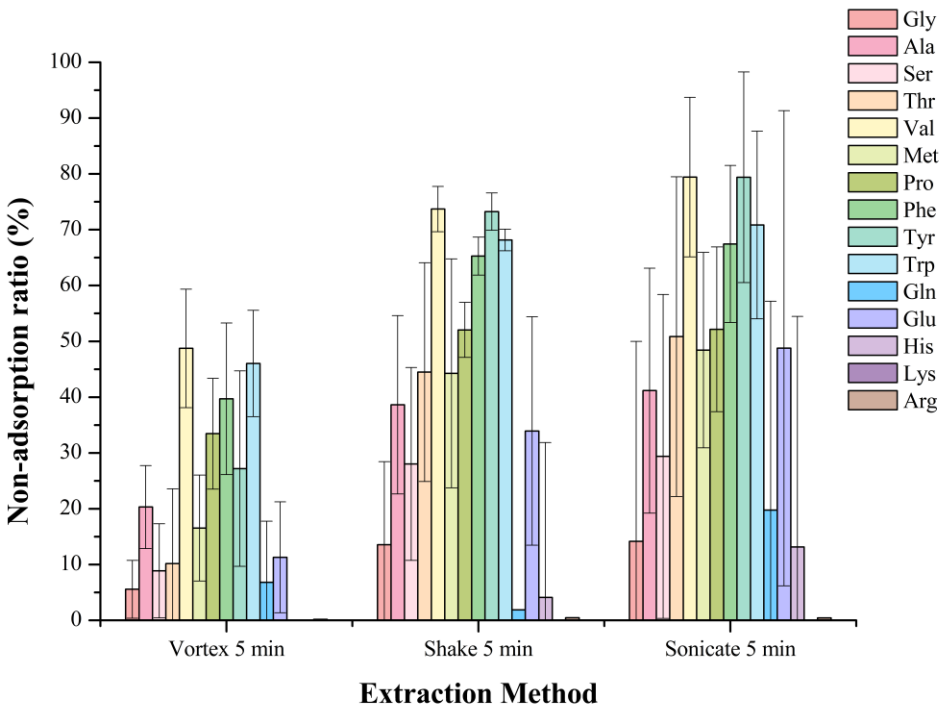

Figure 26. Extraction Method Optimization in Extraction Conditions.

The highest adsorption efficiency was achieved with 10 minutes of vortexing, as shown in Figure 27. This trend—an increase in adsorption efficiency from 5 to 10 minutes, followed by a decline at 15 and 20 minutes—can be explained by the amount of energy applied during vortexing. Excessive energy input, as seen at 15 and 20 minutes, may have driven analyte desorption from the MOF surface, thereby reducing adsorption efficiency. In contrast, insufficient energy at 5 minutes may have limited analyte–MOF interactions, resulting in lower adsorption efficiency than at 10 minutes. At 10 minutes, the applied energy was sufficient to promote optimal analyte adsorption. Accordingly, vortexing for 10 minutes was selected as the optimal extraction time.

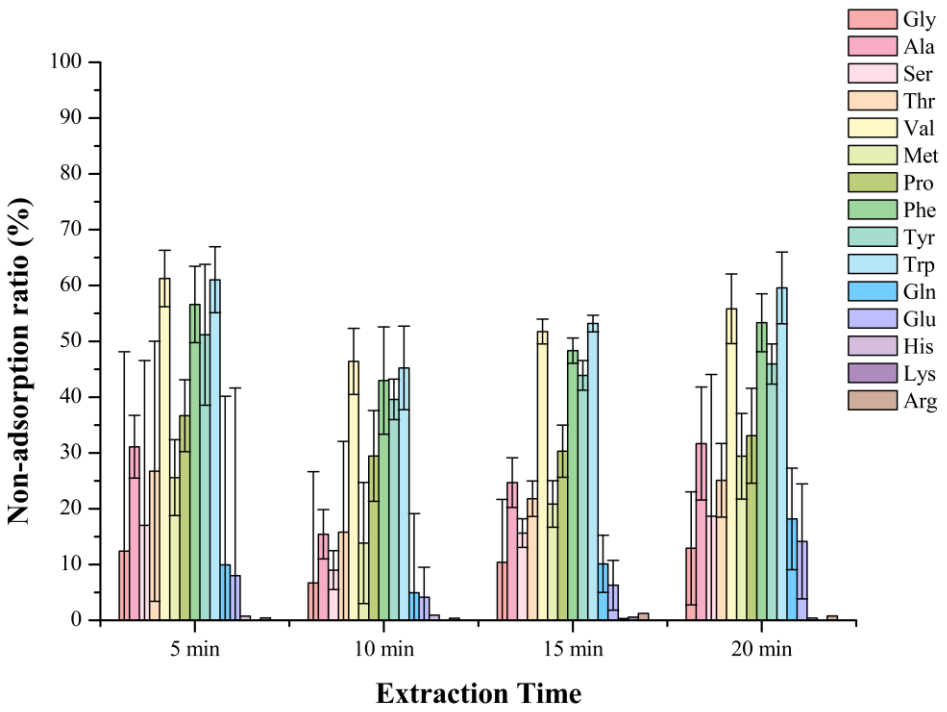

Figure 27. Extraction Time Optimization in Extraction Conditions.

3.3.5 Adsorbent Amount

Considering the balance between the analyte concentrations typically found in food samples after dilution, the effective detection range of the instrument, and the necessity to clearly evaluate adsorption capacity differences, a concentration of 1000 ng/mL for the 15-amino-acid mixture was selected for optimizing the adsorbent amount.

As shown in Figure 28, the non-adsorption ratio significantly decreased as the adsorbent amount increased from 10 mg to 50 mg, with the rate of decrease becoming less pronounced between 50 mg and 110 mg. Although the extraction performance at 110 mg of adsorbent was slightly superior to other conditions, the incremental improvement compared to 50 mg was limited. Additionally, noticeable agglomeration and poor dispersion of adsorbent particles were observed at higher loadings,

potentially affecting reproducibility. Therefore, considering cost-effectiveness, practicality, and analytical reliability, 50 mg was selected as the optimal adsorbent amount for subsequent elution optimization.

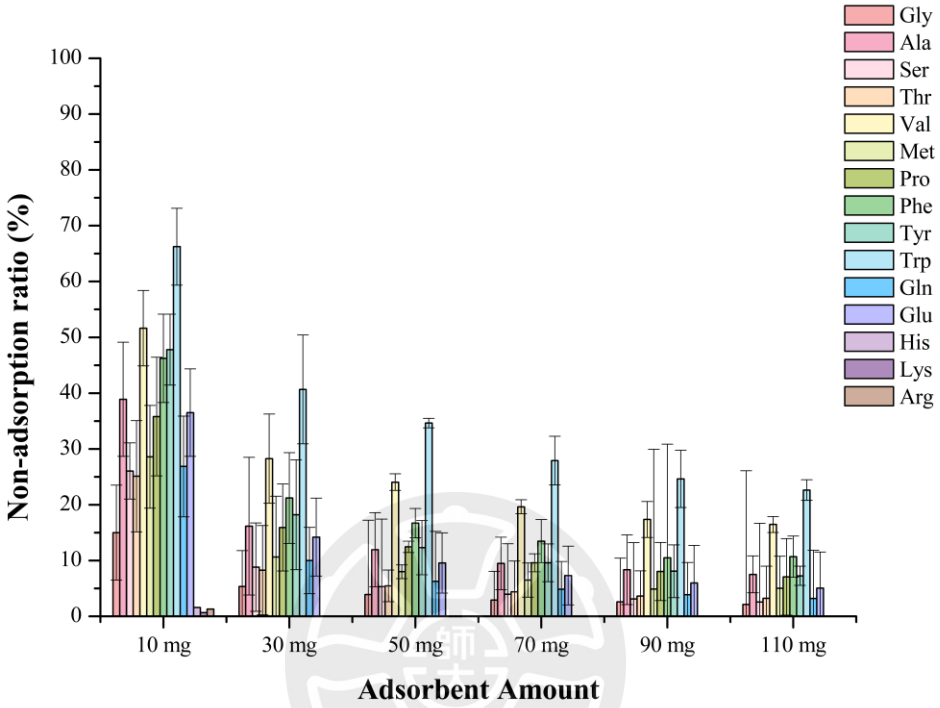

Figure 28. Adsorbent Amount Optimization for Extraction of Fifteen Amino Acids at 1000 ng/mL.

3.3.6 Elution Solution

Given the zwitterionic nature of amino acids (with pKa values ~2-3 for carboxylic groups and ~9-10 for ammonium groups, yielding pI from ~3 for acidic Glu to ~11 for basic Arg), the elution solvent was selected to disrupt interactions with the cationic Cu-PyC NH_4^+ MOF framework. Nine solvents across acidic (hydrochloric acid at 1-5%, formic acid), neutral (pH ~6-7), and basic (ammonium hydroxide, sodium hydroxide) ranges were tested to optimize desorption while preserving MOF stability.

Figure 29 illustrates recovery percentages (%) for each amino acid, with error bars indicating variability. High recoveries occur in acidic conditions (5% HCl, 3% HCl, 1% HCl), peaking at 1% HCl for non-polar (e.g., Ala, Val, Met, Pro, Phe > 80%) and acidic (e.g., Glu ~70-90%) amino acids. Recoveries decline slightly at 5% and 3% HCl, especially for polar or basic amino acids (e.g., Ser, Thr, Tyr, Trp, Gln, His, Lys, Arg < 50%). In mildly acidic (pH 1.0, 3.0) conditions, recoveries are moderate (~40-70%), but drop sharply in neutral (pH 6.0 ~20-40%) and basic (pH 9.0-12.0 < 20%) conditions, with basic amino acids (Lys, Arg) showing consistently low recoveries. Small/non-polar amino acids (Gly, Ala, Val) achieve the highest recoveries (>90% at 1% HCl), while aromatic (Tyr, Trp, Phe) and charged ones (Glu, His, Lys, Arg) vary more, with charged species showing greater sensitivity to pH shifts. These trends confirm that acidic eluents favor desorption, but excessive acidity introduces trade-offs, as evidenced by the slight dip at 5% HCl.

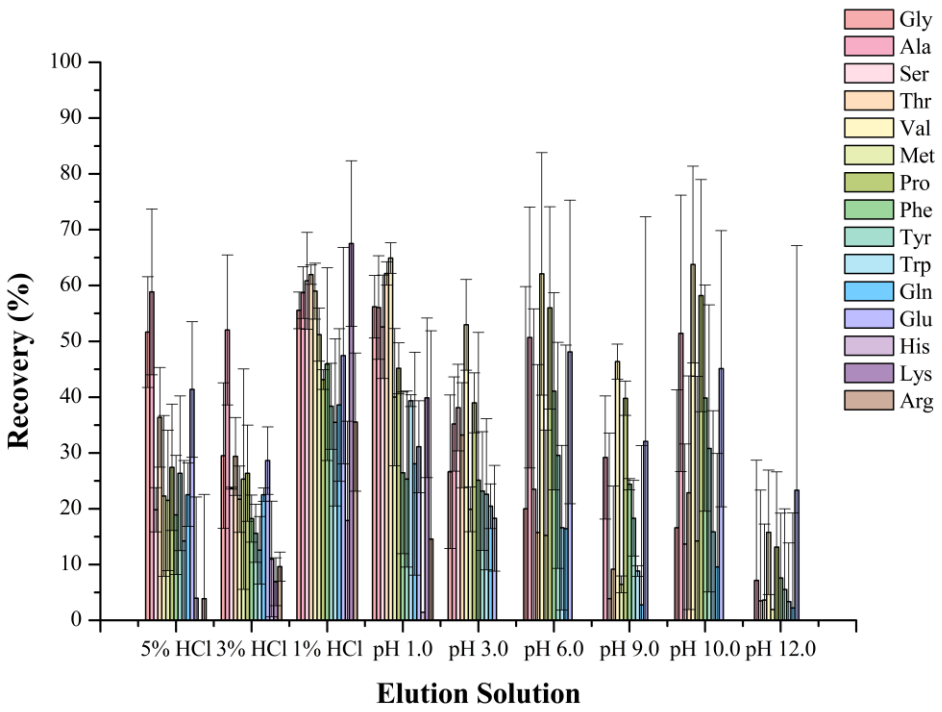

Figure 29. Elution Solution Optimization in Elution Conditions.

We hypothesize that this phenomenon arises from the ion-exchange mechanism inherent to the anionic framework of the Cu-PyC NH_4^+ MOF, which is a key structural feature enabling selective extraction of amino acids. The anionic charge of the framework originates primarily from the doubly deprotonated pyrazole-4-carboxylate (PyC) ligands, where both the carboxylate ($–COO^–$) and pyrazolate anions contribute negative charges, forming a robust $[Cu_3(\mu_3\text{-}OH)(\mu_3\text{-}4\text{-}PyC)_3]^–$ network. This anionic framework is electrostatically balanced by NH_4^+ counterions, which occupy the pores and maintain overall structural neutrality and stability. During extraction, zwitterionic amino acids, with their protonated ammonium groups ($–NH_3^+$), undergo ion exchange with these NH_4^+ ions, displacing them to bind to the anionic sites on the framework. This cation-exchange process is particularly advantageous for amino acids, as it combines electrostatic attraction with additional interactions such as

hydrogen bonding from the framework's N/O functional groups, enhancing selectivity and efficiency in complex matrices.

In the elution step, the strong acidity of HCl solutions facilitates desorption through a secondary ion-exchange mechanism. The hydronium ions (H_3O^+) from HCl compete with and displace the bound amino acids from the anionic framework, allowing successful elution. This is evident in the high recoveries observed at moderate HCl concentrations (e.g., 1% HCl), where the process disrupts analyte-framework interactions without compromising MOF integrity. However, excessive HCl concentrations (e.g., 3% and 5%) lead to a decline in amino acid recovery, likely due to over-acidification. In such environments, surplus H_3O^+ cations and Cl^- anions may coordinate directly with the anionic framework or Cu^{2+} centers, causing partial structural disruption. This could involve competitive binding of Cl^- to metal nodes or protonation-induced weakening of metal-ligand bonds, ultimately leading to localized framework collapse and reduced adsorption capacity.

Evidence of structural damage under strongly acidic conditions is presented in Figure 30 and Figure 31. The appearance of blue coloration in the elution solutions (Figure 30) suggests Cu^{2+} ion release from the MOF structure, indicative of coordination bond breakage. The PXRD patterns (Figure 31) further reveal significant peak loss and broadening, confirming partial framework degradation at higher HCl concentrations. These observations underscore the importance of balancing elution efficiency with MOF stability, highlighting the anionic framework's role not only in extraction but also in dictating the material's chemical resilience.

Based on a comprehensive evaluation of amino acid recoveries, analyte stability, and MOF structural integrity, a 1% hydrochloric acid solution was ultimately selected as the optimal elution solvent. Under this condition, the desorption behavior is considered to be predominantly governed by the second proposed mechanism—anion competition—wherein chloride ions effectively displace amino acids from adsorption sites. The acid concentration is sufficient to promote this interaction without inducing excessive structural degradation of the MOF. Nonetheless, relatively poor recoveries were still observed for basic amino acids, likely due to their strong electrostatic or coordinative interactions with the MOF framework, which hinder efficient desorption. Overall, 1% hydrochloric acid offers a practical compromise between analyte elution efficiency, structural preservation of the MOF, and reproducible analytical performance. This ion-exchange-driven approach, enabled by the anionic framework and NH_4^+ counterions, positions the Cu-PyC NH_4^+ MOF as a superior adsorbent for zwitterionic analytes, distinguishing it from neutral or cationic MOFs in terms of selectivity and versatility for real-world applications.

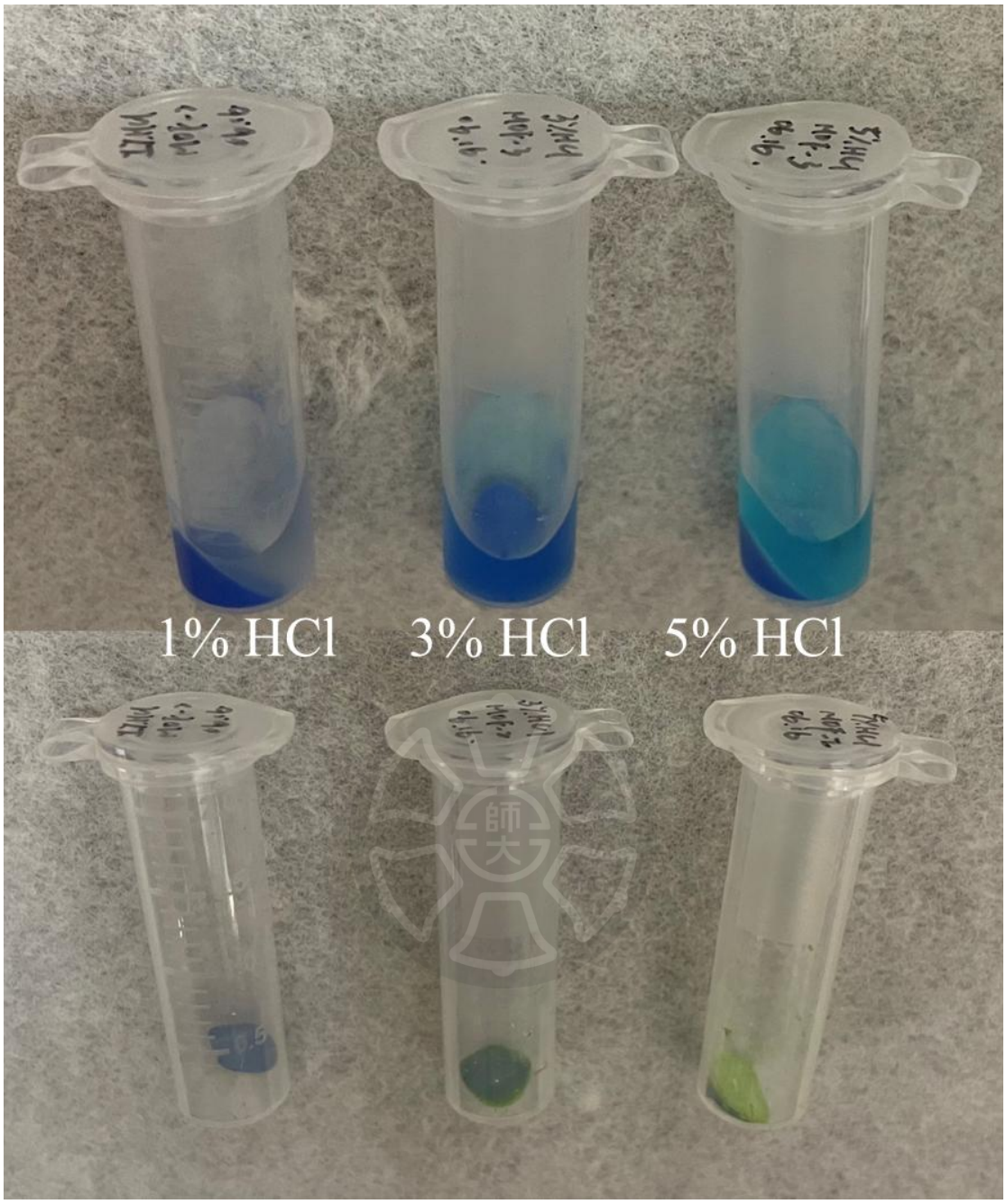

Figure 30. Visual Appearance of Cu-PyC NH_4^+ MOF After Elution with Different HCl Concentrations.

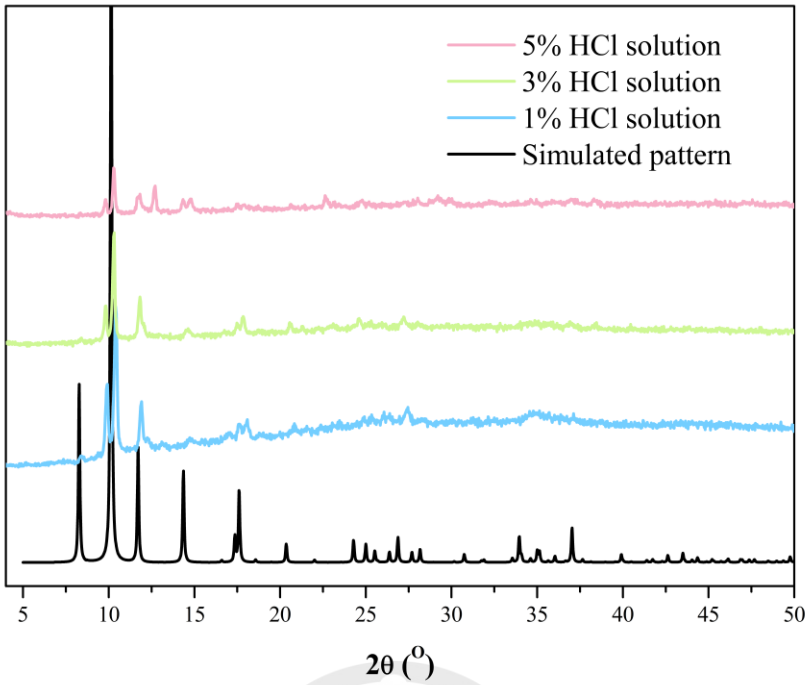

Figure 31. PXRD Patterns Comparison of Cu-PyC NH_4^+ MOF After Exposure to Eluents with Different HCl Concentrations.

3.3.7 Elution Method

Referring to the principle and considerations mentioned in section 3.3.4, three elution methods were evaluated as presented in Figure 32. Although amino acid recoveries obtained from vortexing and shaking methods appeared similar, recoveries achieved by vortexing were slightly higher overall. Notably, the recoveries of basic amino acids under vortexing conditions were significantly higher compared to shaking. In summary, the vortexing method was selected for subsequent optimization experiments.

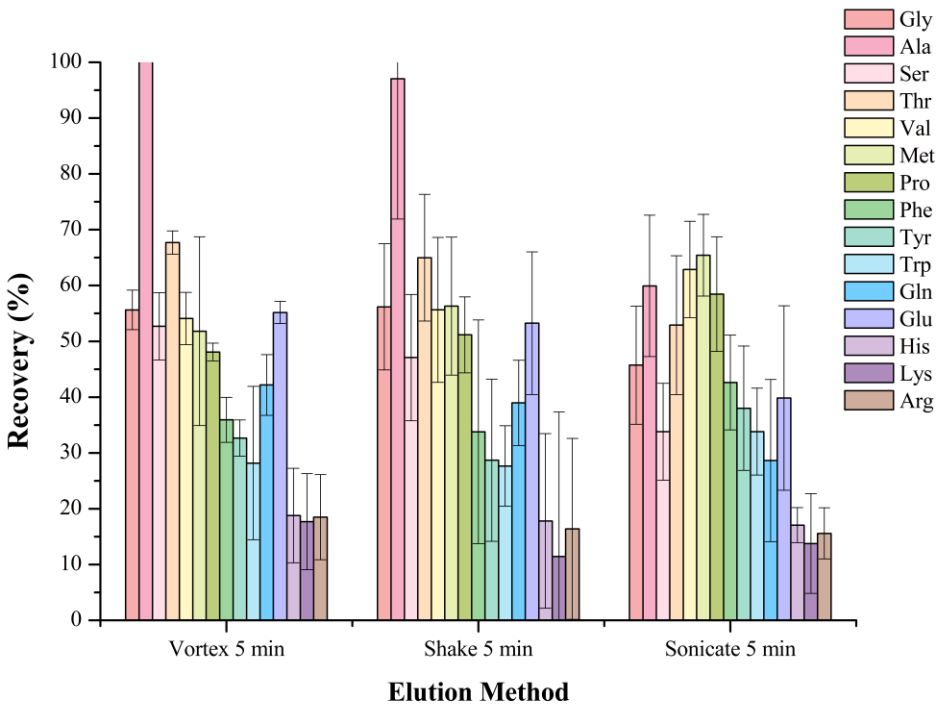

Figure 32. Elution Method Optimization in Elution Conditions.

3.3.8 Elution Time

As illustrated in Figure 33, the elution efficiency obtained using 10-minute vortexing was higher compared to other conditions. This phenomenon could be explained by insufficient energy provided in the 5-minute condition, resulting in incomplete analyte desorption, while excessive vortexing time (longer than 10 minutes) might provide excess energy, causing unintended interactions between analytes and adsorption sites or promoting re-adsorption, thus reducing recovery. Therefore, the 10-minute vortexing condition was selected as the optimal elution method and duration for subsequent optimization experiments.

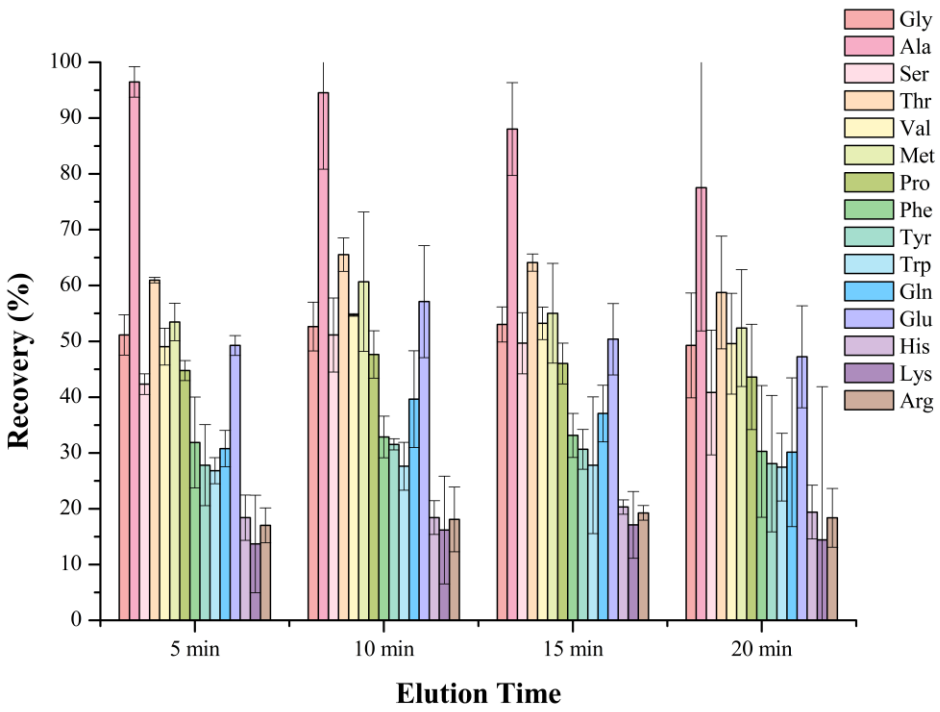

Figure 33. Elution Time Optimization in Elution Conditions.

3.3.9 Elution Solution Volume

The elution solution volume influences the dispersibility of the adsorbent in the solvent system, thereby affecting analyte transport dynamics and spatial distribution, which ultimately impacts amino acid recovery. To evaluate this effect, elution volumes from 500 μL to 1200 μL were tested, as shown in Figure 34.

An increasing recovery trend was observed with increasing elution volume, and the highest recoveries were achieved using 1200 μL. However, due to the acidity of the 0.1% hydrochloric acid eluent, direct injection into the HPLC system could damage the amide column. Therefore, a 5-fold dilution will be applied prior to analysis. Balancing dilution needs and detection sensitivity, 1200 μL was selected as the optimal elution volume.

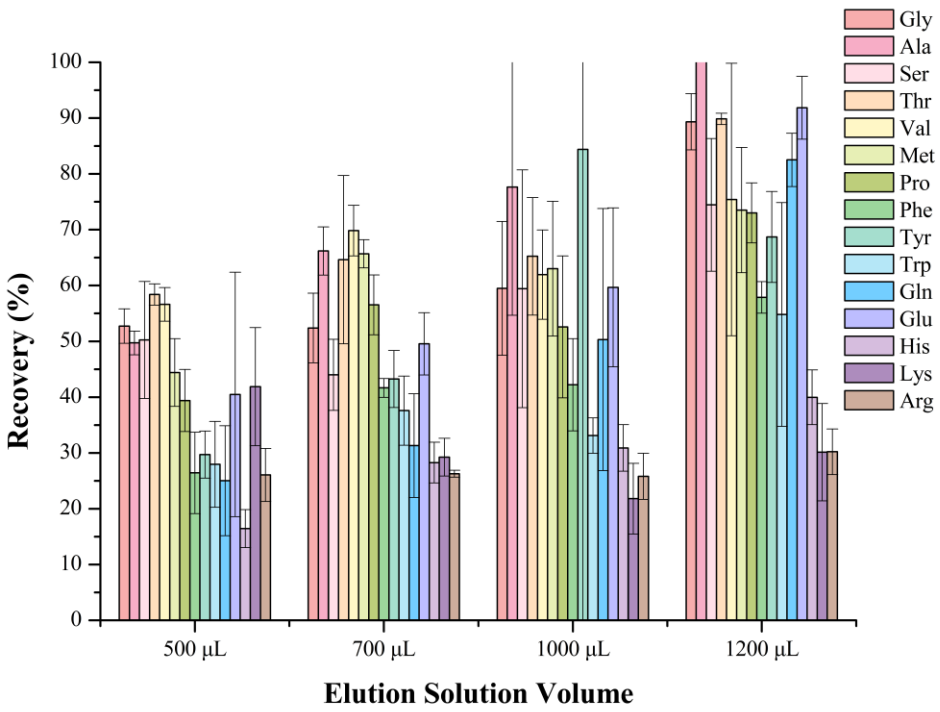

Figure 34. Elution Solution Volume Optimization in Elution Conditions.

3.3.10 Stability test of MOF

The stability of the synthesized MOF throughout the extraction and elution procedures was evaluated using multiple analytical techniques. PXRD patterns (Figure 35) indicated that the MOF maintained structural integrity without significant changes across all tested conditions, including the original synthesized material, immersion in extraction solvent, amino acid extraction, and elution solvent exposure.

Similarly, ATR-FTIR spectra (Figure 36) revealed no distinct differences among these conditions. Although one would expect characteristic amino acid peaks, such as N–H stretching (~3300 cm^{-1}) and C=O stretching vibrations, these were not prominently observed, likely due to the low loading of amino acids on the MOF or overlapping vibrational signals from the MOF structure itself.

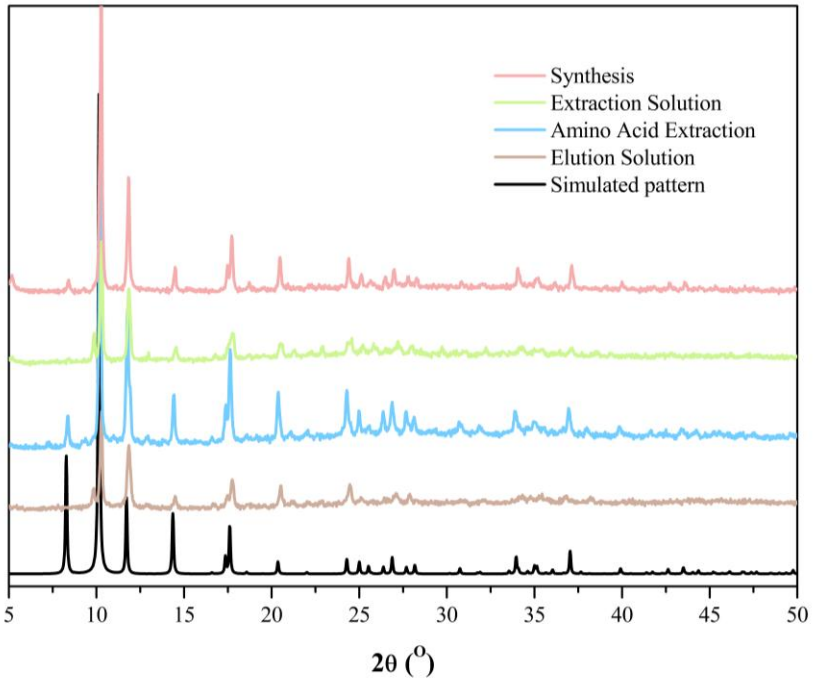

Figure 35. PXRD Patterns of Cu-PyC NH_4^+ MOF Under Different Experimental Conditions and Simulated Structure.

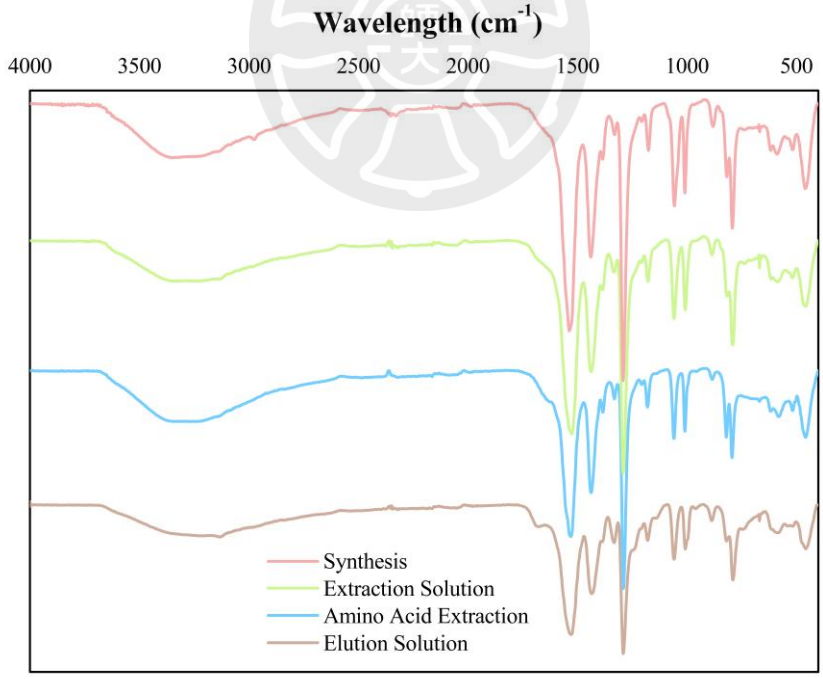

Figure 36. ATR-FTIR Spectra of Cu-PyC NH_4^+ MOF Under Different Experimental Conditions.

Furthermore, morphological analysis by FE-SEM (Figure 37) confirmed no observable morphological differences or significant particle agglomeration before and after the extraction and elution steps. The MOF consistently retained its uniform morphology throughout all processes.

Overall, based on structural (PXRD), chemical (ATR-FTIR), and morphological (FESEM) analyses, the MOF demonstrated excellent stability throughout the optimized extraction and elution protocol, validating its suitability as a robust adsorbent for amino acid analysis.

(a) **(b)**

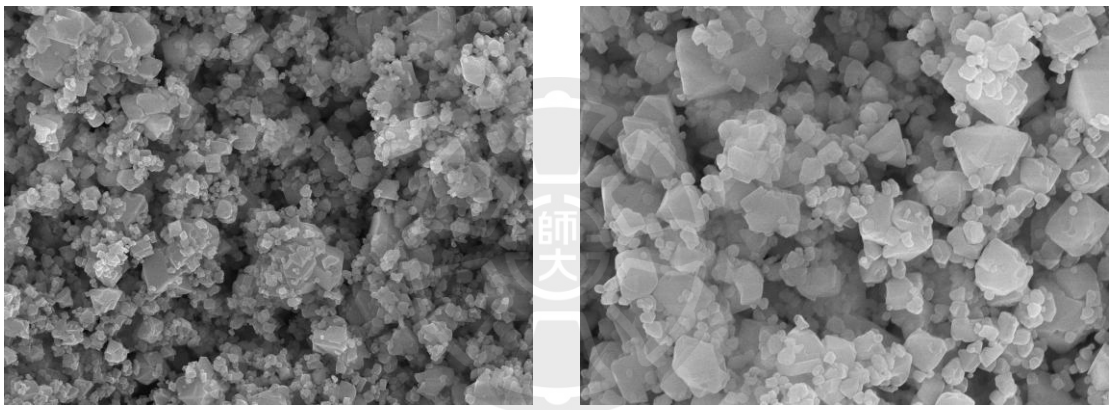

(c) **(d)**

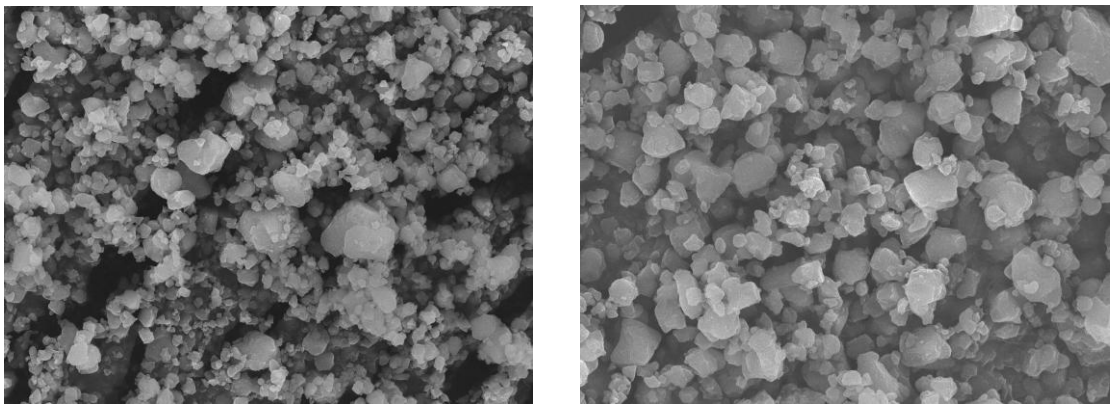

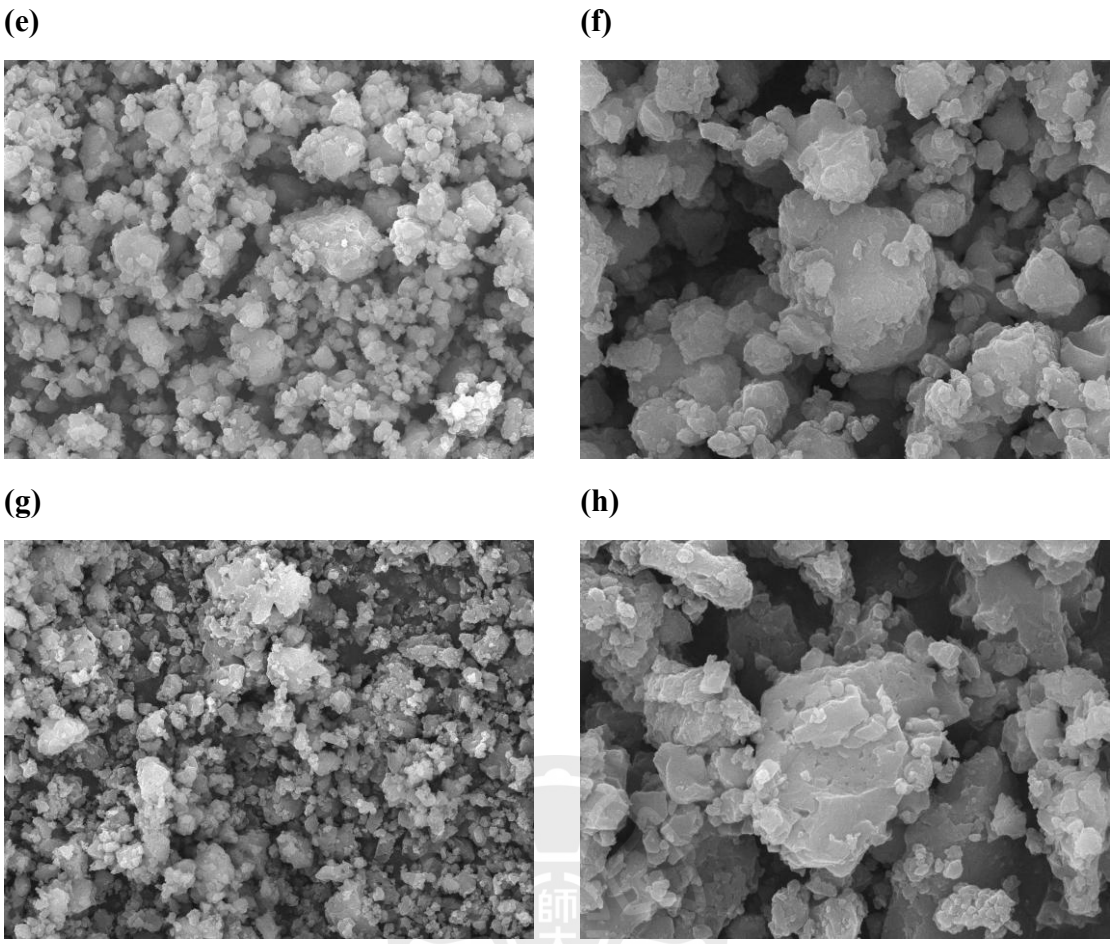

Figure 37. FESEM images of Cu-PyC NH_4^+ MOF Under Different Experimental Conditions.

(a, b) Synthesized MOF – ×5,000, ×10,000

(c, d) After extraction solvent immersion – ×5,000, ×10,000

(e, f) After amino acid extraction – ×5,000, ×10,000

(g, h) After elution treatment – ×5,000, ×20,000

3.4 Adsorption Mechanism

The adsorption mechanism of amino acids onto the Cu-PyC NH_4^+ MOF in the dispersive solid-phase extraction (dSPE) process is primarily driven by a cation-exchange process, facilitated by the unique anionic framework of the MOF. This framework, formulated as $[Cu_3(\mu_3\text{-}OH)(\mu3\text{-}4\text{-}PyC)_3]^-$, derives its negative charge from the doubly deprotonated pyrazole-4-carboxylate (PyC) ligands. Each PyC ligand contributes two negative charges—one from the carboxylate group ($–COO^–$) and one from the pyrazolate anion formed by deprotonation of the pyrazole ring N-H. These ligands coordinate with Cu^{2+} ions in a μ_3-bridging mode, forming a microporous structure with high surface area and functionalized sites rich in nitrogen and oxygen atoms. The overall anionic charge of the framework is balanced by NH_4^+ counterions, which occupy the pores and ensure structural stability and electrical neutrality. This design not only provides porosity for analyte diffusion but also enables selective ion-exchange capabilities, distinguishing this MOF from neutral or cationic counterparts and making it particularly suited for zwitterionic analytes like amino acids.

During the extraction phase, as illustrated in Figure 38(a) , the zwitterionic form of amino acids—featuring a protonated ammonium group ($–NH_3^+$) and a deprotonated carboxylate group ($–COO^–$)—interacts with the MOF. The $-NH_3^+$ moiety displaces the NH_4^+ counterions through cation exchange, binding electrostatically to the anionic sites on the framework. This process is augmented by secondary interactions, including hydrogen bonding between amino acid's functional groups and N/O atoms in PyC ligands, as well as potential π-π stacking with aromatic pyrazole rings. These multimodal interactions enhance selectivity, allowing efficient capture of amino acids from complex matrices while excluding impurities, as depicted in the sequential steps of vortex mixing, centrifugation, and supernatant removal in the schematic.

The elution mechanism, shown in Figure 38(b), involves a reverse ion-exchange process using HCl solutions. Hydronium ions (H_3O^+) from the acid compete with and displace the bound -NH_3^+ groups of the amino acids, facilitating their release into the eluent. Additionally, chloride ions (Cl^-) may contribute via anion competition, further disrupting analyte-framework interactions. At optimal concentrations (e.g., 1% HCl), this yields high recoveries without compromising MOF integrity. However, excessive acidity (e.g., 3-5% HCl) leads to structural degradation, as surplus H_3O^+ and Cl^- ions coordinate with Cu^{2+} centers or protonate ligand sites, causing partial framework collapse. This is evidenced by the blue coloration in elution solutions (Figure 30), indicative of Cu^{2+} leaching, and the loss of characteristic peaks in PXRD patterns (Figure 31), confirming diminished crystallinity at higher acid levels.

Supporting evidence for this ion-exchange-dominated mechanism includes the MOF's high selectivity for charged analytes, as demonstrated by recovery trends in optimization experiments. For instance, basic amino acids exhibit stronger binding due to their higher positive charge density, resulting in lower elution efficiencies, while neutral or acidic ones desorb more readily. Additionally, the stability of the MOF after mild elution process, indicated by minimal changes in FT-IR spectra post-extraction (Figure 36), supports the reversible nature of the cation exchange without irreversible covalent modifications. This mechanism aligns with the hard-soft acid-base (HSAB) principle[69], where the soft Cu^{2+} nodes prefer coordination with softer ligands, but the anionic framework prioritizes electrostatic interactions with hard cations like -NH_3^+ or NH_4^+.

Overall, the anionic framework enabled by PyC ligands offers a robust, selective, and eco-friendly platform for ion-exchange-based adsorption, surpassing traditional sorbents and highlighting the Cu-PyC NH_4^+ MOF's potential for analyte enrichment across diverse matrices.

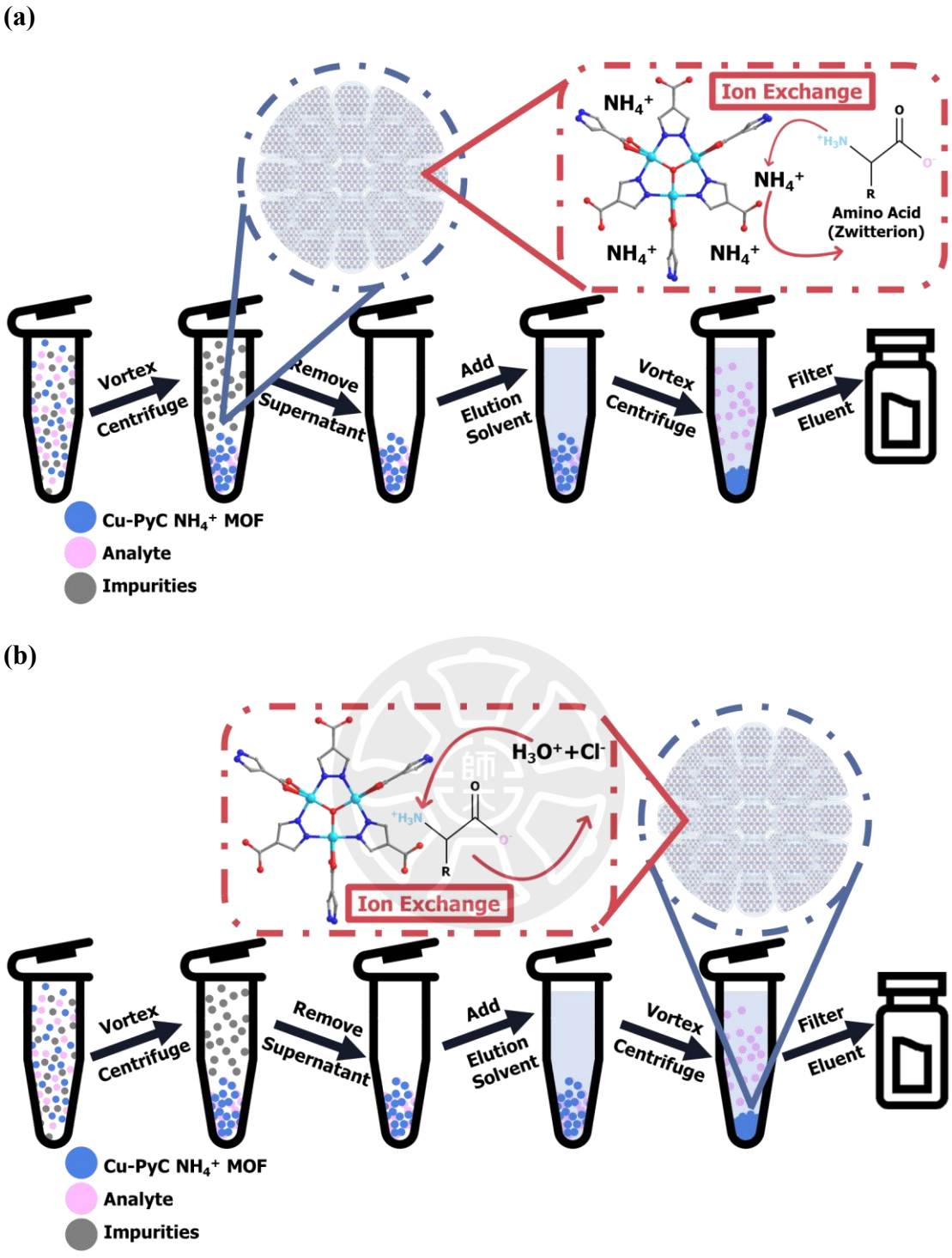

Figure 38. Cu-PyC NH_4^+ MOF dispersive SPE mechanism:

(a) cation-exchange adsorption of amino acids;

(b) HCl-assisted ion exchange releases amino acids.

3.5 Application

The developed dSPE method was further applied to instant coffee samples to assess its practical utility. As shown in Figure 39(a) , the chromatogram of a 100 ng/mL mixed amino acid standard displays excellent signal intensity, resolution, and peak shape, serving as a reference for method performance. In comparison, the chromatogram of the real coffee sample diluted 500-fold without pretreatment (Figure 39b) shows poor sensitivity and significant baseline noise, highlighting the matrix complexity and the need for efficient sample clean-up. Following dSPE treatment, the chromatogram of the sample diluted 600-fold (Figure 39c) exhibits markedly improved peak clarity, signal intensity, and reduced background noise, enabling reliable analyte detection. Additionally, the dSPE-treated sample spiked with 100 ng/mL standard (Figure 39d) shows enhanced peak intensities with no observable matrix interference, demonstrating high sensitivity and recovery.

These results confirm the method's robustness and effectiveness for trace-level amino acid analysis in complex matrices. The developed dSPE procedure offers an efficient, reproducible, and interference-free extraction strategy suitable for real-world applications such as food sample analysis.

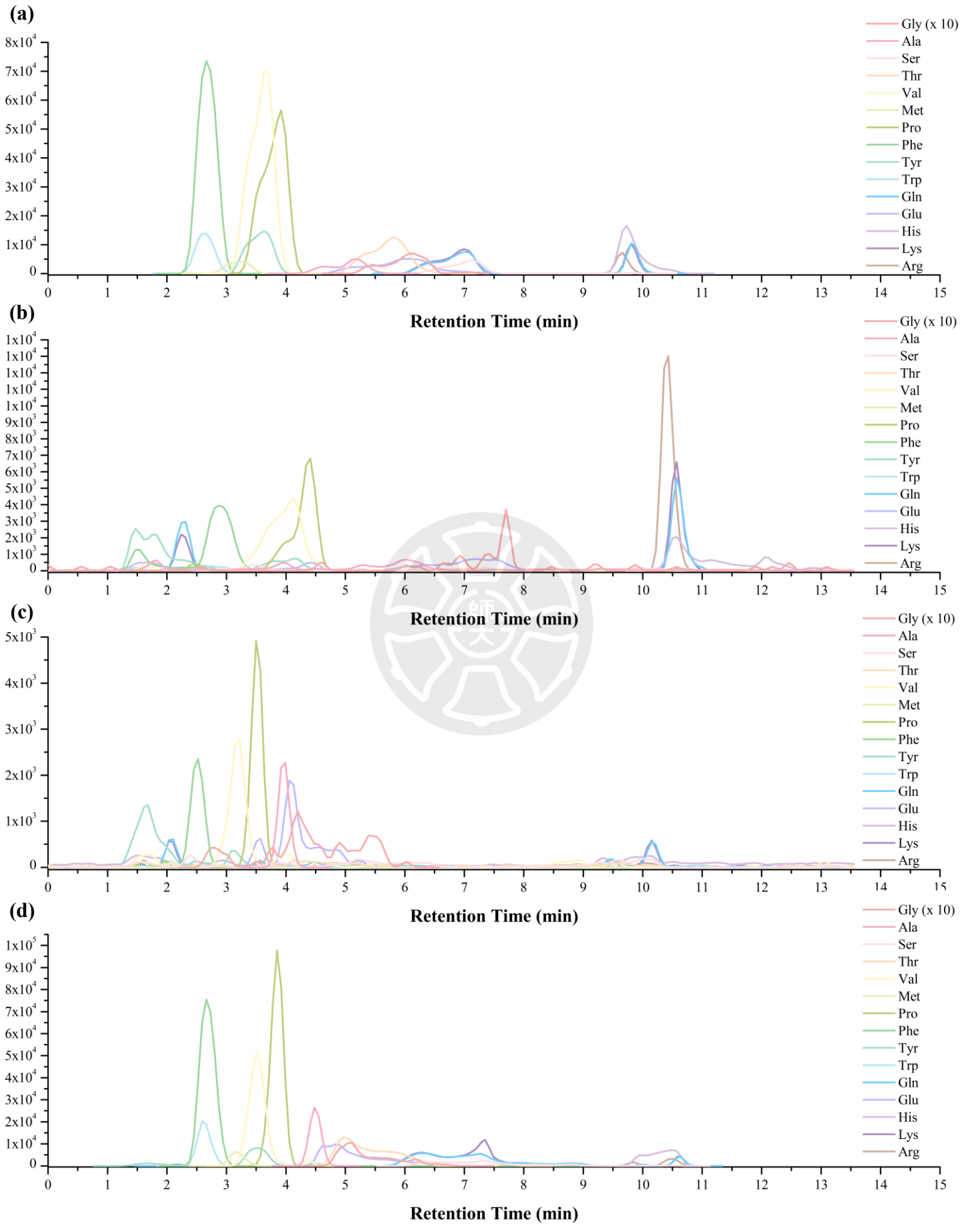
(a)
8x10^4
7x10^4
6x10^4
5x10^4
4x10^4
3x10^4
2x10^4
1x10^4
0
0 1 2 3 4 5 6 7 8 9 10 11 12 13 14 15
Retention Time (min)
Gly (x 10)
Ala
Ser
Thr
Val
Met
Pro
Phe
Tyr
Trp
Gln
Glu
His
Lys
Arg
(b)
1x10^4
9x10^3
8x10^3
7x10^3
6x10^3
5x10^3
4x10^3
3x10^3
2x10^3
1x10^3
0
0 1 2 3 4 5 6 7 8 9 10 11 12 13 14 15
Retention Time (min)
Gly (x 10)
Ala
Ser
Thr
Val
Met
Pro
Phe
Tyr
Trp
Gln
Glu
His
Lys
Arg
(c)
5x10^3
4x10^3
3x10^3
2x10^3
1x10^3
0
0 1 2 3 4 5 6 7 8 9 10 11 12 13 14 15
Retention Time (min)
Gly (x 10)
Ala
Ser
Thr
Val
Met
Pro
Phe
Tyr
Trp
Gln
Glu
His
Lys
Arg
(d)
1x10^5
9x10^4
8x10^4
7x10^4
6x10^4
5x10^4
4x10^4
3x10^4
2x10^4
1x10^4
0
0 1 2 3 4 5 6 7 8 9 10 11 12 13 14 15
Retention Time (min)
Gly (x 10)
Ala
Ser
Thr
Val
Met
Pro
Phe
Tyr
Trp
Gln
Glu
His
Lys
Arg

Figure 39. Representative LC-MS/MS Chromatograms of Fifteen Amino Acids under the Different Conditions.
(a) 100 ng/mL standard,
(b) real sample (×500), (c) dSPE-treated sample (×600),
and (d) dSPE-treated sample (×600) spiked with 100 ng/mL standard.

Chapter 4 Conclusion

In this study, we successfully synthesized and applied a novel anionic Cu-based metal-organic framework, $NH_4[Cu_3(\mu_3\text{-}OH)(\mu_3\text{-}4\text{-carboxypyrazolato})_3]$ (Cu-PyC NH_4^+ MOF), as a dispersive solid-phase extraction (dSPE) adsorbent for the selective enrichment of amino acids from complex matrices. The anionic framework of this MOF, derived from doubly deprotonated pyrazole-4-carboxylate ligands and balanced by NH_4^+ counterions, represents a groundbreaking feature that enables a highly efficient cation-exchange mechanism. This unique structure facilitates robust electrostatic interactions with the zwitterionic forms of amino acids, allowing their protonated ammonium groups ($–NH_3^+$) to displace NH_4^+ ions and bind selectively to the framework's anionic sites. Augmented by secondary hydrogen bonding and π-π stacking, this multimodal adsorption process outperforms traditional neutral or cationic MOFs, providing exceptional selectivity and efficiency in capturing polar, charged analytes like amino acids—compounds that are notoriously challenging to extract due to their hydrophilicity and matrix interferences.

The value of this approach cannot be overstated: amino acid extraction is inherently vital across biochemistry, nutrition, clinical diagnostics, and environmental monitoring, where precise quantification informs everything from metabolic disorder detection to food quality assurance. By leveraging an anionic MOF, our method addresses longstanding limitations in conventional sorbents, such as poor retention of zwitterions and high solvent consumption, while promoting sustainability through reduced reagent use and recyclability. Systematic optimization of extraction parameters—including pH, additives, adsorbent dosage, and elution conditions—yielded high recoveries (> 80% for most analytes) and reproducibility, culminating in a derivatization-free LC-MS/MS workflow using an amide-based HILIC column in

MRM mode for 15 amino acids quantification.

Applied to real-world samples like instant coffee, the method demonstrated superior matrix cleanup and trace-level detection, highlighting its transformative potential in food safety, biomedical research, and beyond. This innovation not only expands the frontiers of MOF-based adsorbents but also establishes a rapid, reliable, and eco-friendly platform for routine amino acid analysis, paving the way for broader adoption in high-impact fields where accurate analyte isolation can drive scientific and societal advancements.

Reference

(1) Vickery, H. B.; Schmidt, C. L. A. The History of the Discovery of the Amino Acids. *Chemical Reviews* **1931**, *9* (2), 169-318. DOI: 10.1021/cr60033a001.

(2) Bradford Vickery, H. The History of the Discovery of the Amino Acids II. A Review of Amino Acids Described Since 1931 as Components of Native Proteins. In *Advances in Protein Chemistry*, Anfinsen, C. B., Edsall, J. T., Richards, F. M. Eds.; Vol. 26; Academic Press, 1972; pp 81-171.

(3) Wu, G. Amino acids: metabolism, functions, and nutrition. *Amino Acids* **2009**, *37* (1), 1-17. DOI: 10.1007/s00726-009-0269-0 From NLM Medline.

(4) Galili, G.; Amir, R.; Fernie, A. R. The Regulation of Essential Amino Acid Synthesis and Accumulation in Plants. *Annu Rev Plant Biol* **2016**, *67*, 153-178. DOI: 10.1146/annurev-arplant-043015-112213 From NLM Medline.

(5) Violi, J. P.; Bishop, D. P.; Padula, M. P.; Steele, J. R.; Rodgers, K. J. Considerations for amino acid analysis by liquid chromatography-tandem mass spectrometry: A tutorial review. *TrAC Trends in Analytical Chemistry* **2020**, *131*, 116018. DOI: https://doi.org/10.1016/j.trac.2020.116018.

(6) Weber, A. L.; Miller, S. L. Reasons for the occurrence of the twenty coded protein amino acids. *J Mol Evol* **1981**, *17* (5), 273-284. DOI: 10.1007/BF01795749 From NLM Medline.

(7) Hunt, S. The Non-Protein Amino Acids. In *Chemistry and Biochemistry of the Amino Acids*, Barrett, G. C. Ed.; Springer Netherlands, 1985; pp 55-138.

(8) Ilardo, M.; Meringer, M.; Freeland, S.; Rasulev, B.; Cleaves, H. J., 2nd. Extraordinarily adaptive properties of the genetically encoded amino acids. *Sci Rep* **2015**, *5*, 9414. DOI: 10.1038/srep09414 From NLM Medline.

(9) Ding, Y.; Ting, J. P.; Liu, J.; Al-Azzam, S.; Pandya, P.; Afshar, S. Impact of non-proteinogenic amino acids in the discovery and development of peptide therapeutics. *Amino Acids* **2020**, *52* (9), 1207-1226. DOI: 10.1007/s00726-020-02890-9 From NLM Medline.

(10) Rose, W. C. The Nutritive Significance of the Amino Acids and Certain Related Compounds. *Science* **1937**, *86* (2231), 298-300. DOI: 10.1126/science.86.2231.298 From NLM PubMed-not-MEDLINE.

(11) Rodwell, V. W.; Murray, R. K. Biochemistry & Medicine. In *Harper's Illustrated Biochemistry, 31e*, Rodwell, V. W., Bender, D. A., Botham, K. M., Kennelly, P. J., Weil, P. A. Eds.; McGraw-Hill Education, 2018.

(12) Ambrogelly, A.; Palioura, S.; Söll, D. Natural expansion of the genetic code. *Nature Chemical Biology* **2007**, *3* (1), 29-35. DOI: 10.1038/nchembio847.

(13) Finkelstein, J. D. Methionine metabolism in mammals. *The Journal of*

Nutritional Biochemistry **1990**, *1* (5), 228-237. DOI: https://doi.org/10.1016/0955-2863(90)90070-2.
(14) Haussinger, D. Nitrogen metabolism in liver: structural and functional organization and physiological relevance. *Biochem J* **1990**, *267* (2), 281-290. DOI: 10.1042/bj2670281 From NLM Medline.
(15) Phang, J. M.; Liu, W.; Zabirnyk, O. Proline metabolism and microenvironmental stress. *Annu Rev Nutr* **2010**, *30*, 441-463. DOI: 10.1146/annurev.nutr.012809.104638 From NLM Medline.
(16) Rodgers, K. J. Non-protein amino acids and neurodegeneration: the enemy within. *Exp Neurol* **2014**, *253*, 192-196. DOI: 10.1016/j.expneurol.2013.12.010 From NLM Medline.
(17) Dunlop, R. A.; Cox, P. A.; Banack, S. A.; Rodgers, K. J. The non-protein amino acid BMAA is misincorporated into human proteins in place of L-serine causing protein misfolding and aggregation. *PLoS One* **2013**, *8* (9), e75376. DOI: 10.1371/journal.pone.0075376 From NLM Medline.
(18) Olsen, R. W.; Sieghart, W. GABA A receptors: subtypes provide diversity of function and pharmacology. *Neuropharmacology* **2009**, *56* (1), 141-148. DOI: 10.1016/j.neuropharm.2008.07.045 From NLM Medline.
(19) Martineau, M.; Baux, G.; Mothet, J. P. D-serine signalling in the brain: friend and foe. *Trends Neurosci* **2006**, *29* (8), 481-491. DOI: 10.1016/j.tins.2006.06.008 From NLM Medline.
(20) Blau, N.; van Spronsen, F. J.; Levy, H. L. Phenylketonuria. *Lancet* **2010**, *376* (9750), 1417-1427. DOI: 10.1016/s0140-6736(10)60961-0 From NLM.
(21) Lardner, A. L. Neurobiological effects of the green tea constituent theanine and its potential role in the treatment of psychiatric and neurodegenerative disorders. *Nutr Neurosci* **2014**, *17* (4), 145-155. DOI: 10.1179/1476830513Y.0000000079 From NLM Medline.
(22) de Koning, T. J.; Snell, K.; Duran, M.; Berger, R.; Poll-The, B. T.; Surtees, R. L-serine in disease and development. *Biochem J* **2003**, *371* (Pt 3), 653-661. DOI: 10.1042/BJ20021785 From NLM Medline.
(23) Fosgerau, K.; Hoffmann, T. Peptide therapeutics: current status and future directions. *Drug Discov Today* **2015**, *20* (1), 122-128. DOI: 10.1016/j.drudis.2014.10.003 From NLM Medline.
(24) Wu, G. *Principles of Animal Nutrition*; CRC Press, 2018.
(25) Voet, D.; Voet, J. G. *Biochemistry*; John Wiley & Sons, 2011.
(26) Holecek, M. Branched-chain amino acids in health and disease: metabolism, alterations in blood plasma, and as supplements. *Nutr Metab (Lond)* **2018**, *15*, 33. DOI: 10.1186/s12986-018-0271-1 From NLM PubMed-not-MEDLINE.

(27) Blaskovich, M. A. Unusual Amino Acids in Medicinal Chemistry. *J Med Chem* **2016**, *59* (24), 10807-10836. DOI: 10.1021/acs.jmedchem.6b00319 From NLM Medline.
(28) Rodgers, K. J.; Main, B. J.; Samardzic, K. Cyanobacterial Neurotoxins: Their Occurrence and Mechanisms of Toxicity. *Neurotox Res* **2018**, *33* (1), 168-177. DOI: 10.1007/s12640-017-9757-2 From NLM Medline.
(29) Nunn, P. B.; Bell, E. A.; Watson, A. A.; Nash, R. J. Toxicity of non-protein amino acids to humans and domestic animals. *Nat Prod Commun* **2010**, *5* (3), 485-504. From NLM.
(30) Lefebvre, K. A.; Robertson, A. Domoic acid and human exposure risks: A review. *Toxicon* **2010**, *56* (2), 218-230. DOI: https://doi.org/10.1016/j.toxicon.2009.05.034.
(31) Cox, P. A.; Davis, D. A.; Mash, D. C.; Metcalf, J. S.; Banack, S. A. Dietary exposure to an environmental toxin triggers neurofibrillary tangles and amyloid deposits in the brain. *Proc Biol Sci* **2016**, *283* (1823). DOI: 10.1098/rspb.2015.2397 From NLM Medline.
(32) Rubenstein, E. Biologic effects of and clinical disorders caused by nonprotein amino acids. *Medicine (Baltimore)* **2000**, *79* (2), 80-89. DOI: 10.1097/00005792-200003000-00002 From NLM Medline.
(33) Banack, S. A.; Metcalf, J. S.; Spáčil, Z.; Downing, T. G.; Downing, S.; Long, A.; Nunn, P. B.; Cox, P. A. Distinguishing the cyanobacterial neurotoxin β-N-methylamino-l-alanine (BMAA) from other diamino acids. *Toxicon* **2011**, *57* (5), 730-738. DOI: https://doi.org/10.1016/j.toxicon.2011.02.005.
(34) Violi, J. P.; Bishop, D. P.; Padula, M. P.; Steele, J. R.; Rodgers, K. J. Considerations for amino acid analysis by liquid chromatography-tandem mass spectrometry. *A tutorial review* **2020**, *131*, Review Article. DOI: 10.1016/j.trac.2020.116018.
(35) Kaspar, H.; Dettmer, K.; Gronwald, W.; Oefner, P. J. Advances in amino acid analysis. *Anal Bioanal Chem* **2009**, *393* (2), 445-452. DOI: 10.1007/s00216-008-2421-1 From NLM Medline.
(36) Bosch, L.; Alegría, A.; Farré, R. Application of the 6-aminoquinolyl-N-hydroxysccinimidyl carbamate (AQC) reagent to the RP-HPLC determination of amino acids in infant foods. *Journal of Chromatography B* **2006**, *831* (1), 176-183. DOI: https://doi.org/10.1016/j.jchromb.2005.12.002.
(37) Fountoulakis, M.; Lahm, H.-W. Hydrolysis and amino acid composition analysis of proteins. *Journal of Chromatography A* **1998**, *826* (2), 109-134. DOI: https://doi.org/10.1016/S0021-9673(98)00721-3.
(38) Weiss, M.; Manneberg, M.; Juranville, J.-F.; Lahm, H.-W.; Fountoulakis, M. Effect of the hydrolysis method on the determination of the amino acid composition

of proteins. *Journal of Chromatography A* **1998**, *795* (2), 263-275. DOI: https://doi.org/10.1016/S0021-9673(97)00983-7.
(39) Uy, R.; Wold, F. Posttranslational Covalent Modification of Proteins. *Science* **1977**, *198* (4320), 890-896. DOI: 10.1126/science.337487 (acccessed 2025/08/11).
(40) Stadtman, E. R.; Levine, R. L. Free radical-mediated oxidation of free amino acids and amino acid residues in proteins. *Amino Acids* **2003**, *25* (3), 207-218. DOI: 10.1007/s00726-003-0011-2.
(41) Friedman, M. Chemistry, Nutrition, and Microbiology of d-Amino Acids. *Journal of Agricultural and Food Chemistry* **1999**, *47* (9), 3457-3479. DOI: 10.1021/jf990080u.
(42) Genchi, G. An overview on d-amino acids. *Amino Acids* **2017**, *49* (9), 1521-1533. DOI: 10.1007/s00726-017-2459-5.
(43) Hartman, M. C. T.; Josephson, K.; Szostak, J. W. Enzymatic aminoacylation of tRNA with unnatural amino acids. *Proceedings of the National Academy of Sciences* **2006**, *103* (12), 4356-4361. DOI: 10.1073/pnas.0509219103 (acccessed 2025/08/11).
(44) Nomenclature and symbolism for amino acids and peptides (Recommendations 1983). **1984**, *56* (5), 595-624. DOI: doi:10.1351/pac198456050595 (acccessed 2025-08-12).
(45) Cahn, R. S.; Ingold, C.; Prelog, V. Specification of Molecular Chirality. *Angewandte Chemie International Edition in English* **1966**, *5* (4), 385-415. DOI: https://doi.org/10.1002/anie.196603851 (acccessed 2025/08/11).
(46) Periat, A.; Krull, I. S.; Guillarme, D. Applications of hydrophilic interaction chromatography to amino acids, peptides, and proteins. *J Sep Sci* **2015**, *38* (3), 357-367. DOI: 10.1002/jssc.201400969 From NLM Medline.
(47) Cook, T. R.; Zheng, Y. R.; Stang, P. J. Metal-organic frameworks and self-assembled supramolecular coordination complexes: comparing and contrasting the design, synthesis, and functionality of metal-organic materials. *Chem Rev* **2013**, *113* (1), 734-777. DOI: 10.1021/cr3002824 From NLM Medline.
(48) Rosi, N. L.; Eckert, J.; Eddaoudi, M.; Vodak, D. T.; Kim, J.; O'Keeffe, M.; Yaghi, O. M. Hydrogen storage in microporous metal-organic frameworks. *Science* **2003**, *300* (5622), 1127-1129. DOI: 10.1126/science.1083440 From NLM PubMed-not-MEDLINE.
(49) Noro, S.; Kitagawa, S.; Kondo, M.; Seki, K. A New, Methane Adsorbent, Porous Coordination Polymer. *Angew Chem Int Ed Engl* **2000**, *39* (12), 2081-2084. DOI: 10.1002/1521-3773(20000616)39:12<2081::aid-anie2081>3.0.co;2-a From NLM PubMed-not-MEDLINE.
(50) Li, H. E., Mohamed; Groy, Thomas L.; Yaghi, Omar M. Establishing Microporosity in Open Metal-Organic Frameworks: Gas Sorption Isotherms for

Zn(BDC). *Journal of the American Chemical Society* **1998**, *120* (33), 8571–8572. DOI: 10.1021/ja981669x.
(51) Bavykina, A.; Kolobov, N.; Khan, I. S.; Bau, J. A.; Ramirez, A.; Gascon, J. Metal-Organic Frameworks in Heterogeneous Catalysis: Recent Progress, New Trends, and Future Perspectives. *Chem Rev* **2020**, *120* (16), 8468-8535. DOI: 10.1021/acs.chemrev.9b00685 From NLM PubMed-not-MEDLINE.
(52) Kreno, L. E.; Leong, K.; Farha, O. K.; Allendorf, M.; Van Duyne, R. P.; Hupp, J. T. Metal-organic framework materials as chemical sensors. *Chem Rev* **2012**, *112* (2), 1105-1125. DOI: 10.1021/cr200324t From NLM Medline.
(53) Sohrabi, H.; Ghasemzadeh, S.; Ghoreishi, Z.; Majidi, M. R.; Yoon, Y.; Dizge, N.; Khataee, A. Metal-organic frameworks (MOF)-based sensors for detection of toxic gases: A review of current status and future prospects. *Materials Chemistry and Physics* **2023**, *299*. DOI: 10.1016/j.matchemphys.2023.127512.
(54) Luo, Z.; Fan, S.; Gu, C.; Liu, W.; Chen, J.; Li, B.; Liu, J. Metal-Organic Framework (MOF)-based Nanomaterials for Biomedical Applications. *Curr Med Chem* **2019**, *26* (18), 3341-3369. DOI: 10.2174/0929867325666180214123500 From NLM Medline.
(55) Xue, Y.; Zheng, S.; Xue, H.; Pang, H. Metal–organic framework composites and their electrochemical applications. *Journal of Materials Chemistry A* **2019**, *7* (13), 7301-7327. DOI: 10.1039/c8ta12178h.
(56) Furukawa, H.; Cordova, K. E.; O'Keeffe, M.; Yaghi, O. M. The chemistry and applications of metal-organic frameworks. *Science* **2013**, *341* (6149), 1230444. DOI: 10.1126/science.1230444 From NLM PubMed-not-MEDLINE.
(57) Yusuf, V. F.; Malek, N. I.; Kailasa, S. K. Review on Metal-Organic Framework Classification, Synthetic Approaches, and Influencing Factors: Applications in Energy, Drug Delivery, and Wastewater Treatment. *ACS Omega* **2022**, *7* (49), 44507-44531. DOI: 10.1021/acsomega.2c05310 From NLM PubMed-not-MEDLINE.
(58) Jonckheere, D.; Steele, J. A.; Claes, B.; Bueken, B.; Claes, L.; Lagrain, B.; Roeffaers, M. B. J.; De Vos, D. E. Adsorption and Separation of Aromatic Amino Acids from Aqueous Solutions Using Metal-Organic Frameworks. *ACS Appl Mater Interfaces* **2017**, *9* (35), 30064-30073. DOI: 10.1021/acsami.7b09175 From NLM Medline.
(59) Li, L.; Han, J.; Huang, X.; Qiu, S.; Liu, X.; Liu, L.; Zhao, M.; Qu, J.; Zou, J.; Zhang, J. Organic pollutants removal from aqueous solutions using metal-organic frameworks (MOFs) as adsorbents: A review. *Journal of Environmental Chemical Engineering* **2023**, *11* (6). DOI: 10.1016/j.jece.2023.111217.
(60) Manousi, N.; Plastiras, O.-E.; Kalogiouri, N.; Zacharis, C.; Zachariadis, G. Metal-Organic Frameworks in Bioanalysis: Extraction of Small Organic Molecules.

Separations **2021**, *8* (5). DOI: 10.3390/separations8050060.
(61) Bazargan, M.; Ghaemi, F.; Amiri, A.; Mirzaei, M. Metal–organic framework-based sorbents in analytical sample preparation. *Coordination Chemistry Reviews* **2021**, *445*. DOI: 10.1016/j.ccr.2021.214107.
(62) del Rio, M.; Grimalt Escarabajal, J. C.; Turnes Palomino, G.; Palomino Cabello, C. Zinc/Iron mixed-metal MOF-74 derived magnetic carbon nanorods for the enhanced removal of organic pollutants from water. *Chemical Engineering Journal* **2022**, *428*. DOI: 10.1016/j.cej.2021.131147.
(63) Ma, X.; Wang, L.; Wang, H.; Deng, J.; Song, Y.; Li, Q.; Li, X.; Dietrich, A. M. Insights into metal-organic frameworks HKUST-1 adsorption performance for natural organic matter removal from aqueous solution. *J Hazard Mater* **2022**, *424* (Pt C), 126918. DOI: 10.1016/j.jhazmat.2021.126918 From NLM Medline.
(64) Edebali, S. Synthesis and characterization of MIL-101 (Fe) as efficient catalyst for tetracycline degradation by using NaBH4: Artificial neural network modeling. *Applied Surface Science Advances* **2023**, *18*. DOI: 10.1016/j.apsadv.2023.100496.
(65) Yang, D.; Odoh, S. O.; Borycz, J.; Wang, T. C.; Farha, O. K.; Hupp, J. T.; Cramer, C. J.; Gagliardi, L.; Gates, B. C. Tuning Zr6 Metal–Organic Framework (MOF) Nodes as Catalyst Supports: Site Densities and Electron-Donor Properties Influence Molecular Iridium Complexes as Ethylene Conversion Catalysts. *ACS Catalysis* **2015**, *6* (1), 235-247. DOI: 10.1021/acscatal.5b02243.
(66) Padinjareveetil, A. K. K.; Perales-Rondon, J. V.; Zaoralova, D.; Otyepka, M.; Alduhaish, O.; Pumera, M. Fe-MOF Catalytic Nanoarchitectonic toward Electrochemical Ammonia Production. *ACS Appl Mater Interfaces* **2023**, *15* (40), 47294-47306. DOI: 10.1021/acsami.3c12822 From NLM PubMed-not-MEDLINE.
(67) Reinsch, H.; Marszalek, B.; Wack, J.; Senker, J.; Gil, B.; Stock, N. A new Al-MOF based on a unique column-shaped inorganic building unit exhibiting strongly hydrophilic sorption behaviour. *Chem Commun (Camb)* **2012**, *48* (76), 9486-9488. DOI: 10.1039/c2cc34909d From NLM PubMed-not-MEDLINE.
(68) Kalmutzki, M. J.; Hanikel, N.; Yaghi, O. M. Secondary building units as the turning point in the development of the reticular chemistry of MOFs. *Sci Adv* **2018**, *4* (10), eaat9180. DOI: 10.1126/sciadv.aat9180 From NLM PubMed-not-MEDLINE.
(69) Hamisu, A. M.; Ariffin, A.; Wibowo, A. C. Cation exchange in metal-organic frameworks (MOFs): The hard-soft acid-base (HSAB) principle appraisal. *Inorganica Chimica Acta* **2020**, *511*. DOI: 10.1016/j.ica.2020.119801.
(70) Quartapelle Procopio, E.; Linares, F.; Montoro, C.; Colombo, V.; Maspero, A.; Barea, E.; Navarro, J. A. Cation-exchange porosity tuning in anionic metal-organic frameworks for the selective separation of gases and vapors and for catalysis. *Angew Chem Int Ed Engl* **2010**, *49* (40), 7308-7311. DOI: 10.1002/anie.201003314 From

NLM PubMed-not-MEDLINE.
(71) Kulandaivel, S.; Wang, Y. M.; Chen, S. F.; Lin, C. H.; Yeh, Y. C. A Cu-based metal-organic framework synthesized via a green method exhibits unique catecholase-like activity for epigallocatechin gallate detection in teas. *Anal Methods* **2024**, *16* (48), 8307-8315. DOI: 10.1039/d4ay01733a From NLM Medline.
(72) Soxhlet, F. Die gewichtsanalytische Bestimmung des Milchfettes. *Dingler's Polytechnisches Journal* **1879**, *232*, 461-465.
(73) Martin, A. J. P.; Synge, R. L. M. Separation of the higher monoamino-acids by counter-current liquid-liquid extraction: the amino-acid composition of wool. *Biochemical Journal* **1941**, *35* (1-2), 91-121. DOI: 10.1042/bj0350091 (acccessed 7/22/2025).
(74) Buszewski, B.; Szultka, M. Past, Present, and Future of Solid Phase Extraction: A Review. *Critical Reviews in Analytical Chemistry* **2012**, *42* (3), 198-213. DOI: 10.1080/07373937.2011.645413.
(75) Anastassiades, M.; Lehotay, S. J.; Štajnbaher, D.; Schenck, F. J. Fast and Easy Multiresidue Method Employing Acetonitrile Extraction/Partitioning and "Dispersive Solid-Phase Extraction" for the Determination of Pesticide Residues in Produce. *Journal of AOAC INTERNATIONAL* **2003**, *86* (2), 412-431. DOI: 10.1093/jaoac/86.2.412 (acccessed 7/23/2025).
(76) Horvath, C. G.; Lipsky, S. R. Use of liquid ion exchange chromatography for the separation of organic compounds. *Nature* **1966**, *211* (5050), 748-749. DOI: 10.1038/211748a0 From NLM Medline.
(77) Horvath, C. G.; Preiss, B. A.; Lipsky, S. R. Fast liquid chromatography: an investigation of operating parameters and the separation of nucleotides on pellicular ion exchangers. *Anal Chem* **1967**, *39* (12), 1422-1428. DOI: 10.1021/ac60256a003 From NLM Medline.
(78) Harris, D. C. *Quantitative chemical analysis*; W. H. Freeman, 2007.
(79) Skoog, D. A.; Holler, F. J.; Crouch, S. R. *Principles of instrumental analysis*; Cengage Learning, 2018.
(80) Wu, F.; Liu, L.; Wang, S.; Xu, J.; Lu, P.; Yan, W.; Peng, J.; Wu, D.; Li, H. Solid state ionics – Selected topics and new directions. *Progress in Materials Science* **2022**, *126*. DOI: 10.1016/j.pmatsci.2022.100921.
(81) Squires, G. Francis Aston and the mass spectrograph. *Journal of the Chemical Society, Dalton Transactions* **1998**, *1998*, 3893–3899.
(82) Mattauch, J. H., Richard. Über einen neuen Massenspektrographen. *Zeitschrift für Physik* **1934**, *89*, 786–795. DOI: https://doi.org/10.1007/BF01341392.
(83) Wolfgang Paul, H. S. Ein neues Massenspektrometer ohne Magnetfeld. *Zeitschrift für Naturforschung A* **1953**, *8* (7), 448-450. DOI:

https://doi.org/10.1515/zna-1953-0710.
(84) Wolff, M. M.; Stephens, W. E. A Pulsed Mass Spectrometer with Time Dispersion. *Review of Scientific Instruments* **1953**, *24* (8), 616-617. DOI: 10.1063/1.1770801.
(85) Alastair Ewan Cameron, D. F. E., Jr. An Ion 'Velocitron'. *Review of Scientific Instruments* **1948**, *19* (9), 605-606.
(86) Wiley, W. C.; McLaren, I. H. Time-of-Flight Mass Spectrometer with Improved Resolution. *Review of Scientific Instruments* **1955**, *26* (12), 1150-1157. DOI: 10.1063/1.1715212.
(87) Melvin Stephen Bruce Munson, F. H. F. Chemical Ionization Mass Spectrometry. I. General Introduction. *Journal of the American Chemical Society* **1966**, *88* (12), 2621-2630. DOI: 10.1021/ja00964a001.
(88) Dole, M.; Mack, L. L.; Hines, R. L.; Mobley, R. C.; Ferguson, L. D.; Alice, M. B. Molecular Beams of Macroions. *The Journal of Chemical Physics* **1968**, *49* (5), 2240-2249. DOI: 10.1063/1.1670391 (acccessed 6/29/2025).
(89) Horning, E. C.; Horning, M. G.; Carroll, D. I.; Dzidic, I.; Stillwell, R. N. New picogram detection system based on a mass spectrometer with an external ionization source at atmospheric pressure. *Analytical Chemistry* **1973**, *45* (6), 936-943. DOI: 10.1021/ac60328a035.
(90) Comisarow, M. B.; Marshall, A. G. Fourier transform ion cyclotron resonance spectroscopy. *Chemical Physics Letters* **1974**, *25* (2), 282-283. DOI: https://doi.org/10.1016/0009-2614(74)89137-2.
(91) Muller, R. A. Radioisotope Dating with a Cyclotron. *Science* **1977**, *196* (4289), 489-494. DOI: doi:10.1126/science.196.4289.489.
(92) Karas, M.; Bachmann, D.; Hillenkamp, F. Influence of the wavelength in high-irradiance ultraviolet laser desorption mass spectrometry of organic molecules. *Analytical Chemistry* **1985**, *57* (14), 2935-2939. DOI: 10.1021/ac00291a042.
(93) Tanaka, K.; Waki, H.; Ido, Y.; Akita, S.; Yoshida, Y.; Yoshida, T.; Matsuo, T. Protein and polymer analyses up to m/z 100 000 by laser ionization time-of-flight mass spectrometry. *Rapid Communications in Mass Spectrometry* **1988**, *2* (8), 151-153. DOI: https://doi.org/10.1002/rcm.1290020802.
(94) Griffiths, J. A brief history of mass spectrometry. *Anal Chem* **2008**, *80* (15), 5678-5683. DOI: 10.1021/ac8013065 From NLM PubMed-not-MEDLINE.
(95) Dronsfield, A. Mass spectrometry - the early days. Royal Society of Chemistry: 2010.
(96) McLafferty, F. W. A century of progress in molecular mass spectrometry. *Annu Rev Anal Chem (Palo Alto Calif)* **2011**, *4*, 1-22. DOI: 10.1146/annurev-anchem-061010-114018 From NLM Medline.

(97) Zhou, G.; Pang, H.; Tang, Y.; Yao, X.; Mo, X.; Zhu, S.; Guo, S.; Qian, D.; Qian, Y.; Su, S.; et al. Hydrophilic interaction ultra-performance liquid chromatography coupled with triple-quadrupole tandem mass spectrometry for highly rapid and sensitive analysis of underivatized amino acids in functional foods. *Amino Acids* **2013**, *44* (5), 1293-1305. DOI: 10.1007/s00726-013-1463-7 From NLM Medline.
(98) Zhang, P.; Chan, W.; Ang, I. L.; Wei, R.; Lam, M. M. T.; Lei, K. M. K.; Poon, T. C. W. Revisiting Fragmentation Reactions of Protonated alpha-Amino Acids by High-Resolution Electrospray Ionization Tandem Mass Spectrometry with Collision-Induced Dissociation. *Sci Rep* **2019**, *9* (1), 6453. DOI: 10.1038/s41598-019-42777-8 From NLM Medline.
(99) Virgiliou, C.; Theodoridis, G.; Wilson, I. D.; Gika, H. G. Quantification of endogenous aminoacids and aminoacid derivatives in urine by hydrophilic interaction liquid chromatography tandem mass spectrometry. *J Chromatogr A* **2021**, *1642*, 462005. DOI: 10.1016/j.chroma.2021.462005 From NLM Medline.
(100) Kulandaivel, S.; Lo, W. C.; Lin, C. H.; Yeh, Y. C. Cu-PyC MOF with oxidoreductase-like catalytic activity boosting colorimetric detection of Cr(VI) on paper. *Anal Chim Acta* **2022**, *1227*, 340335. DOI: 10.1016/j.aca.2022.340335 From NLM Medline.
(101) Zhao, Y.-G.; Cai, M.-Q.; Chen, X.-H.; Pan, S.-D.; Yao, S.-S.; Jin, M.-C. Analysis of nine food additives in wine by dispersive solid-phase extraction and reversed-phase high performance liquid chromatography. *Food Research International* **2013**, *52* (1), 350-358. DOI: 10.1016/j.foodres.2013.03.038.
(102) Jung, W. T.; Hsieh, Y. H.; Kuo, Y. J.; Yu, Y. H.; Liu, Y. H.; Lu, K. L.; Lee, H. L. Rapid microwave synthesis of MOF microrods: Dispersive SPE coupled with UHPLC-MS/MS to determine fluoroquinolones in honey. *Talanta* **2023**, *263*, 124733. DOI: 10.1016/j.talanta.2023.124733 From NLM Medline.